

Copyright Warning & Restrictions

The copyright law of the United States (Title 17, United States Code) governs the making of photocopies or other reproductions of copyrighted material.

Under certain conditions specified in the law, libraries and archives are authorized to furnish a photocopy or other reproduction. One of these specified conditions is that the photocopy or reproduction is not to be “used for any purpose other than private study, scholarship, or research.” If a user makes a request for, or later uses, a photocopy or reproduction for purposes in excess of “fair use” that user may be liable for copyright infringement,

This institution reserves the right to refuse to accept a copying order if, in its judgment, fulfillment of the order would involve violation of copyright law.

Please Note: The author retains the copyright while the New Jersey Institute of Technology reserves the right to distribute this thesis or dissertation

Printing note: If you do not wish to print this page, then select “Pages from: first page # to: last page #” on the print dialog screen



The Van Houten library has removed some of the personal information and all signatures from the approval page and biographical sketches of theses and dissertations in order to protect the identity of NJIT graduates and faculty.

ABSTRACT

RELATIONSHIP BETWEEN THE AUTONOMIC NERVOUS SYSTEM AND THE RECOVERING HEART POST EXERCISE USING HEART RATE VARIABILITY

**by
Pierre Asselin**

The goal of this thesis is to determine if a relationship exists between the activity of the autonomic nervous system (ANS) and the speed of heart rate recovery post maximal exercise. The parasympathetic branch of the ANS was assessed during rest by obtaining the high frequency (HF) component of the heart rate variability (HRV) frequency spectrum. The recovery time was estimated by fitting an exponential curve to the heart rate post exercise where the exponent was used to calculate the time constant to indicate recovery time. A regression was then performed on the HF and recovery time in order to find a relationship between the ANS activity and the recovery time.

Changes in the ANS through all stages of the experiment were characterized using two different time-frequency methods; Continuous Wavelet Transform (CWT) and the Short Time Fourier Transform (STFT).

A moderate relationship ($R^2=0.5164$) exists between the HF and the rate of recovery. Changes in the ANS throughout the experiment indicated a drop in both the LF and HF (where LF represents a mixture of sympathetic and parasympathetic activity) values during exercise and may indicate sympathetic saturation. The normalized LF and HF values contained a large spike in the LF and a corresponding drop in the HF at the start of exercise and again at the start recovery indicating sympathetic activation and sympathetic desaturation, respectively.

**RELATIONSHIP BETWEEN THE AUTONOMIC NERVOUS SYSTEM AND
THE RECOVERING HEART POST EXERCISE USING HEART RATE
VARIABILITY**

**by
Pierre Asselin**

**A Thesis
Submitted to the Faculty of
New Jersey Institute of Technology
in Partial Fulfillment of the Requirements for the Degree of
Master of Science in Biomedical Engineering**

Department of Biomedical Engineering

May 2005

Blank Page

APPROVAL PAGE

**RELATIONSHIP BETWEEN THE AUTONOMIC NERVOUS SYSTEM AND
THE RECOVERING HEART POST EXERCISE USING HEART RATE
VARIABILITY**

Pierre Asselin

Dr. Stanley Reisman, Thesis Advisor
Professor of Biomedical Engineering, NJIT

Date

Dr. Ronald Rockland, Committee Member
Associate Professor of Engineering Technology, NJIT
Associate Professor of Biomedical Engineering, NJIT

Date

Dr. Joel Schesser, Committee Member
Special Lecturer in Biomedical Engineering, NJIT

Date

Dr. Sina Zaim, Committee Member
Assistant Professor of Medicine, UMDNJ

Date

BIOGRAPHICAL SKETCH

Author: Pierre Asselin
Degree: Master of Science
Date: May 2005

Undergraduate and Graduate Education:

- Masters of Science in Biomedical Engineering,
New Jersey Institute of Technology, Newark, NJ, 2005
- Bachelor of Science in Computer Engineering,
New Jersey Institute of Technology, Newark, NJ, 2003

Major: Biomedical Engineering

Presentations and Publications:

Jerome Allen, Pierre Asselin and Richard Foulds, "American Sign Language Finger Spelling Recognition System," Proceedings of the 29th Annual Northeast Bioengineering Conference, Newark, March 2003.

To my parents, Andre and Magda Asselin,
who never stopped believing in me

ACKNOWLEDGMENT

I would like to express my sincerest appreciation to Dr. Stanley Reisman, who not only served as my research supervisor, providing valuable and countless resources, insight, and intuition, but also constantly gave me support, reassurance, and encouragement. Special thanks to Dr. Joel Schesser, without his advice and guidance the completion of this thesis would not have been impossible. I would also like to acknowledge Dr. Ronald Rockland, without his creation of the peak detector and insight the completion of the work would have been much more tedious and drawn out. Another integral person involved with the research was Dr. Sina Zaim, as the principal investigator in the study, none of this would have been feasible. I would also like to thank the above mentioned for actively participating in my committee.

I would also like to extend my deepest gratitude to all the staff at UMDNJ especially Dr. Jennifer Zimmer, who worked tirelessly to keep the study running as smooth as possible.

To Anne Marie Petrock, Jason Steffener, Diane Donnelly, and Binoy Mathew, my fellow graduate students in the Biomedical Signal Processing Research Laboratory, thank you for your friendship, support and for keeping sometimes stressful moments enjoyable.

I would also like to thank my family who never stopped believing in me. My sincerest appreciation to my parents Andre and Magda, who always pushed me to do better, my brother, Ramy, who tough me to be stubborn enough to never give up and to my sister who always set a good example, I will always love you.

I am truly blessed for my friends whose support seems boundless, I thank you. I could not have accomplished this without the humor extended from Ralph Jimenez; The

countless sleepless nights, working in the lab, with Jerome Allen; the nourishment received from the numerous barbequed cookies provided by Simon Dwyer and Muhammad Mian; and lastly my deepest gratitude to Abayomi Soyeju, without his efforts during my undergraduate career my time in graduate school would have been short lived. For the countless others whom I have not named you will always remain dear to me.

TABLE OF CONTENTS

Chapter	Page
1 BACKGROUND	1
1.1 Introduction.....	1
1.2 Autonomic Nervous System.....	3
1.2.1 Divisions of the Autonomic Nervous System	3
1.2.2 Physiology of Autonomic Nervous System.....	6
1.2.3 Effects of Drugs.....	7
1.3 Physiological Effects of Exercise.....	9
1.4 Heart Rate Variability (HRV)	10
1.4.1 Physiological Correlates of HRV.....	11
1.4.2 Time Domain Methods of HRV.....	12
1.4.3 Frequency Domain Methods of HRV.....	13
2 ENGINEERING BACKGROUND.....	15
2.1 Signal Acquisition	15
2.2 Power Spectral Analysis.....	17
2.3 Short Time Fourier Transform.....	18
2.4 Wavelet Transform.....	19
3 METHODS	23
3.1 Subjects	23
3.2 Experimental Design for Test A Patients.....	23
3.3 Experimental Design for Test B.....	25
3.4 Data Processing	26

TABLE OF CONTENTS
(Continued)

Chapter	Page
3.4.1 Peak Detection.....	26
3.4.2 Test B Filtering.....	27
3.4.3 IIBI Creation.....	28
3.4.4 Spectral Analysis.....	30
3.4.5 Short Time Fourier Transform.....	31
3.4.6 Wavelet Transform.....	35
3.4.7 Curve Fitting.....	36
3.5 Statistical Analysis	37
4 RESULTS AND DISCUSSION	39
5 CONCLUSION AND FUTURE WORK	77
APPENDIX A PEAK DETECTOR.....	79
APPENDIX B POWER SPECTRUM NORMALIZATION	80
APPENDIX C WAVELET TRANSFORM PROGRAM CODE	82
APPENDIX D SHORT TIME FOURIER TRANSFORM PROGRAM CODE.....	90
APPENDIX E EXPANDING PROGRAM	94
APPENDIX F PEAK DETECTOR PROGRAM.....	99
APPENDIX G IIBI FILTERING PROGRAM.....	121
APPENDIX H PLOTS FROM THE TIME FREQUENCY ANALYSIS	122
REFERENCES	152

LIST OF TABLES

Table		Page
1.1	Sympathetic and Parasympathetic Divisions Effects on Various Organs.....	5
1.2	Cholinergic and Adrenergic Receptors	8
3.1	Stages of the Bruce Protocol	25
4.1	Data Used for the Regression Analysis.....	42

LIST OF FIGURES

Figure	Page
2.1(a) Time-Frequency plane for WTs (b) Time-Frequency plane for STFT	21
3.1 Diagram showing the process flow required to perform the peak detection....	27
3.2 Diagram showing the process flow to filter the IBI acquired by the Polar heart rate monitor.....	28
3.3 Creation of the IIBI signal interpolated at 5 Hz.....	30
3.4 STFT output results for the entire experiment for one UMDNJ patient.	34
3.5 WT output results for the entire experiment for one UMDNJ patient.	36
4.1 Frequency spectrum for the paced breathing section of the IIBI for one of the UMDNJ patients.	41
4.2 Output of the curve fitting program plotting the IIBI (blue) and the best fitting exponential curve (red).....	41
4.3 Plot of the HF vs. the exponent.	43
4.4 STFT output results for the entire experiment for one UMDNJ patient.	48
4.5 WT output results for the entire experiment for one UMDNJ patient.	49
4.6 STFT output for the paced breathing portion of the experiment.....	51
4.7 WT output for the paced breathing portion of the experiment.....	52
4.8 STFT output for the time period the patient was in the process of standing. ...	54
4.9 WT output for the time period the patient was in the process of standing.....	55
4.10 STFT output for the exercise portion of the experiment.	56
4.11 WT output for the exercise portion of the experiment.	57
4.12 STFT output for the recovery portion of the experiment.	59
4.13 WT output for the recovery portion of the experiment.	60

**LIST OF FIGURES
(Continued)**

Figure	Page
4.14 Output from the STFT program running a file with an extended 30 minute recovery period.	63
4.15 Output from the WT program running a file with an extended 30 minute recovery period.	64
4.16 STFT output for the resting portion of the experiment.	66
4.17 WT output for the resting portion of the experiment.	67
4.18 STFT output for the exercise portion of the experiment.	69
4.19 WT output for the exercise portion of the experiment.	70
4.20 STFT output for the recovery portion of the experiment.	72
4.21 WT output for the recovery portion of the experiment.	73
E.1 Front panel of the main program used to expand data view.	95
E.2 Block Diagram of the main program used to expand data view.	96
E.3 Front panel of sub program that will calculate the significance of one group being greater then the other.	97
E.4 Block Diagram of sub program that will calculate the significance of one group being greater then the other.	97
F.1 Main program for peak detection front panel.	99
F.2 Main program for peak detection block diagram.	100
F.3 Expand ECG front panel.	101
F.4 Expand ECG block diagram.	101
F.5 Interval Rwave array front panel.	102
F.6 Interval Rwave array block diagram.	102
F.7 Final Rdetect 032704 front panel.	103

**LIST OF FIGURES
(Continued)**

Figure	Page
F.8 Final Rdetect 032704 block diagram.	103
F.9 Rwave array segment front panel.	104
F.10 Rwave array segment block diagram.	104
F.11 Spectrum front panel.	105
F.12 Spectrum block diagram.	106
F.13 EGG amplif 032104 front panel.	107
F.14 EGG amplif 032104 block diagram.	107
F.15 Single Rdetect 032704 front panel.	108
F.16 Single Rdetect 032704 block diagram.	108
F.17 R wave filter deriv 2 front panel.	109
F.18 R wave filter deriv 2 block diagram.	109
F.19 IIBI create 040104 front panel.	110
F.20 IIBI create 040104 block diagram.	110
F.21 Start group front panel.	111
F.22 Start group block diagram.	111
F.23 Peak find v2 Rwave front panel.	112
F.24 Peak find v2 Rwave block diagram.	112
F.25 Rwave >level 031704 front panel.	113
F.26 Rwave >level 031704 block diagram.	113
F.27 Clipped median 032704 front panel.	114
F.28 Clipped median 032704 block diagram.	114

LIST OF FIGURES
(Continued)

Figure	Page
F.29 Peak levels 032104 front panel.	115
F.30 Peak levels 032104 block diagram.....	115
F.31 Decimate front panel.	116
F.32 Decimate block diagram.....	116
F.33 Sub difference front panel.	117
F.34 Sub difference block diagram.....	117
F.35 Refractory front panel.....	118
F.36 Refractory block diagram.....	118
F.37 Signal greater then level front panel.	119
F.38 Signal greater then level block diagram.....	119
F.39 Meet conditions front panel.....	120
F.40 Meet conditions block diagram.	120
H.1 STFT output for subject 1.....	122
H.2 STFT output for subject 2.....	123
H.3 STFT output for subject 3.....	124
H.4 STFT output for subject 4.....	125
H.5 STFT output for subject 5.....	126
H.6 STFT output for subject 6.....	127
H.7 STFT output for subject 7.....	128
H.8 STFT output for subject 8.....	129
H.9 STFT output for subject 9.....	130

LIST OF FIGURES
(Continued)

Figure	Page
H.10 STFT output for subject 10	131
H.11 STFT output for subject 11	132
H.12 STFT output for subject 12	133
H.13 STFT output for subject 13	134
H.14 STFT output for subject 14	135
H.15 STFT output for subject 15	136
H.16 STFT output for subject 16	137
H.17 STFT output for subject 17	138
H.18 STFT output for subject 18	139
H.19 STFT output for subject 19	140
H.20 STFT output for subject 20	141
H.21 STFT output for subject 21	142
H.22 STFT output for subject 22	143
H.23 STFT output for subject 23	144
H.24 STFT output for subject 24	145
H.25 STFT output for subject 25	146
H.26 STFT output for subject 26	147
H.27 STFT output for subject 27	148
H.28 STFT output for subject 28	149
H.29 STFT output for subject 29	150
H.30 STFT output for subject 30	151

CHAPTER 1

BACKGROUND

1.1 Introduction

The autonomic nervous system (ANS) is the portion of the central nervous system that controls involuntary functions such as sweating, digestion, breathing and heart rate. Of these four functions, heart rate can be utilized to assess the health and fitness level of an individual.

Most people today know of the direct relationship between a person's health and the proper functionality of their heart. However, there exists a deeper relationship than what appears on the surface. For instance, there have been indications of a relationship that exists among patients with slow heart rate recovery and the occurrence of pathological cardiac events, as well as a link identified between low heart rate variability (HRV) and the occurrence of cardiac abnormalities such as myocardial infarctions and diabetic neuropathies [1, 8, 12]. Therefore, it is important to be able to assess the ANS in a noninvasive manner to identify a relationship between its activity, which can be characterized by the variability of a person's heart rate, and the rate at which the heart recovers after an exercise or stress.

This thesis examines the relationship between heart rate variability at a resting state and the rate at which heart rate recovers after exercise. In addition this thesis will map changes in autonomic activity during both exercise and recovery stages.

In order to assess the relationship between the ANS and heart rate recovery two different testing procedures were used. The first, Test A, had participants perform three

tasks: resting while breathing at a controlled rate, exercise, and seated recovery. The second, Test B also performed three similar tasks: rested breathing at a self selected rate, exercise, and an extended seated recovery.

Depending on the testing procedure and task performed, different methods of analyzing changes in the heart rate were used. The HRV method used to analyze data acquired from the controlled breathing task of Test A was power spectrum analysis, which was implemented with the use of the Fourier transform. The heart rate during the seated recovery stage was assessed by fitting an exponential curve, where the time constant of the curve represented the estimated rate of recovery. A relation was then developed between the high frequency (HF) component obtained from the analysis of the paced breathing data and the above mentioned time constant. This was done since the HF is associated with the activity of the parasympathetic nervous system [6, 8, 12], which is the section of the ANS thought to be associated with reducing heart rate [2].

It is unknown how the two branches of the ANS function in order to cause heart rate recovery. There are four possibilities that can explain the initial changes within the ANS which bring about the return of the heart rate to its resting values. The first theory is that there is no change in sympathetic activity and an increase in parasympathetic activity. The second theory explains the phenomenon with a decrease in sympathetic activity while the parasympathetic activity remains the same. The third explanation is a combination of the first two; it supports an increase in parasympathetic activity and a reduction in sympathetic activity. Finally the last theory is an increase in both branches of the ANS but there is a larger increase in the parasympathetic branch than the sympathetic branch.

In order to visualize what may be happening, a secondary test was employed to analyze both Test A and Test B. This test consisted of two methods, the Wavelet Transform (WT) and the Short Time Fourier Transform (STFT). These methods are capable of measuring changes in frequency with time unlike traditional spectral analysis. This would enable us to quantify the changes in both divisions of the ANS with respect to time.

1.2 Autonomic Nervous System

1.2.1 Divisions of the Autonomic Nervous System

The autonomic nervous system (ANS) is the portion of the central nervous system that controls involuntary functions. It makes the necessary adjustments to cardiac muscle, smooth muscle, and gland activity in order to support the change in the body's activities [2]. It also increases or decreases heart rate, respiratory rate, adjusts blood pressure, body temperature, and stomach secretions. The ANS is divided into two branches, parasympathetic and sympathetic, which serve the same visceral organs but have opposite effects. Generally, both divisions of the ANS are partially active, although one branch will dominate over the other depending on whether the body is under stress or returning to rest. The responsibility of the sympathetic branch is to increase the heart rate under situations of stress (e.g., exercise, flight or fight conflicts, etc.) and the responsibility of parasympathetic branch is to decrease the heart rate to recover to a resting state [2].

The sympathetic nervous system increases the heart rate while inhibiting digestion when a person is in fear, rage, or exercising. When the sympathetic nervous system is active, it dilates heart vessels and skeletal muscles, and constricts cutaneous and visceral blood vessels [2]. This causes an increased flow of blood to skeletal muscles and raises

the heart rate as well as dampens gastrointestinal and urinary tract motility. Another reaction to an increase in sympathetic activity is dilation of the bronchioles in order to increase ventilation [2].

The branch of the ANS that allows us to relax, conserve energy and decrease the heart rate is the parasympathetic nervous system. When it is active, blood pressure, heart and breath rates become regulated at low normal levels. Also the gastrointestinal tract becomes active in digestion to replenish the body and pupils constrict to protect the retinas from being damaged from excessive light [2]. A more detailed list of how both branches affect different target organs is listed in Table 1.1

Table 1.1 Sympathetic and Parasympathetic Divisions Effects on Various Organs

TARGET ORGAN/SYSTEM	SYMPATHETIC EFFECTS	PARASYMPATHETIC EFFECTS
Eye (iris)	Stimulates dilator muscles, dilates eye pupils	Stimulates constrictor muscles; constricts eye pupils
Eye (ciliary muscle)	No effect	Stimulates muscles, which results in bulging of the lens for accommodation and close vision
Glands (nasal, lacrimal, salivary, gastric, pancreas)	Inhibits secretory activity; Causes Vasoconstriction of blood vessels supplying the glands	Stimulates secretory activity
Sweat glands	Stimulates copious sweating (cholinergic fibers)	No effect
Adrenal medulla	Stimulates medulla cells to secrete epinephrine and norepinephrine	No effect
Arrector pili muscles attached to hair follicles	Stimulates to contract (erects hairs and produces "Goosebumps")	No effect
Heart muscle	Increases rate and force of heart beat	Decreases rate; slows and steadies heart
Heart: coronary blood vessels	Causes vasodilation	constricts coronary vessels
Bladder/urethra	Causes relaxation of smooth muscle of bladder wall; constricts urethral sphincters (e.g., anal sphincter)	Causes contraction of smooth muscle of bladder wall; relaxes urethral sphincter; promotes voiding
Lungs	Dilates bronchioles and mildly constricts blood vessels	Constricts bronchioles
Digestive tract organs	Decreases activity of glands and muscles of digestive system and constricts sphincters (e.g., anal sphincter)	Increases motility (peristalsis) and amount of secretion by digestive organs; relaxes sphincters to allow movement of food stuffs along tract
Liver	Epinephrine stimulates liver to release glucose to blood	No effect
Gallbladder	Inhibits (gallbladder is relaxed)	Excites (gallbladder contracts to expel bile)
Kidney	Causes vasoconstriction; decreases urine output; promotes rennin formation	No effect
Penis	Causes ejaculation	Causes erection (vasodilation)
Vagina, clitoris	Causes reverse peristalsis (contraction) of vagina	Causes erection (vasodilation of clitoris)
Blood vessels	Constricts most vessels and increases blood pressure; constricts vessels of abdominal viscera and skin to divert blood to systemic circulation when necessary; dilates vessels of the skeletal muscles (cholinergic fibers) during exercise	Little or no effect
Blood coagulation	Increases coagulation	No effect
Cellular metabolism	Increases metabolic rate	No effect
Adipose tissue	Stimulates lipolysis (fat breakdown)	No effect
Mental activity	Increases alertness	No effect

(Source: E. N. Marieb, Human Anatomy and Physiology, 3rd Ed. New York: The Benjamin/Cummings Publishing Company, Inc., 1989.)

1.2.2 Physiology of Autonomic Nervous System

The major neurotransmitters released by the ANS are acetylcholine (ACh) and norepinephrine (NE). Fibers which release ACh are called cholinergic fibers and those releasing NE are called adrenergic fibers. The exceptions of adrenergic fibers which secrete ACh are the fibers innervating the sweat glands of the skin, the blood vessels within skeletal muscles and the external genitalia [2]. There is no straight forward generalization that can explain the effects of ACh and NE such as excitation or inhibition, their effects depend on which receptors they attach to.

Each autonomic transmitter has two main kinds of receptors which allow different effects caused by the same chemicals. The cholinergic receptor contains nicotinic receptors and muscarinic receptors. Nicotinic receptors are affected the same way when nicotine binds to them as when ACh does. Muscarinic receptors are activated with the mushroom poison, muscarine which will not affect nicotinic receptors just as nicotine will not affect muscarinic receptors [2]. Nicotinic receptors are found in neuromuscular junctions of skeletal muscle cells, such as all post ganglionic neurons of both sympathetic and parasympathetic nervous system. When ACh binds to the nicotinic receptor it will always stimulate or excite the neuron or effector cell. The effect ACh has on muscarinic receptors will generally excite all parasympathetic target organs except it will inhibit cardiac muscle [2]. For example ACh will stimulate receptors on the smooth muscle of the gastrointestinal tract and cause the cardiac muscle receptors of the heart to slow its activity.

Adrenergic receptors are divided into two major classes, the alpha (α) and beta (β) receptors. Generally NE or epinephrine binding to α receptors is stimulatory but has the

opposite effect when it binds to β receptors. These receptors have been divided into subclasses α_1 , α_2 , β_1 and β_2 [2]. A description of how these receptors affect their target organ is described in Table 1.2.

1.2.3 Effects of Drugs

Certain drugs can be administered to suppress or stimulate selected organs. An example of this is an adrenergic blocker, also referred to as beta-blockers that attach to β_1 receptors of the cardiac muscle. This will reduce heart rate without interfering with sympathetic effects. Another example is neostigmine, an anticholinesterase drug, which prevents the breakdown of ACh allowing it to accumulate. This drug is used with patients suffering from myasthenia gravis, where skeletal muscle activity is impaired due to a lack of ACh stimulation.

Table 1.2 Cholinergic and Adrenergic Receptors

NEUROTRANSMITTER	RECEPTOR TYPE	MAJOR LOCATIONS	EFFECT OF BINDING
Acetylcholine	Cholinergic		
	Nicotinic	All post ganglionic neurons; adrenal medullary cells (also neuromuscular junctions of skeletal muscle)	excitation
	Muscarinic	All parasympathetic target organs	Excitation in most cases; inhibition of cardiac muscle
		Select sympathetic targets; <ul style="list-style-type: none"> • Sweat glands • Blood vessels in skeletal muscles 	Activation inhibition (causes vasodilation)
Norepinephrine (and epinephrine released by adrenal medulla)	Adrenergic		
	β_1	Heart, kidneys, adipose tissue	Increases heart rate and strength; stimulates secretion of rennin; stimulates lipolysis
	β_2	Lungs and most other sympathetic target organs; abundant on blood vessels serving skeletal muscles	Inhibition : dilation of blood vessels and bronchioles; relaxes smooth muscle walls of digestive and urinary visceral organs
	α_1	Most importantly blood vessel, but virtually all sympathetic target organs except heart	Activation: constricts blood vessels and visceral organ sphincters
	α_2	Membrane of adrenergic axon terminals; blood platelets	Mediates inhibition of NE release from adrenergic terminals; promotes blood clotting

(Source: E. N. Marieb, Human Anatomy and Physiology, 3rd Ed. New York: The Benjamin/Cummings Publishing Company, Inc., 1989.)

1.3 Physiological Effects of Exercise

At any given work load, chronic training is associated with lower HR. This is caused by reduced sympathetic plasma catecholamines and decreased muscle sympathetic nerve activity. In addition, exercise leads to resting bradycardia due to an alteration in autonomic control by either, an increase in vagal activity, a decrease in sympathetic activity or both. Exercise will also help to reduce resting blood pressure (BP) which may also involve reducing resting sympathetic activity. Some indications of reduced sympathetic output due to training could be seen with by decreased plasma catecholamines, catecholamine spillover and muscle sympathetic nerve activity [3].

Exercise not only has a strong correlation with a lower HR, it also has an effect on how quickly a person can recover after exercise. The rate of recovery, however, is dependent on the level of exertion [5]. It also is mediated by both reduction of sympathetic withdrawal and parasympathetic reactivation. As to which part of the ANS has a greater effect on the recovery, Pierpont has looked into the work of several investigators. One investigator postulated that the initial reaction toward the HR recovery is an initial drop in sympathetic tone which would then be followed by an increase in parasympathetic activity [4]. Other theories believe that there is a more rapid reaction of the parasympathetic activity. This explains why at shorter and lower levels of exercise the HR recovers more rapidly than from longer and higher levels of exercise since the sympathetic activity has not had as much of a chance to change [5].

The effects of exercise are not only seen if performed on a regular basis, but even a single bout of exercise introduces some changes up to 24 hours after the exercise bout [1]. Some benefits have been lower density of blood lipids, and increased insulin

sensitivity. Another interesting result after one bout of submaximal exercise is that the heart becomes more reactive to neurological inputs causing heart rate to change more rapidly.

1.4 Heart Rate Variability (HRV)

One of the ways the heart rate is regulated for humans and animals is by the parasympathetic and sympathetic branches of the ANS. The sympathetic branch will cause an increase in heart rate under stress while the parasympathetic branch will have an opposite effect once the stress is removed. These branches are linked to the heart at the Sinoatrial Node (SA node) where the beat is initiated for a normal heart [2, 6]. One approach for understanding the activity in both branches of the autonomic nervous system involves studying HRV [6].

The first important application of HRV was recognized in 1963 by Hon and Lee [7]. In their study, they noted that there was a change in the HRV before any substantial changes in the average heart rate. Hon and Lee analyzed the time between successive heart beats, known as the R-R interval or as the inter-beat-interval (IBI). The time where a heart beat occurs can be obtained from observing the maximum points of the QRS complex of the electrocardiogram (ECG) signal. Other researchers, as noted by Malik, [8] continued the development and expanded the application of HRV. In the 1980s it was confirmed that HRV was a strong predictor of mortality following an acute myocardial infarction [9]. It was at this point when the clinical importance of HRV was finally understood. Since then, there have been different methods of analyzing HRV. The first method applies time domain calculations and is mainly applied to analyzing large sample

sizes such as those obtained from 24 hour data. The second method uses frequency domain calculations and is employed to analyze shorter segments of data generally lasting for 5 minutes.

1.4.1 Physiological Correlates of HRV

The variations seen within each R-R interval represents the beat-to-beat control mechanism adjusting itself to the changing body. The vagal and sympathetic activities are constantly interacting, but under resting conditions the vagal tone would prevail and the HRV is largely due to vagal modulation [8]. The parasympathetic influences exceed sympathetic effects due to two independent mechanisms, the first being a cholinergically induced reduction of norepinephrine released in response to sympathetic activity, and the second being a cholinergic attenuation of the response to an adrenergic stimulus [8]. The sympathetic influence is generated by the release of epinephrine and norepinephrine. The β -adrenergic receptor activation will ultimately result in the acceleration of the diastolic depolarization thereby increasing the heart rate [8].

The HRV representations of sympathetic and vagal activities are derived with respect to the sinus node. Therefore, outside variations affect the HRV model. For instance there is a large influence caused by the central oscillators such as the respiratory and vasomotor centers. The peripheral oscillators, such as oscillation of arterial pressure, and respiratory sinus arrhythmia also help modulate the cardiac cycle. These oscillators will affect the heart period in both the long term and short term due to their rhythmic fluctuations in neural discharge [8]. For example, an increase in breath rate may cause a decrease in the HF even though vagal activity remains unchanged [12]. This can be

shown by observing the change in the energy in the HF band as the breathing frequency is varied.

1.4.2 Time Domain Methods of HRV

Some of the simple time domain measures which can be calculated are the mean R-R interval, mean heart rate, the difference between the longest and shortest R-R interval, etc. Other time domain measurements are statistical measures and come from either the R-R interval itself or from the difference between successive R-R intervals.

One of the simplest statistical time domain variables is the standard deviation of the R-R interval (SDNN). This variable reflects all the cyclical components responsible for variability in the period of recording. The ECG signals used must be the same length in time in order to compare results. The total variance of the signal changes with signals of different lengths.

Another statistical time domain measurement is the standard deviation of the average R-R interval (SDANN) [8]. This method breaks a 24 hour signal into 288 smaller 5 minute windows and calculates the mean for each window. This measure is used to calculate changes in heart rate due to signals with periods greater than 5 min.

The statistical measures which use the time difference between consecutive beats are commonly used to estimate high frequency variations in the heart rate. The first is the square root of the mean squared differences of successive R-R intervals (RMSSD). Another is the number in interval differences of successive R-R intervals greater than 50ms (NN50). Finally there is the proportion derived by dividing the NN50 by the total number of R-R intervals (pNN50) [8].

1.4.3 Frequency Domain Methods of HRV

Heart rate variability may be characterized by its frequency spectrum and has been shown to be a good representation of the activity of both the sympathetic and parasympathetic portions of the autonomic nervous system act [10]. The traditional method of performing HRV in the frequency domain applies a Fourier transform to the IIBI. The HRV frequency spectrum can be broken up into 3 sections: high, low, and very low frequency (HF, LF, and VLF, respectively) components. The HF component ranges from 0.15-0.4Hz and represents the parasympathetic activity. The LF ranges from 0.04-0.15Hz and represents a mixture of parasympathetic and sympathetic activity. Everything below the frequency range of 0.04 is known as the VLF [6, 8,11,12] and it is hypothesized that it may represent an assortment of factors such as thermoregulation fluctuation [11]. Since the known activity of the ANS lies within the LF and HF bands, the main concentration of the analysis involves these two frequency bands.

The measurements of LF and HF can be represented in absolute values of power or in normalized units. Normalized units represent the relative value of each power component in proportion to the total power minus the VLF.

$$NLF = \frac{LF}{LF + HF} \quad (1.1)$$

$$NHF = \frac{HF}{LF + HF} \quad (1.2)$$

The recording time of the signal should last at least 10 times the wavelength of the lowest frequency in the frequency range of interest, which will ensure the proper detection of the signal. Therefore, the minimum signal length to obtain the high frequency component should approximately be a 1 minute signal and a 2 minute signal is

needed to determine the LF component [8]. Typically a 5 minute signal is used to obtain optimal results as well as an easily obtainable standard for analyzing any signal. When comparing results, all the signals must be of the same length in order to be able to compare between two different signals. The total power contained in the frequency spectrum will be increased in signals of longer duration. However, the total power can be normalized to a signal of a fixed length.

Pharmacological experiments which block portions of the ANS have shown how the different branches affect the frequency bands. It was noted that parasympathetic activity is the main contributor to the HF band and the LF component represents a mixture of vagal and sympathetic activity [12, 10]. An increase in LF can be seen under several conditions such as mental stress, during moderate hypotension, physical activity, and occlusion of a coronary artery. An increase in HF can also be induced by controlled respirations, cold stimulation of the face and rotational stimuli. LF/HF ratio is considered by some investigators to mirror sympathetic/parasympathetic balance or to reflect sympathetic modulations [8]. It is important to remember that these components of HRV do not provide a level of autonomic tone but instead show the degree of autonomic variation.

CHAPTER 2

ENGINEERING BACKGROUND

2.1 Signal Acquisition

The first step to properly perform any HRV measurement is to accurately obtain IBI [6]. This is done by first acquiring an ECG signal which is digitized using a high enough sampling rate to accurately identify the QRS complex and to satisfy the sampling theorem[8,13]. An optimal sampling rate choice is between 250-500 Hz since the maximum frequency contained within an ECG signal is 100 Hz.

Next, an R-wave (or peak) detection program is used to calculate the time difference (in ms) between beats. A program was developed which has the added flexibility of manually correcting any falsely detected R-waves. This is accomplished by comparing the abnormalities contained within the IBI signal to the ECG. A more specific explanation of how this is performed is found in the Methods Chapter 3.

The reliability of the processed data is affected by events such as ectopic beats, arrhythmic events, and missing data. If the ECG contains data due to these phenomena, interpolation using preceding and successive beats can be used to fill in the sections containing blemished data. No interpolation was used in this study. If there were sections of data that contained any of the above mentioned events the whole data set was removed from the study.

In order to perform many of the HRV analyses including all of the frequency domain methods, it is important to use a signal with equally spaced samples. The IBI samples are not equally spaced but are indirectly related to time (since it is defined as the

time interval per beat sampled). To make it explicitly depend on time, a transformation is performed by interpolating points according to a desired sampling rate. This results in the interpolated inter-beat-interval (IIBI) signal. Generally the sampling rate chosen is the same as the one used during the ECG acquisition process. For some more complex methods of analysis and long data sets, it may be too time consuming to interpolate the data at such a high sampling frequency. It would be adequate to choose an interpolation frequency as low as 5 to 10 Hz since the highest frequency of interest is 0.4 Hz, in the resting state, and .7 Hz, in strenuous exercise.

Different methods of interpolation include cubic spline interpolation, linear interpolation and backward step function interpolation [6]. The backward step function interpolation method was used in this study since it is the simplest and still produced good results. The backward step function is done by taking the IBI values and multiplying it by the interpolation sampling rate divided by 1000ms.

$$numOfSamples = IBI(ms) \times \left(\frac{iSR(ms)}{1000(ms)} \right) \quad (2.1)$$

That number is then rounded to the nearest whole number. This will set the number of times to fill an array with the IBI value. The number of samples contained within the IIBI will then be in proportion to that of the ECG signal. For example, if the sampling rate of the ECG signal was twice that of the IIBI then the number of samples in the ECG signal will be twice that of the IIBI.

2.2 Power Spectral Analysis

The spectral analysis is based on the Fourier transform. The Fourier transform is a method used to determine the frequency content of a time domain signal. It is defined by the following equation:

$$X(f) = \int_{-\infty}^{\infty} x(t) \cdot e^{-2j\pi ft} dt \quad (2.2)$$

where t is time, f is frequency and $x(t)$ is the time domain signal and $X(f)$ is called the spectral density function and represents the magnitudes and phases of the frequency content of $x(t)$ [14,15]. The Fourier transform converts $x(t)$ from the time domain into the frequency domain in a similar manner as the Fourier series represents a decomposition of a periodic signal time sequence as an infinite series of sinusoids. (Note that $e^{-2j\pi ft}$ is the complex form of a sinusoid since $e^{-2j\pi ft} = \cos(2\pi ft) + j\sin(2\pi ft)$ using Euler's formula [15].) The difference between the Fourier transform and Fourier series is that the Fourier Transform can be applied to non periodic signals while the Fourier series is defined for periodic signals. Therefore, the Fourier transform can be viewed as a Fourier series of a periodic function whose period goes to infinity. Since the Fourier series relates the magnitudes and phases of a periodic signal at a specified frequency, called the spectrum, the Fourier transform becomes a spectral density which represents the contribution of any given frequency to the signal. The power density spectrum $S_{xx}(f)$ is defined as

$$S_{xx}(f) = X^*(f)X(f) = |X(f)|^2 \quad (2.3)$$

where $X(f)$ is the Fourier transform of the input signal $x(t)$ and the $X^*(f)$ is the complex conjugate of $X(f)$ [14].

The Fourier transform analysis assumes that the input signal $x(t)$ is a stationary signal. In general, signals from the ANS are non-stationary. However, for the purposes of this study the ANS will be assumed to be stationary only during paced breathing. This assumption is based on the fact that there are a limited number of influences affecting the ANS during rest. This method, however, is not acceptable during exercise and recovery. Methods needed for this type of analysis must be able to measure changes in frequency over time.

2.3 Short Time Fourier Transform

There are different methods that could be implemented to in order to observe changes in frequency over time. Two methods are the Short Time Fourier Transform (STFT) and the wavelet transform. The STFT method uses the Fourier transform to calculate the power but incorporates a windowing function, obtaining time localization according to the following equation.

$$STFT(\tau, f) = \int_{\tau-\Delta}^{\tau+\Delta} [x(t)\gamma^*(t-\tau)] e^{-j2\pi ft} dt \quad (2.4)$$

This equation defines the STFT as the Fourier transform, at time τ and frequency f , of the signal $x(t)$ multiplied by the complex conjugate of the shifted analysis window $\gamma^*(t-\tau)$ shifted by time τ [14,16]. The integration is over the interval of $\tau - \Delta$ to $\tau + \Delta$ where 2Δ is the window size. The STFT is performed for all time shifts and for all frequencies. From this, the power density spectrum as a function of τ and f is calculated using equation 2.5. The resulting 2-dimensional function is referred to as a spectrogram.

$$\rho(\tau, f) = |STFT(\tau, f)|^2 \quad (2.5)$$

The spectrogram represents a “localized” power for a specific frequency and time period. This localization is a result of eliminating the effects of the signal beyond the window size of 2Δ centered at τ . The result given from the STFT is greatly influenced by the length and shape of the window $\gamma^*(t)$ [16]. Choosing an appropriate window size is a key issue since this is what sets the time-frequency resolution. That is, the window should be small enough to assume that the signal is stationary and using a smaller portion of the signal results in greater time resolution. The drawback to this is that using a smaller sized window lowers the obtainable frequency resolution. Therefore the window size should be large enough to produce an acceptable frequency resolution. The filter size versus the time-frequency resolution is described by the Heisenberg Uncertainty Principle [14]. The uncertainty principle is defined as by the following equation:

$$\Delta t \Delta E \geq h/2\pi \quad (2.6)$$

where, Δt is the uncertainty in time, ΔE is the uncertainty in energy, and h is Planck’s constant [17,18]. It identifies the relationship of the time resolution to the frequency resolution and puts a limitation on the degree of obtainable time resolution by reducing the degree of obtainable frequency resolution and vice versa.

2.4 Wavelet Transform

The problem of obtaining good frequency and time resolution can not be avoided but the WT offers a unique solution. This function is similar to the STFT in that it is based on the Fourier transform and uses a windowing function. However, the windowing function

used has a unique approach in optimizing the time-frequency resolution. The window size is determined according to the frequency.

The WT is defined as follows:

$$WT(s, \tau) = \int_{-\infty}^{\infty} |s|^{-1/2} x(t) \psi^* \left(\frac{t - \tau}{s} \right) dt \quad (2.7)$$

Just as the STFT convolved the signal $x(t)$ with a window $\psi(t)$, this transform convolves the signal $x(t)$ with an analysis window $\psi^*(t)$. This window is also called the mother wavelet and just as the Fourier transform uses sines and cosines to break down the signal the WT uses this mother wavelet. Another difference between the WT and STFT is that in addition to the time shifting parameter, τ , there is a parameter, s , which is used to scale the size of the window. STFT uses a fixed window size. The signal is also multiplied by $|s|^{-1/2}$ in order to normalize the energy contained so that there will be uniform energy at every scale [14,19].

The scale is related to the frequency of the signal, and this relationship depends on the type of wavelet applied but, in general, scale is inversely proportional to frequency. This means that low scales represent high frequencies and high scale values represent low frequencies. Since the scale determines window size and the Uncertainty Principle still applies, better frequency resolution at the expense of time resolution is obtained for low frequencies. For higher frequencies the opposite is true, a better time resolution is obtained at the expense of frequency resolution [14].

The changing window throughout the process provides a unique time frequency resolution pictured in Figure 2.1. The box heights and widths change but the area of the box stays constant making each box represent an equal portion of time and frequency.

The STFT time and frequency resolutions are determined by a window of constant width making the time-frequency plane consist of equal sized squares.

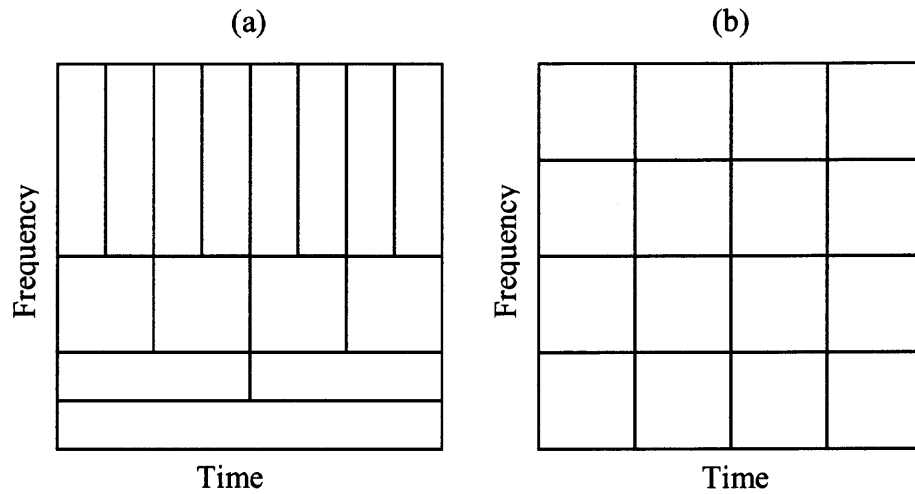


Figure 2.1 (a) Time-Frequency plane for WTs (b) Time-Frequency plane for STFT.

There are different types of mother wavelets that can be used for analyzing different signals. For example the use of the Morlet wavelet favors spectral accuracy whereas the Mexican Hat wavelet favors individual event localization [20]. In order to be a wavelet it must satisfy the following mathematical criteria. It must have finite energy [21]

$$E = \int_{-\infty}^{\infty} |\psi(t)|^2 dt < \infty \quad (2.8)$$

and the area contained within the wavelet is equal to zero [22]

$$\int \Psi(t) dt = 0 \quad (2.9)$$

The choice was made in using the Morlet wavelet in this thesis since it provides spectral accuracy as well as its use in other similar research [19, 21, 26].

The Morlet wavelet is defined as

$$\psi(t) = \frac{1}{\sqrt[4]{\pi}} \left(e^{i\omega_0 t} - e^{-\omega_0^2/2} \right) e^{-t^2/2} \quad (2.10)$$

where ω_0 is the central frequency of the mother wavelet. The $\frac{1}{\sqrt[4]{\pi}}$ term is the normalization factor that will give the wavelet unit energy. The first term in the brackets, $e^{i\omega_0 t}$ contains the complex sinusoidal waveform $\cos(\omega_0 t) + i \sin(\omega_0 t)$. The second term in the brackets $e^{-\omega_0^2/2}$ corrects for non-zero mean of the complex sinusoid of the first term, and is known as the correction term. The last term $e^{-t^2/2}$ is the Gaussian envelope which has unit standard deviation and confines both the real and imaginary part of the complex sinusoidal waveform [21].

CHAPTER 3

METHODS

3.1 Subjects

Both Test A and Test B had their own separate unique group of subjects. Test A's participants were patients at University of Medicine and Dentistry of New Jersey (UMDNJ) who signed an informed consent form. All 128 participants from UMDNJ involved in the study are of either sex, and at least 18 but less than 100 years of age. Participants who were permitted to participate were those who were not currently taking heart medications, did not have heart disease and were in good enough physical health to undergo an exercise test. Any person who had atrial fibrillation, a history of palpitations, a pacemaker or a defibrillator was excluded from the study. All participants in the study were patients that were requested to undergo a stress test by their physician.

In Test B, data was collected from one subject at New Jersey Institute of Technology (NJIT). He was a 24 year old of average health and fit all the above listed inclusion criteria except the requisition to undergo a stress test.

3.2 Experimental Design for Test A Patients

UMDNJ patients in Test A were instrumented with a 12 lead ECG configuration and then monitored with the Quinton QStress TM55. Lead II of the ECG was taken from the rear output of the stress test machine as an analog signal. It was digitized at 250 Hz and was saved on a laptop computer with the use of a National Instruments DAQCard-1200 and a program written in LabView 5.1. The preparation of the ECG electrodes included shaving

of the skin electrode site, lightly abrading, and cleaning the site with alcohol. The data collection was continuous lasting the entire time they spent in the stress test laboratory.

All data were collected between the hours of 9 am to 12 pm, which would limit the effects due to the circadian rhythm. The test was composed of three different sections, resting baseline, exercise and recovery. The resting baseline lasted for a period of 5 minutes, and involved the subject sitting relaxed in the UMDNJ's cardiology division stress test laboratory, breathing at a paced rate of 12 breaths per min or 0.2 Hz. In order to achieve the regulated breath rate the subject followed a series of moving lights that would move up when the subject should inhale and move down indicating that it is time for the subject to exhale. The participant was asked to follow the rhythm and not to take in deep breaths but to try to keep the volume of air in every breath consistent with normal breathing.

Once they completed 5 minutes of uninterrupted paced breathing the subject was asked to stand and walk onto the treadmill where they were explained the exercise portion of the test. This portion of the test followed the Bruce protocol for stress tests involving different stages of exertion. The protocol began at a slow walking pace of 1.7 mph on tread mill with 10% elevation. Every 3 minutes the tread mill increased in speed and elevation according to Table 3.1.

The advancement of stages continued until the subject reached 85% of their designated maximum heart rate, established by their sex, age, height, weight and current medications. The test may be stopped by the subject before he or she reached 85% of their maximum heart rate if they indicated that they could not continue due to shortness

of breath, chest pain, lightheadedness, discomfort or cramping. The physician may also stop the test if any serious abnormalities in the ECG or blood pressure were discovered.

Table 3.1 Stages of the Bruce Protocol

Stage	Time (min)	Velocity (mph)	Slope
1	0	1.70	10%
2	3	2.5	12%
3	6	3.4	14%
4	9	4.2	16%
5	12	5	18%
6	15	5.5	20%
7	18	6	22%
8	21	6.5	24%
9	24	7	26%
10	27	7.5	28%

(Source: <http://www.brianmac.demon.co.uk/bruce.htm> Nov. 11 2004)

3.3 Experimental Design for Test B

The second experiment, Test B, was performed in order to observe the changes in autonomic activity during recovery for a longer period of time. Test A only acquired the recovery data for a time period of 5 minutes. It was thought that this might not be long enough to determine the changes in the ANS since it was observed that the heart rate did not return to baseline levels after 5 minutes.

The single participant involved in Test B used a Polar S810i heart rate monitor to acquire beat to beat time recordings. The accuracy of heart rate measurements during steady state conditions acquired with this system was recorded at $\pm 1\%$ or ± 1 bpm whichever was longer [23]. The validity of the data acquired from a similar system was tested previously by other researchers for HRV analysis [24].

This person did not follow the same testing protocol as the UMDNJ participants. He sat outside in a park for 6 minutes resting, then ran for 8 minutes and finally sat down to recover for 30 minutes. He did not perform the paced breathing and did not run in incremental stages such as what is done in the Bruce protocol. Instead, during the initial resting period he breathed at his own self selected rate and he ran at his own pace. The subject was allowed to breathe at his self selected rate since this test was used to look at the changes in the ANS over a longer recovery period. In addition, during the recovery period the subject will breathe at his self selected rate and this will give a better indication whether or not their heart rate has fully recovered. Following the protocol performed in Test A was not needed since the data acquired from this person's data was used in order to view the changes in the ANS during the extended recovery period. However, the resting and exercise was still recorded and analyzed in order to make any comparisons if needed.

3.4 Data Processing

3.4.1 Peak Detection

The first step of processing the data acquired in Test A is to detect the occurrence of R-waves in the ECG, also referred to as peak detection. This was done in order to determine the time that a heart beat occurred and to compile an inter-beat-interval (IBI) signal. This process was not performed with the data acquired in Test B since its output was already in IBI format. The choice of using the R-wave in order to designate where a heart beat occurred was done since it is very distinct and its peak can easily be found. The program, written in LabView 7 Express, is outlined in Figure 5.1 and described in Appendix A.

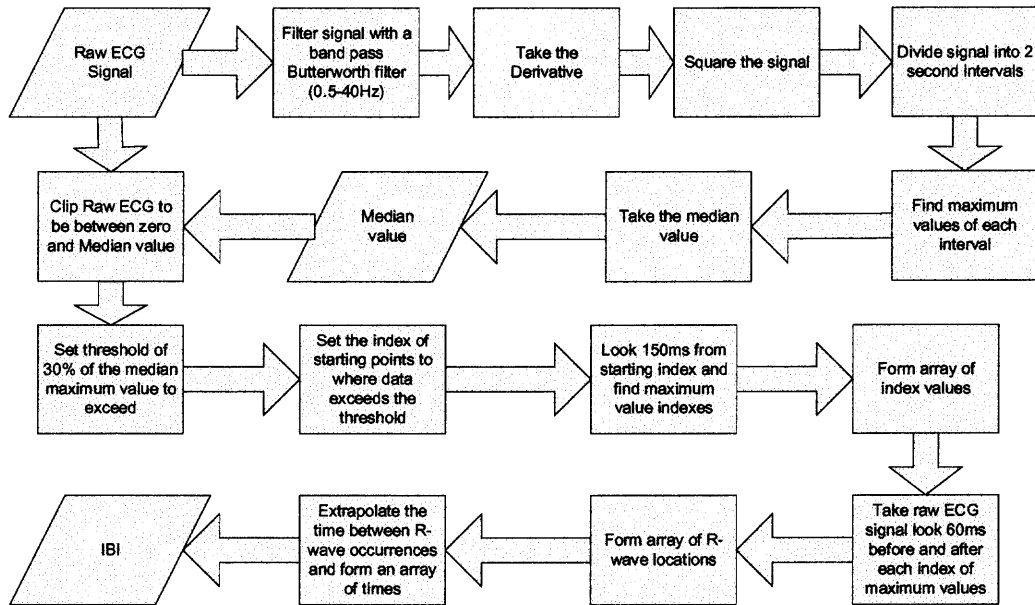


Figure 3.1 Diagram showing the process flow required to perform the peak detection.

Once this program was complete manual correction could be applied to correct any incorrectly detected beats so that any extra beats were removed and any missed beats were added. The changes in the IBI would then be edited according to where the additions and deletions were made. A simple method of locating miss detected beats was done by plotting the IBI and looking for spikes in the data. The indication of a miss detected beat or set of beats would be shown in the IBI plot as a spike pointing upward. Having a spike pointing downward would indicate that there was at least one extra R-wave found.

3.4.2 Test B Filtering

The data in Test B were acquired in IBI format; however the signal still needed to be filtered. The Polar system used to acquire the data missed some beats in the process. This

left sections in the data where the time between beats would be at least twice the mean of previous heart beats. In order to clean the data and make it usable, a filtering program, described in Figure 3.2, was written to split these long intervals. The program started with the fifth point in the data set and tested to see if it was 70% longer than the mean of the previous 4 points. If this was the case the point was tested to see how much longer than the mean it was and was divided into equal parts. For instance, if the current point was twice the mean of the previous 4 points then this point was divided into two equally valued points.

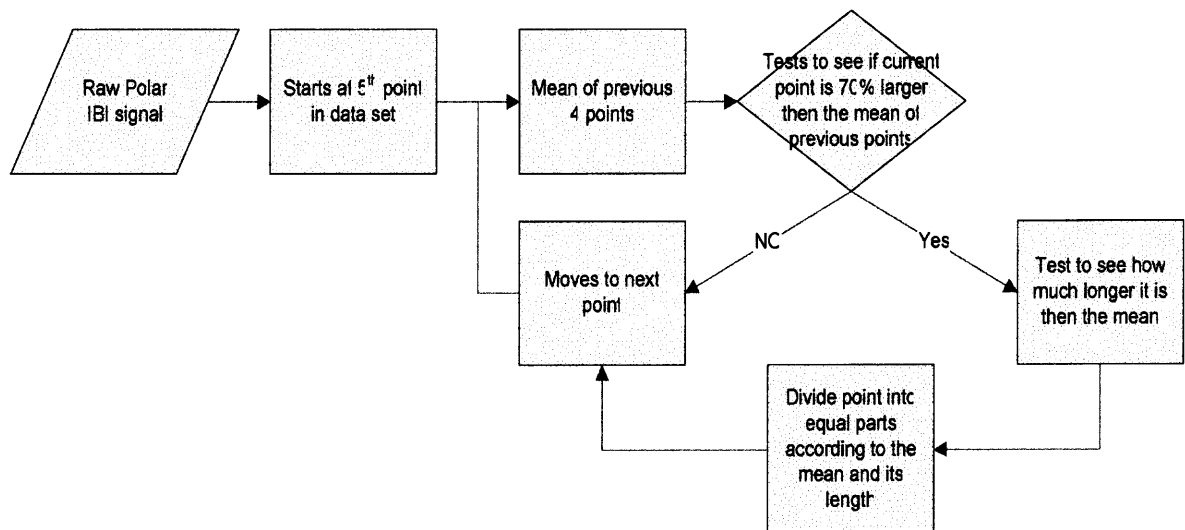


Figure 3.2 Diagram showing the process flow to filter the IBI acquired by the Polar heart rate monitor.

3.4.3 IIBI Creation

Once the IBI was formed it was converted into interpolated inter-beat-interval (IIBI) form which keeps the time occurrence between each data point evenly spaced. The formation of an IIBI is done by inserting data points of the same IBI value into the array depending on the value of the IBI sample and the interpolation sampling rate. The process of

forming an IIBI is illustrated in Figure 3.3 where Figure 3.3b represents the acquired IBI signal extrapolated from the ECG signal of Figure 3.3a by measuring the time between successive R-waves. Figure 3.3c then represents the IIBI formation with a 5 Hz interpolation sampling rate. The number of samples inserted into the IIBI array was chosen by the following equation:

$$\left(\frac{IBI(ms)}{1000ms} \right) \times samplingRate \quad (3.1)$$

The IIBI was then used with the frequency domain analysis as well as the curve fitting process. The interpolation was done at different frequencies depending on the method used. Programs such as the STFT and the WT used an interpolating frequency of 5 Hz. because the time needed to process the data was much greater than the time for a basic power spectrum. However, the power spectral analysis used an interpolating frequency of 250 Hz, equal to that of the ECG sampling frequency. It could have also used the 5 Hz sampling frequency but the available program to interpolate the signal was written to sample at 250 Hz.

When sampling the IIBI at 250 samples per second the resulting signal has data samples separated by the same time resolution as the ECG. However when the IIBI is sampled at 5 Hz there is a large difference in time resolution. The time separating the samples will be 0.2 seconds instead of 0.004 seconds, consequently causing time intervals 800ms and 875ms to be represented with the same number of samples. This will not affect the resulting frequency power output since the frequency range of interest is 0.04 Hz to 0.7 Hz where such small variations are not noticed.

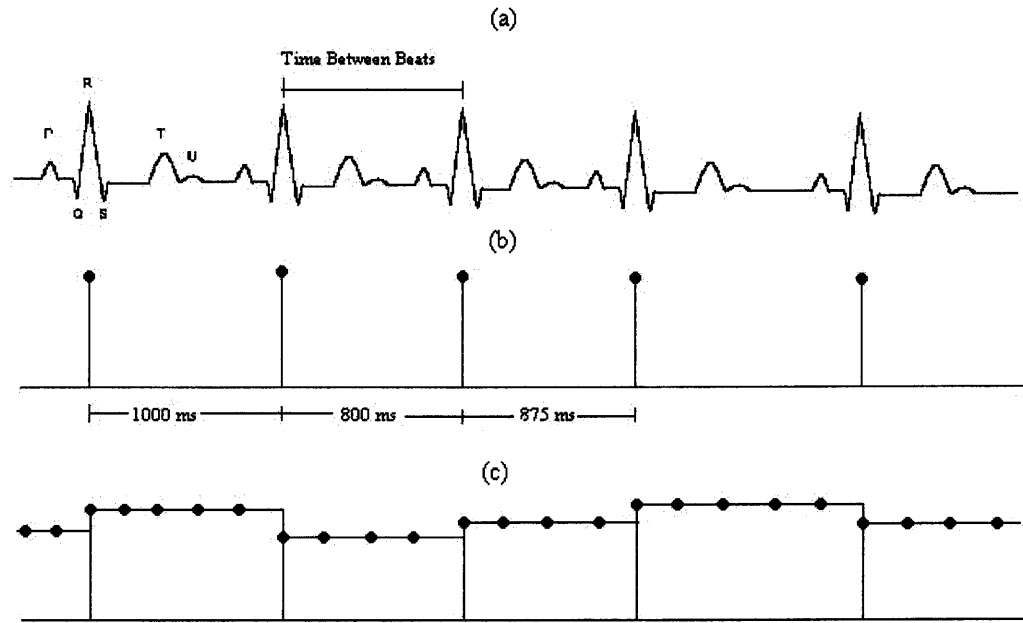


Figure 3.3 Creation of the IIBI signal interpolated at 5 Hz.

- (a) ECG signal
- (b) IBI
- (c) IIBI values interpolated at 5 Hz

3.4.4 Spectral Analysis

The paced breathing portion of the test was analyzed using power spectral analysis. The power spectrum $S_{xx}(f)$ is defined in chapter 2 is

$$S_{xx}(f) = X^*(f)X(f) = |X(f)|^2 \quad (3.2)$$

where $X(f)$ is the Fourier transform of the input signal $x(t)$, in this case it is the IIBI, and the $X^*(f)$ is the complex conjugate of $X(f)$. The power spectrum shows the power contained at each sampled frequency of a stationary signal. We assume that during the paced breathing, the body is not changing, therefore producing a stationary signal. This assumption is not ideal but there are no other alternatives. However, the use of this method is not suitable for the exercise and recovery portions of the test.

The spectral analysis was also programmed using the LabView programming language. This program loaded the IIBI that was interpolated at the same rate as the ECG collection and passed it through the FFT.vi to compute the Fourier transform. The algorithm of calculating the Fourier transform depended on the length of the IIBI. If the length was a power of 2 then it used the fast Fourier transform (FFT) if it was not, it used the discrete Fourier transform (DFT).

Once the power spectrum was calculated the next step was to quantify the energy contained within both the LF and HF portions of the signal. This was accomplished by dividing the power spectrum into frequency bands. The first division is from 0.04-0.15 Hz representing LF and 0.15-0.4 Hz representing the HF. The areas contained in these two frequency bands were calculated by summing the power spectrum array representing the LF and then the HF.

3.4.5 Short Time Fourier Transform

The STFT program was written in Matlab and it is closely related to the power spectrum program described previously. The main difference between the two programs is that the STFT produces changes in frequency over time by applying a small time window to the data and calculating the power spectral analysis to the data in the window. The window is then shifted and another spectral analysis was obtained until it has reached the end of the data set. This program was used during the exercise and recovery stage of the data set in order to show how the frequencies change with time.

This program uses an IIBI that was sampled at 5 Hz in order to speed up processing time. The first step was to set up the windowing properties. A window size of 30 seconds was used since it provided reasonable time-frequency resolution for the

lowest frequency of 0.04 Hz. Any window size could have been chosen, but when testing with a 0.04 Hz sine wave, the spread of the spike in the frequency spectrum that leaked into the other frequency bands could be tolerated more than with shorter window sizes. The next windowing property was how much of a time shift each window would have. The window could be shifted over several samples to reduce processing time by limiting the amount of overlap each window would have on the other window. Since the program's processing time was not reduced that significantly with a shift of several samples as opposed to just one, the window was shifted by one sample.

Once the windowing properties were established the next step was to form a matrix containing all the windowed data. The first window was applied to the first 30 seconds of data. Then the mean was removed from that window and the result was multiplied by a Hanning window. The Hanning window was applied in order to reduce leakage or spreading of energy when taking a Fourier transform of a signal that was not periodic. [25] The windowed section was then contained within its own column of the matrix.

The power spectrum of the matrix was calculated using equation 3.2 by taking the FFT of the window matrix. Then the power spectrum was calculated by multiplying each column of the matrix by its complex conjugate.

The next step was to calculate how the LF and HF power changed through time. However, the frequencies that comprise the HF band were changed. The power spectrum used the range of 0.15-0.4 Hz where the STFT used 0.15-0.7 Hz. This change was incorporated due to the different breathing frequencies during exercise and recovery from exercise. Since breathing frequency may exceed the .4 hz breath rate during exercise and

recovery, a higher frequency range was needed to obtain all the energy due to a higher breathing frequency. The power spectral analysis used a known breathing frequency of 0.2 Hz and therefore, the standard frequency range of 0.15-0.4 Hz could be used.

The LF power was calculated for every time shift by taking the sum of the values between the sample numbers representing 0.04 and 0.15 Hz. The same was done to calculate HF except it used the region between 0.15 and 0.7 Hz.

In order to present the LF and HF data in different formats, the LF and HF values were also normalized using the following equations.

$$NLF = \frac{LF}{LF + HF} \quad (3.3)$$

$$NHF = \frac{HF}{LF + HF} \quad (3.4)$$

where NLF and NHF are the normalized values of LF and HF, respectively and they represent a percentage of energy associated with each frequency band. Viewing the normalized data makes it easier to see how the power changes with respect to each other. The program plotted a series of 2D graphs of the original signal, LF, HF, NLF and NHF. Then it would show a 3D representation of the data by plotting the power spectrum in two formats, mesh and contour. This was done to give a better view of what the data was doing. An example representing the output for one subject in Test A is shown in Figure 3.4.

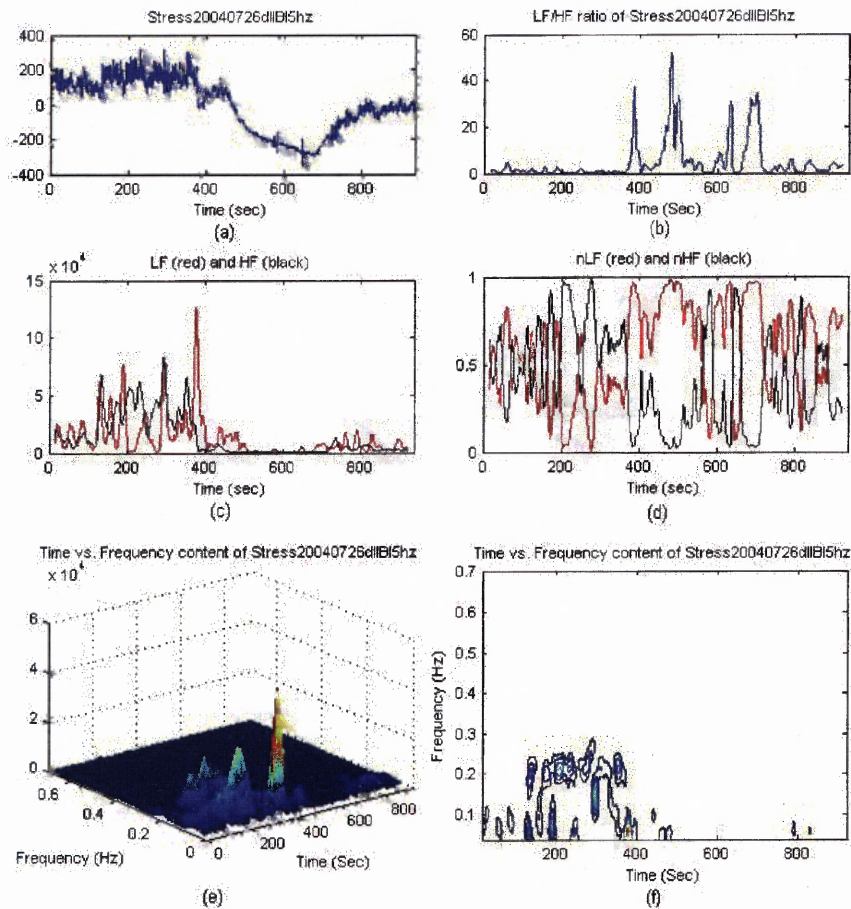


Figure 3.4 STFT output results for the entire experiment for one UMDNJ patient.

- (a) IIBI with the mean removed.
- (b) LF/HF ratio.
- (c) Absolute values of the LF and HF.
- (d) LF and HF in normalized unit.
- (e) 3D representations of the frequency data as a mesh.
- (f) 3D representations of the frequency data contour plot.

3.4.6 Wavelet Transform

The wavelet transform program, written in Matlab 6.5, is also able to represent how frequencies change with time. This program was used in order to have a secondary method of analysis to ensure the results obtained were accurate. It analyzed the same IIBI signals sampled at 5 Hz and also had its mean removed. The frequency ranges for the LF and HF of 0.04-0.15 Hz and 0.15-0.7 Hz, respectively were also unchanged. The function

used to transform the data was the CWT function, which is part of the Matlab wavelet toolbox that performs a continuous wavelet transform. The mother wavelet applied was the Morlet wavelet. This was done since other papers have used this for analyzing HRV. [26, 27, 28] Once the wavelet coefficients were calculated, they were converted from scale to frequency using the following equation.

$$F_a = \frac{F_c}{a \times \Delta} \quad (3.5)$$

Where F_a is the frequency, in Hz, corresponding to scale a , F_c is the center frequency of the wavelet in Hz, and Δ is the sampling period [29].

After processing the data, large edge effects appeared at the beginning and the end of the signal so padding was added. The padding added to the start of the signal was 1 minute worth of the first data value in the signal. The same padding process was performed to the end of the signal but it used last data value of the signal.

The IIBI as well as the LF, HF and the ratio LF/HF were plotted in order to see how they changed with time. Contour plots of both the wavelet coefficients and their converted values into frequency were also plotted. An example representing the output for the same subject as the one in the STFT section is shown in Figure 3.5.

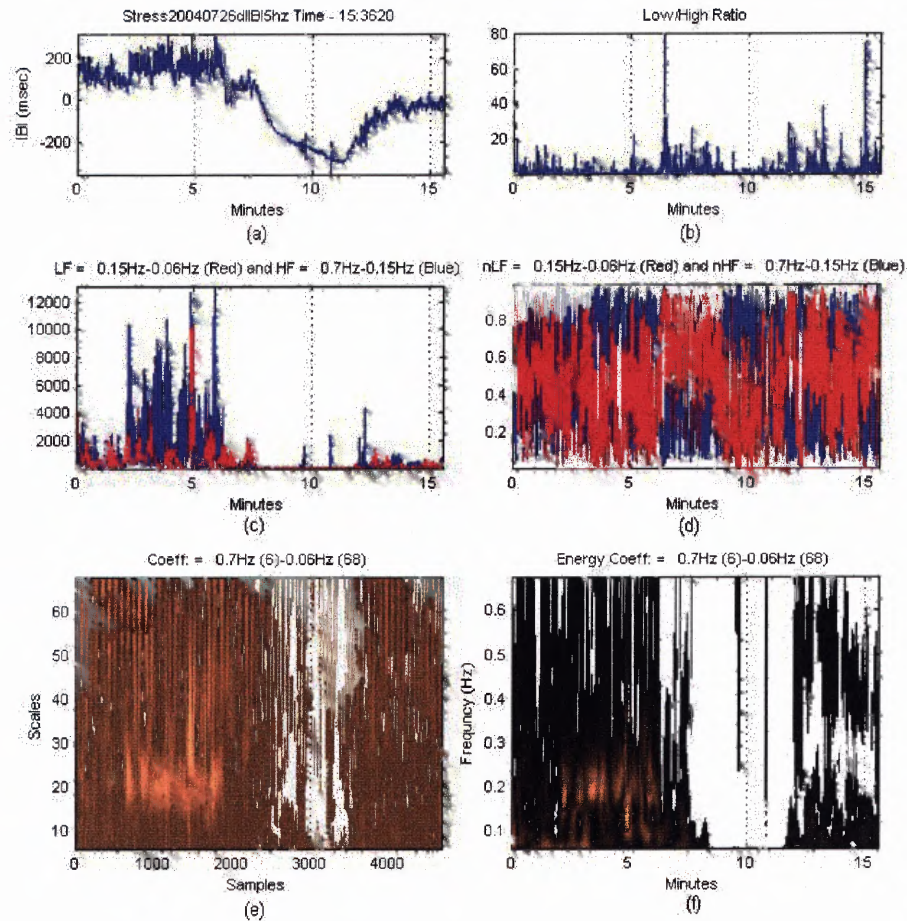


Figure 3.5 WT output results for the entire experiment for one UMDNJ patient.

- (a) IIBI with the mean removed.
- (b) LF/HF ratio.
- (c) Absolute values of the LF and HF.
- (d) LF and HF in normalized units.
- (e) 3D representations of the frequency data as a mesh.
- (f) 3D representations of the frequency data contour plot.

3.4.7 Curve Fitting

A curve fitting program was written in order to model the rate of recovery and obtain its time constant as an indication of the rate of recovery. The program used the Levenberg-Marquardt algorithm to determine the set of coefficients for the recovery model. The model we used was an exponential equation defined as

$$1 - Ae^{Bt} + C \quad (3.6)$$

where the exponent B is the inverse of the time constant of the exponential function.

The curve fitting program, written in LabView, uses the IIBI that was interpolated at 5 Hz. Once the IIBI was loaded the values were normalized so that the minimum value was equal to zero and the maximum value was one. This was done by subtracting the minimum value from every point in the data set. Then the maximum value was divided from every point in the data.

This data was then input into the LabView curve fitting function as well as an array representing the time component of each sample. The curve fitting function was set up to fit the a curve according to equation 3.5 and an initial guess for the values A, B, and C were set as 20, -1, and 0, respectively. These numbers were chosen to set the initial shape of the curve since the program uses these numbers as a starting point for the algorithm. The program then outputs the best fit curve, its coefficients, residuals and the mean square error of the fitted curve.

3.5 Statistical Analysis

Since the results were assessed using qualitative assessment, limited statistical analysis was necessary. Statistical analysis was used to examine the relationship between the HF during the paced breathing portion obtained from Test A and the exponent B obtained during the corresponding estimated recovery curve. This was done by forming a scatter plot of the HF value versus the exponent B. Then a regression line was obtained from this plot also producing a correlation coefficient which gives an indication of how well these two variables correlate with each other. This indication will be represented as a number

ranging from 0 to 1, where 0 indicates there is no correlation and 1 indicates a perfect correlation.

A correlation coefficient was also obtained for all the estimated recovery curves. This would denote the accuracy of the how well the estimated curve fit the recovery data. This was not used to exclude any of the curves from the analysis but just as a reference.

CHAPTER 4

RESULTS AND DISCUSSION

This section presents the results and discussion for all the methods performed using both Test A and Test B data sets. The first method discussed is the regression of HF values and recovery time constant. This method used only the data obtained from Test A in order to form a correlation between the HRV indicator of parasympathetic activity (i.e. HF) and the time of recovery (i.e. recovery time constant). The data obtained from Test B was omitted from this analysis method since it did not follow the same exercise protocol and used a different method of acquiring data. The results of both the STFT and the wavelet transform techniques will be presented next. These methods used the data from both Test A and Test B in order to visualize the changes in ANS over time.

4.1 Results from Regression of HF and Recovery Data From Test A

Of the 128 subject data collected from Test A, 20 met the requirements to properly analyze the data. It was important to obtain data that met the requirements so that the HF obtained from the paced breathing, and the exponential fit from the recovery phase would be reliable. The excluded data was disqualified due to the following reasons:

1. The presence of one or more ectopic beats or arrhythmic events where the heart beat was not initiated by the SA node. However, if these irregular beats occurred at the start or end of the paced breathing section some of the data could be salvaged through truncation if the section of unaffected data is at least three minutes in duration.
2. Inability of the subject to adhere to the proper paced breathing rate of 12 breaths per minute which was indicated by a spike in the spectrum at 0.2Hz, as shown in Figure 4.1.

3. Inability to detect one or more R-waves due to noise contained in the data or sections of data being lost due to equipment malfunction. In similar fashion to reason one, if an undetectable R-wave occurred at the start or end of the data, the data could then be used if at least three minutes of uncorrupted data could be salvaged.

Once all the raw data was converted into IIBI format, a frequency spectrum was obtained for the paced breathing section of the data shown in Figure 4.1. The HF area in the band (0.15 – 0.4 Hz) was calculated. This data is presented in the second column of Table 4.1.

The next step was to obtain the best fitting exponential curve for the recovery portion of the IIBI. Figure 4.2 represents an example of the calculated recovery curve (in red) plotted against the raw IIBI (in blue). The program that calculated the best fit curve also produced an equation for this curve in the following format:

$$1 - Ae^{Bt} + C \quad (4.1)$$

where the exponent B was used as an indication of how quickly the heart rate recovered. This is presented in the third column of Table 4.1. In order to obtain a quantitative estimate of the goodness of fit, a correlation coefficient was calculated using the following formula

$$R^2 = 1 - \frac{SS_{reg}}{SS_{tot}} \quad (4.2)$$

where R^2 is the correlation coefficient, SS_{reg} is the sum of squares of the residuals, and the SS_{tot} is the sum of squares of the difference between the data points and the mean value.

This is presented in the fourth column of Table 4.1.

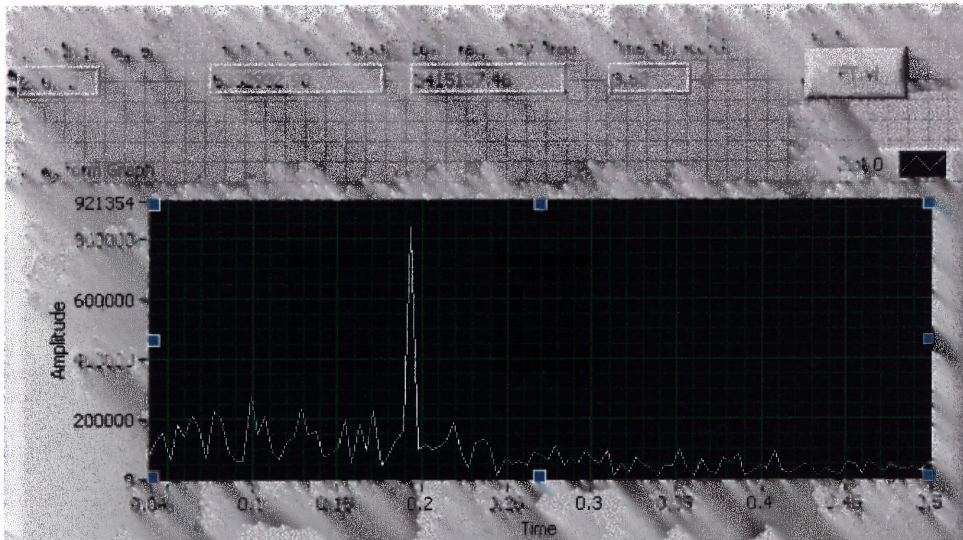


Figure 4.1 Frequency spectrum for the paced breathing section of the IIBI for one of the UMDNJ patients.

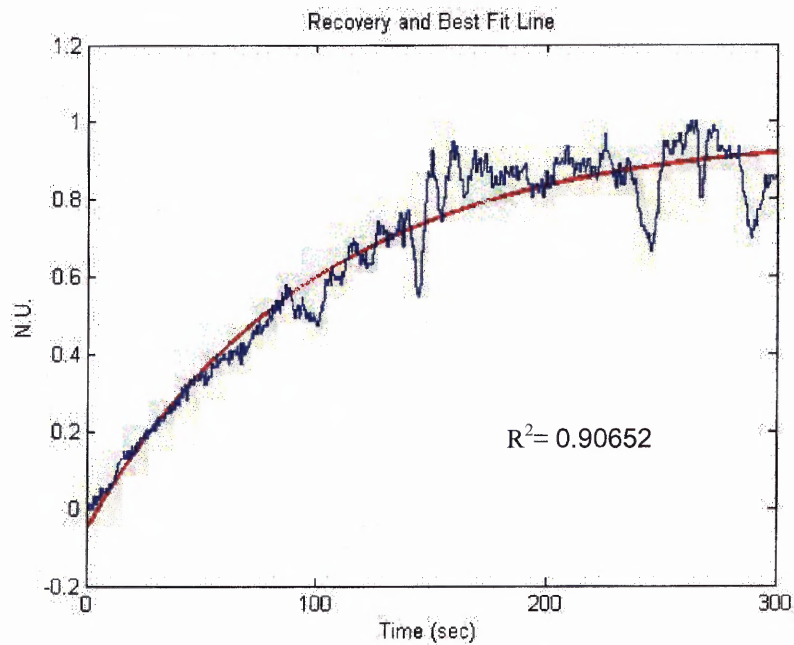


Figure 4.2 Output of the curve fitting program plotting the IIBI (blue) and the best fitting exponential curve (red).

Table 4.1 Data Used for the Regression Analysis

PATIENT	HF	EXPONENT	GOODNESS OF FIT
1	7756577.70	-0.035029	0.86216
2	1691655.36	-0.013790	0.94405
3	3465384.34	-0.019411	0.76123
4	4225154.31	-0.015947	0.87599
5	1773006.89	-0.010911	0.63372
6	4250668.56	-0.016881	0.91042
7	1391535.79	-0.008273	0.98179
8	3524441.34	-0.014016	0.85013
9	5854292.53	-0.009403	0.74911
10	5332932.90	-0.015928	0.90652
11	5458687.23	-0.009699	0.95567
12	3366225.32	-0.008686	0.95262
13	7372798.31	-0.022919	0.86701
14	14530238.55	-0.030719	0.42381
15	1380178.49	-0.005610	0.94884
16	5860812.73	-0.016403	0.85542
17	3219474.72	-0.018422	0.86753
18	3919086.49	-0.018976	0.94407
19	2590910.48	-0.010249	0.94041
20	5935655.89	-0.027966	0.83524

After obtaining the HF component from the power spectrum and the exponent from the regression curve, they were plotted against each other as represented in Figure 4.3. A regression line was then obtained in order to determine the correlation between the HF from paced breathing and the exponent B from the recovery, which is plotted in Figure 4.3 as a solid black line.

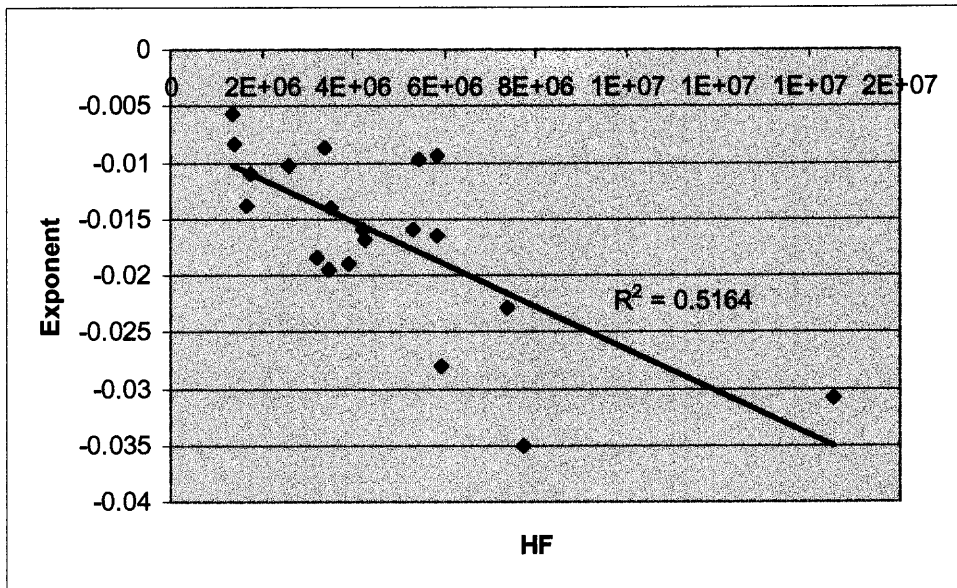


Figure 4.3 Plot of the HF vs. the exponent.

4.2 Discussion of Regression of HF and Recovery Data From Test A

As a person's fitness level increases, the amount of activity contained within the HF is expected to increase while in a resting state. Fitness level of a person is also expected to affect the rate of recovery for the heart. The more fit an individual is the more rapid the recovery. However, the correlation coefficient of Figure 4.3 ($R^2=0.5164$) indicates that there is a moderate relationship between the HF and the rate of recovery. This could be partially due to a substantial variance in HRV for healthy individuals [32] or a small sample size. A larger sample size may have helped reduced the effects of the variance in HRV, since some of subjects may or may not have been healthy. Some of the unhealthy subjects may have had their HRV spectrum more affected by their health than their recovery time or vice versa. A similar situation was observed in a study observing mean heart rate and HRV power spectrum on patients with ventricular tachyarrhythmia (VTA). These investigators observed changes in the mean heart rate as well as changes in the

HRV power spectrum. Patients taking antiarrhythmic (AA) drugs indicated an increase in heart rate as well as a decrease in HRV before VTA. Patient that were not taking AA medication showed no difference in mean heart rate while there was a significant decrease in HRV [30].

During the analysis process, a problem was discovered with the software that calculates the frequency spectrum. The problem occurred when analyzing two identical signals with only one difference. The difference in the signal is the time duration. The output produced a greater power output for the shorter signal then the longer signal. Since this program was used to process the paced breathing data, the problem was not obvious because the duration of most signals was five minutes. The instance of a data set that had a duration different then five minutes came about if there was a section of the data where an R-wave could not be detected or the occurrence of an ectopic beat. Only the segment of data containing a continuous signal with all R-waves that were properly detected was used.

After inspecting the program, the problem found dealt with the normalization of the data. The LabView block, which computes the power spectrum, normalized the data according to the number of samples contained within the data set. In addition there was another normalization function added which normalized the data to represent power contained in an equivalent five minute signal. Therefore a data set that was shorter then five minutes would have proportionally more power added to it and if the signal was longer then the power was decreased proportionally. This problem and its resolution are described in more detail in Appendix B. Once the problem was resolved all of the data was reprocessed producing the results presented in Table 4.1 and Figure 4.3.

4.3 Expected Results for Time Frequency Methods

The absolute values of the LF and HF are expected to oscillate at a constant level during paced breathing, where one may dominate more than the other. If there is one frequency band that dominates, then it should remain proportionally higher for the entire paced breathing period. During the exercise stage we would expect to see these values change in one of the following ways:

1. An increase in LF with a decrease in HF
2. An increase in LF while the HF stays constant
3. A decrease in HF while the LF stays constant
4. A decrease in both LF and HF but a larger decrease in the HF

During the recovery stage these values are expected to revert back to baseline values according to any of these four methods:

1. A decrease in the LF and an increase in the HF
2. A decrease in the LF while the HF stays constant
3. An increase in the HF while the LF stays constant
4. An increase in both the LF and HF but a larger increase in the HF

The LF and HF, when presented in normalized units, are expected to oscillate at a constant level where the LF or the HF could dominate during the paced breathing phase. The domination of one branch is an indication of having either sympathetic or parasympathetic domination. During the exercise portion, the normalized LF should increase at the start of exercise and continue to increase when compared to the paced breathing values. The normalized HF should do the opposite, with a corresponding decrease in the normalized HF. When the subject starts the recovery stage, there should

be an immediate jump within the normalized HF and a corresponding drop within the normalized LF. As recovery continues these values should revert back to the baseline values. Since the normalized HF and LF are normalized to each other, when one increases then the other will have a corresponding decrease. This will leave one possible result representing all three theories describing how the absolute values of the HF and LF are expected to change during recovery.

The LF/HF ratio, during the paced breathing section, should indicate little difference between the HF and LF with values close to 1. Once the person stands and starts to exercise there should be an increase of the ratio and it should stay elevated for the duration of exercise. Once the subject finishes exercising and is seated there should then be a drop in this ratio with values close to zero and well below 1.

4.4 Results of Time Frequency Analysis for Test A

The acquired IIBI data were also analyzed using the previously mentioned STFT and WT programs. These results both show how the ANS change throughout the experiment. Due to noise contained mainly during the exercise portion of the data 5 more data sets were eliminated from this analysis. The results for all remaining 15 data sets from both programs are shown in Appendix H. This chapter presents one of the files, shown in Figure 4.4 and Figure 4.5 representing the output from the STFT analysis and the wavelet analysis, respectively. This file represents all of the most common features contained within the other data files. Due to the similarity between the outputs of the STFT and the WT they will be explained in parallel.

Figure 4.4a and Figure 4.5a, show the same IIBI for one subject. From this plot it is clear that the resting, exercise and recovery stages are easily distinguished from one

another. The resting stage is indicated by a plateau in the graph, the exercise stage by the following negative slope, and the recovery by a final positive slope. Another instance that can be seen is the assumed point in which the person stood after performing the seated paced breathing. This instance is indicated by a momentary dip in the IIBI after the paced breathing but before the exercise stage and is noticeable in 12 out of the 15 data sets.

The subsequent graphs, Figure 4.4b and Figure 4.5b, show the LF/HF ratio for the same subject. These plots exhibit little difference between the LF and HF values during the paced breathing since the values are small and close to 1 which can be more easily seen in Figure 4.6e and Figure 4.7e. However, once the subject stands up and walks onto the treadmill there is a significant increase in the ratio followed by an immediate drop. This occurrence was noticed in all 12 of the STFT and Wavelet data sets that contained a noticeable point where the person stood. This occurrence was also noticed when exercise started in 13 of the STFT data sets and 14 of the WT data sets. Again during the start of the recovery a similar event was noticed in 12 of the STFT data sets and 11 of the WT data sets.

Figure 4.4c and Figure 4.5c represents the absolute values of the LF and HF where both analysis methods also produced results consistent with one another. Although the results produced by the STFT were smoother and more evident than the WT the same conclusion can be made from both analysis methods. This graph indicates first an equal mixture of LF and HF during rest, a subsequent significant drop in the amplitude of these two values during exercise, then finally, an approach to baseline values once the subject has stopped exercising and is seated. This sequence consistently occurred among all

participants. This graph also indicates that 5 minutes of rest is not enough time to bring these values back to the baseline level.

Figure 4.4d and Figure 4.5d represent the LF and HF in normalized units. It shows the LF and HF as a percentage of their activation. It is difficult to see what is happening with the normalized LF and HF values; therefore they have been expanded into different sections represented in Figure 4.6 through Figure 4.13, which will be discussed in detail later.

Figure 4.4e and Figure 4.4f both show how the frequencies change with time over the entire testing session; however, they are illustrated differently. The mesh plot of Figure 4.4e illustrates the data in 3D where the X, Y and Z axis correspond to time, frequency, and amplitude. This plot has a clearer view of the change in amplitudes of each frequency component contained in the signal. The contour plot of Figure 4.4f illustrates the data in a 2D format where the X and Y axis correspond to time and frequency respectively and the change in amplitude is indicated by the change in color. This plot better reveals which frequencies become active throughout the testing session. The large activation of the 0.2 Hz component indicating the paced breathing rate of the subject is more noticeable in the contour plot.

Figure 4.5e and Figure 4.5f also show how the frequencies change with time in a similar fashion as Figure 4.4e. These graphs are both contour plots in which Figure 4.5e represents how the scales change with time and Figure 4.5f represents how the converted frequencies change with time.

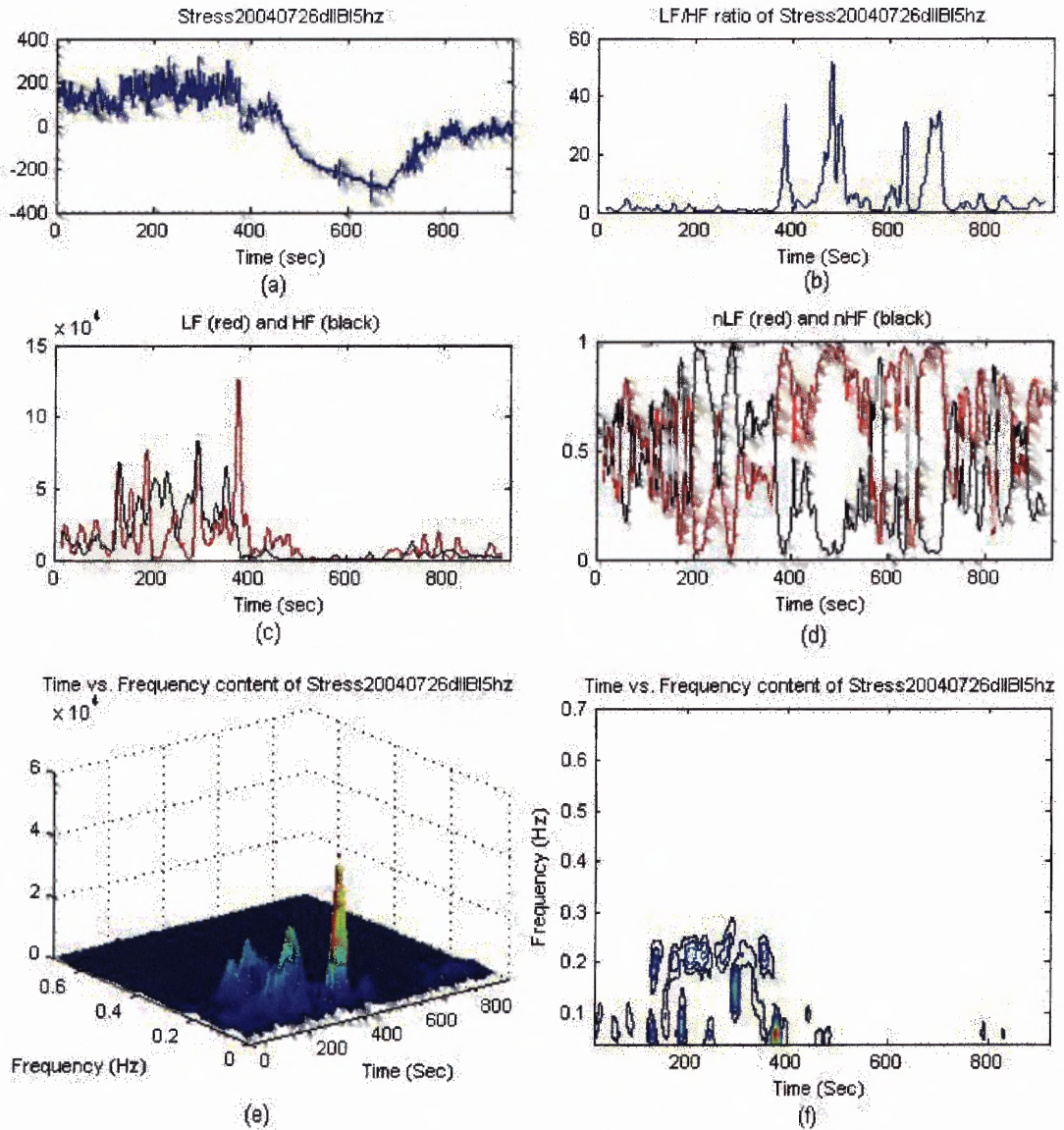


Figure 4.4 STFT output results for the entire experiment for one UMDNJ patient.

- (a) IIBI with the mean removed.
- (b) LF/HF ratio.
- (c) Absolute values of the LF and HF.
- (d) LF and HF in normalized unit.
- (e) 3D representations of the frequency data as a mesh.
- (f) 3D representations of the frequency data contour plot.

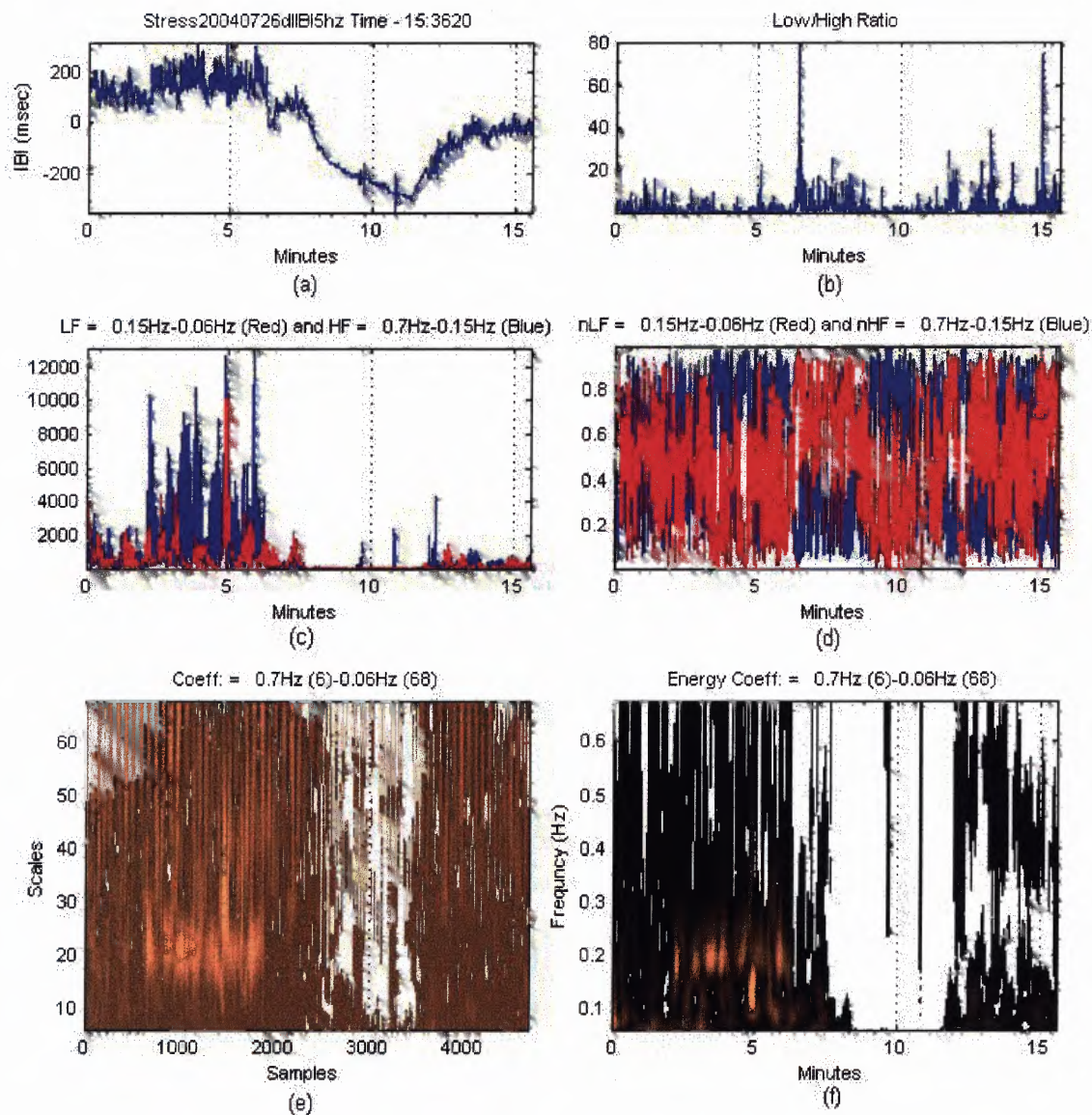


Figure 4.5 WT output results for the entire experiment for one UMDNJ patient.

- (a) IIBI with the mean removed.
- (b) LF/HF ratio.
- (c) Absolute values of the LF and HF.
- (d) LF and HF in normalized units.
- (e) 3D representations of the frequency data as a mesh.
- (f) 3D representations of the frequency data contour plot.

The STFT output for the paced breathing portion of the data can be seen below in Figure 4.6 and the portion from the WT in Figure 4.7. The entire IIBI data collected is plotted in Figure 4.6a and Figure 4.7a. The current area of interest, highlighted in red, represents the paced breathing portion of the testing session. This section is expanded in Figure 4.6b and Figure 4.7b, with the subsequent plots corresponding to the same time line, in order to give a clearer view of how the data behaves. The paced breathing IIBI is level with apparent variations caused by the effects of the ANS and respiration. The results shown in Figure 4.6c through Figure 4.6e and Figure 4.7c through 4.7e exhibit an even mixture of LF and HF since they oscillated closely about the 0.5 level. However, this is not consistent for all subjects; some consistently have a dominating LF or HF and may oscillate slightly higher or lower than the 0.5 level. Even though these values will oscillate they will do so about a constant level, which shows the activation of both branches of the ANS stay at a relatively constant level. The output from the STFT indicated that two subjects had an elevated LF and one had an elevated HF while the WT indicated only one person with an elevated LF and 5 had an elevated HF.

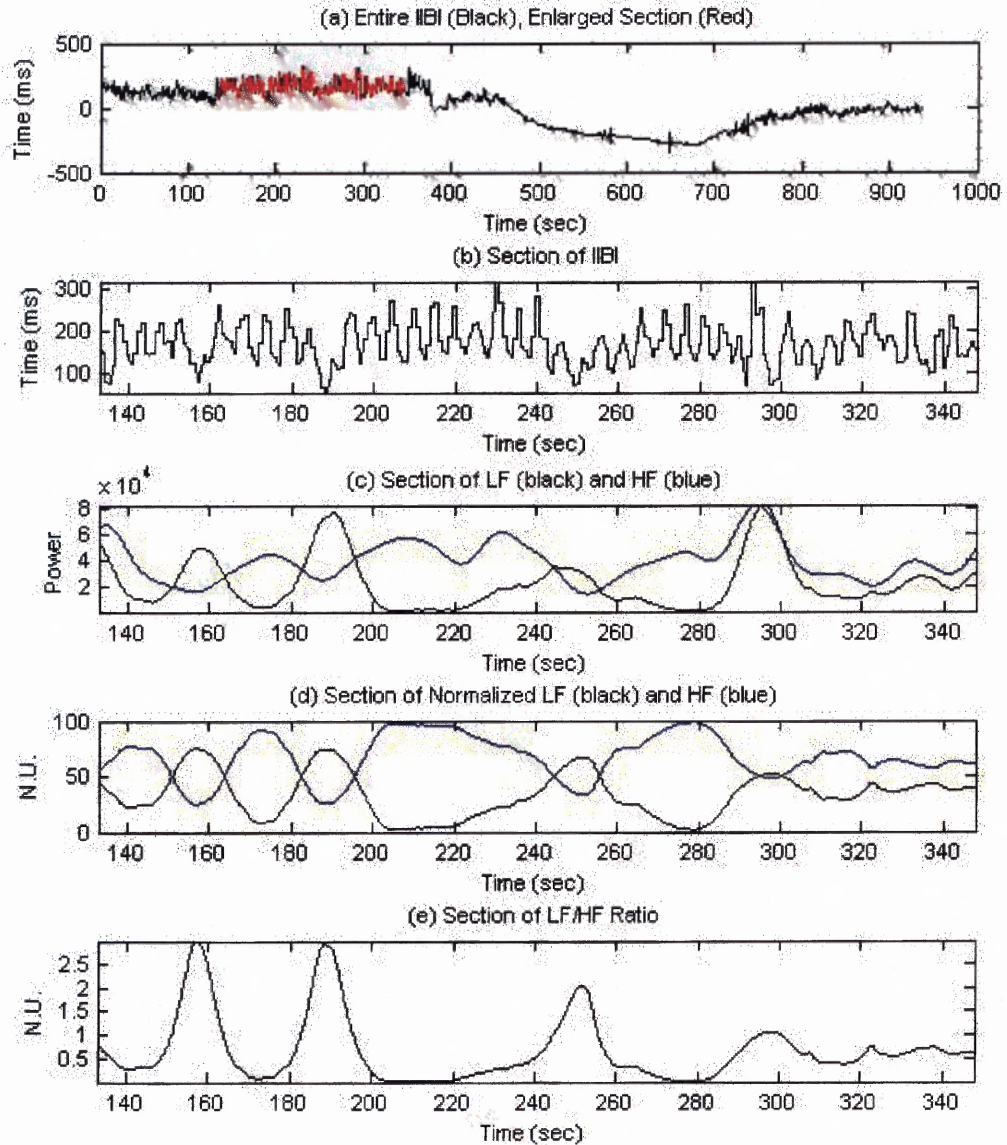


Figure 4.6 STFT output for the paced breathing portion of the experiment.

- (a) IIBI of the entire collection period (black), paced breathing IIBI section (red).
- (b) Expanded view of the paced breathing IIBI.
- (c) Expanded view of the absolute LF (black) and HF (blue) values.
- (d) LF (black) and HF (blue) in normalized units.
- (e) LF/HF ratio.

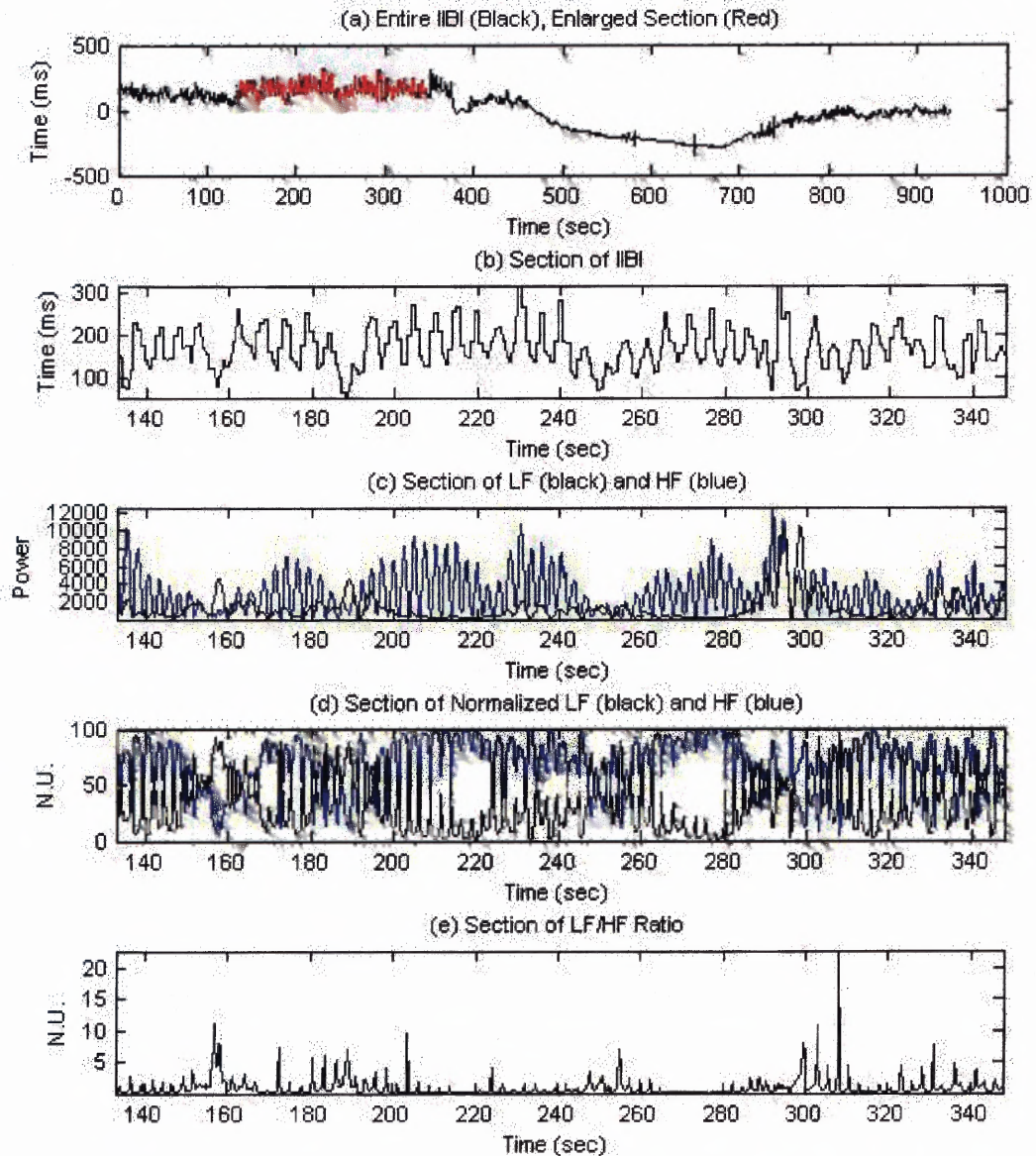


Figure 4.7 WT output for the paced breathing portion of the experiment.
 (a) IIBI of the entire collection period (black), paced breathing IIBI section (red).
 (b) Expanded view of the paced breathing IIBI.
 (c) Expanded view of the absolute LF (black) and HF (blue) values.
 (d) LF (black) and HF (blue) in normalized units.
 (e) LF/HF ratio.

Figure 4.8a and Figure 4.9a show the portion of the IIBI highlighted in red, assumed to be the point at which the subject stood up. There is a relationship between the rapid drop of the IIBI (Figure 4.8b and Figure 4.9b) and the spike in the LF/HF ratio (Figure 4.8e and Figure 4.9e). This immediate drop in IIBI following paced breathing consistently appeared in each subject's data. This drop correlates with the point where the subject would stand just prior to the start of exercise. The extent of the drop and its rebound would be variable, and is hypothesized to be dependent on the subject's muscle activity [31]. This hypothesis was made from a study that compared lying-to-standing data to tilt test data. The individuals in this study went from a lying position to a standing position in four different ways. Two of the methods involved active standing and the other two passive tilting. The four methods are described in detail below:

1. Manually go from a lying position to a standing position as fast as they could.
2. Manually go from a lying position to a standing position in a manner that would take 10 to 15 seconds.
3. Tilt table brought the person from a lying position to an 80° head up position in 2-3 seconds
4. Tilt table brought the person from a lying position to an 80° head up position in 12 seconds.

There was a difference in the drop and rebound of the heart activity between the active standing data and the passive tilting data. The data showed a more significant drop in inter-beat-interval during active standing than during passive tilting. The explanation for this is thought to be related to the involvement of muscle activity during active standing.

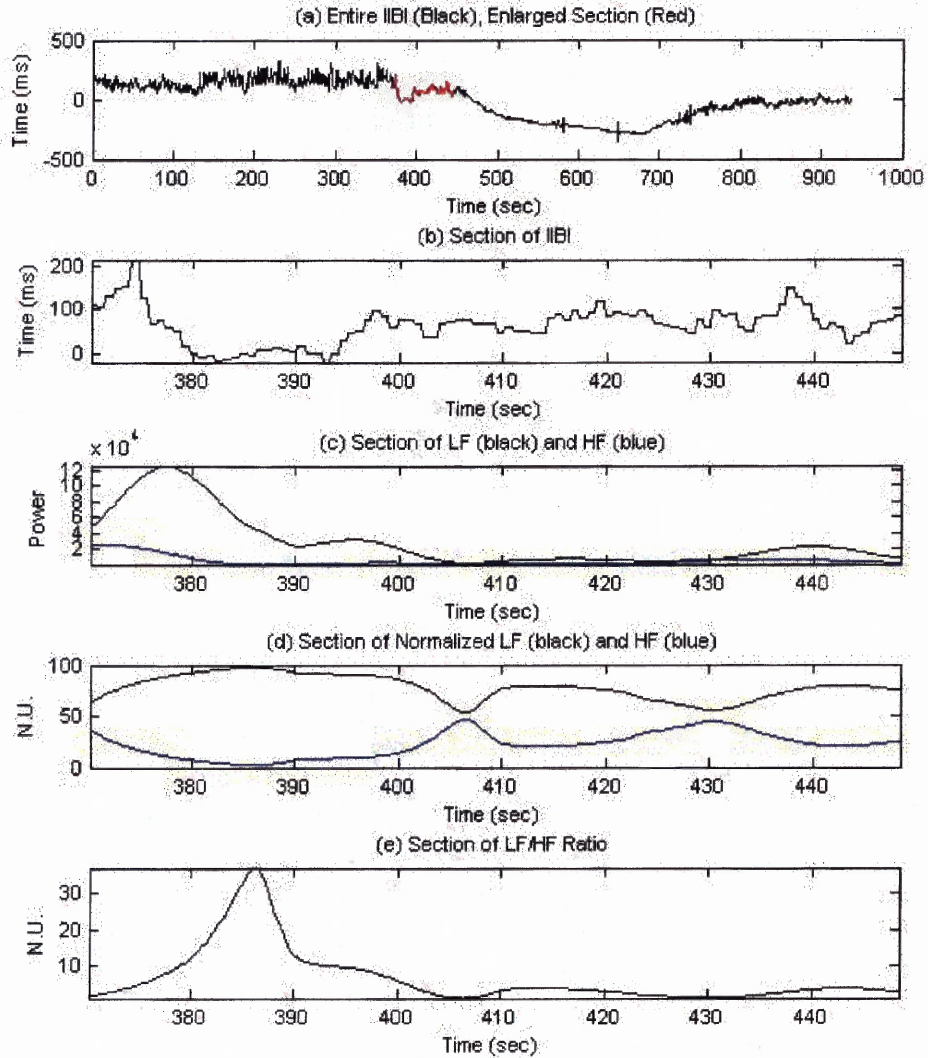


Figure 4.8 STFT output for the time period the patient was in the process of standing.
 (a) IIBI of the entire collection period (black), standing section of the IIBI (red).
 (b) Expanded view of the standing section IIBI.
 (c) Expanded view of the absolute LF (black) and HF (blue) values.
 (d) LF (black) and HF (blue) in normalized units.
 (e) LF/HF ratio.

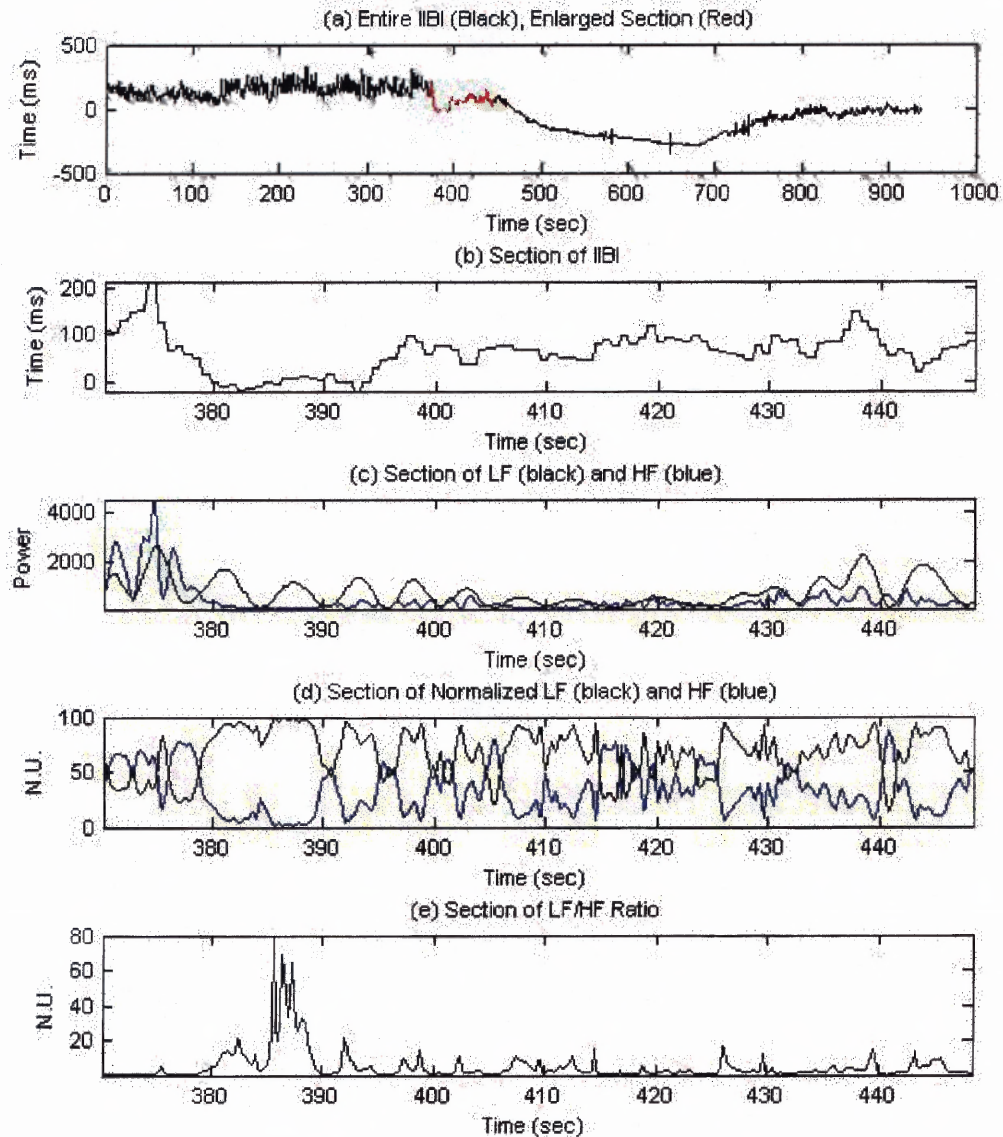


Figure 4.9 WT output for the time period the patient was in the process of standing.
 (a) IIBI of the entire collection period (black), standing section of the IIBI (red).
 (b) Expanded view of the standing section IIBI.
 (c) Expanded view of the absolute LF (black) and HF (blue) values.
 (d) LF (black) and HF (blue) in normalized units.
 (e) LF/HF ratio.

Figure 4.10 and Figure 4.11 represent the exercise portion of the experiment, which took place immediately after the subject stood up. Figure 4.10c through Figure 4.10e and Figure 4.11c through Figure 4.11e show the LF as the dominant frequency range at the start of exercise, where it increases until it peaks, then slowly drops until it equalizes with the HF. This demonstrates that the sympathetic activity has increased resulting in the increase of the heart rate.

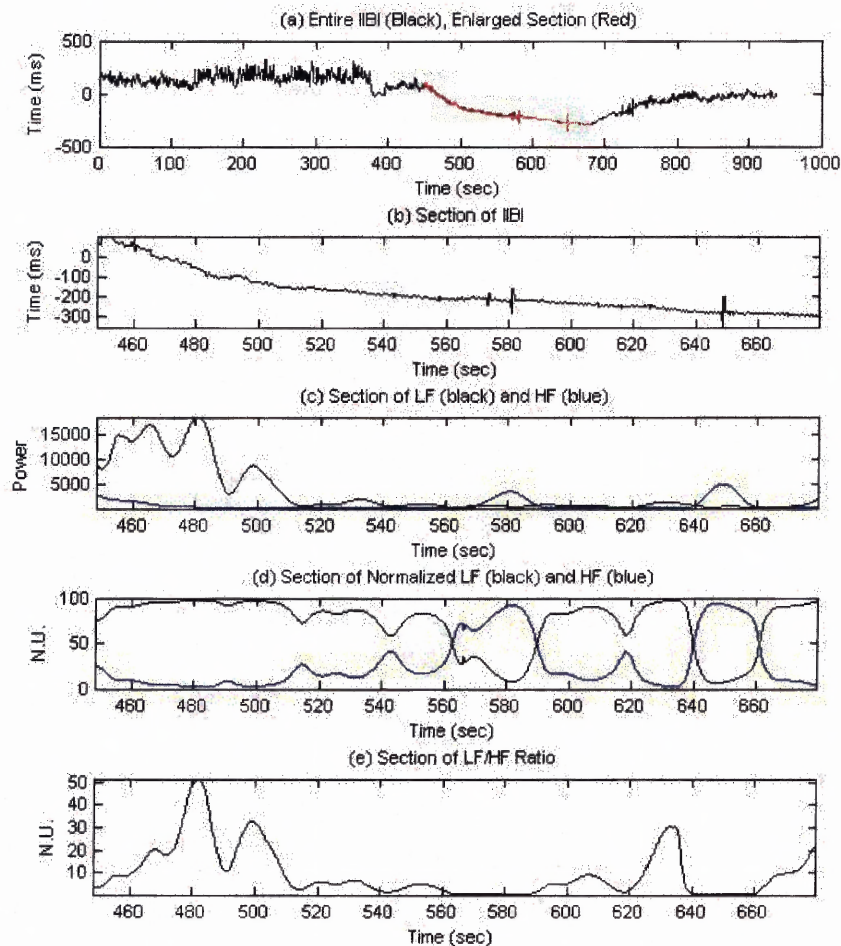


Figure 4.10 STFT output for the exercise portion of the experiment.

- (a) IBI of the entire collection period (black), exercise IBI section (red).
- (b) Expanded view of the exercise IBI.
- (c) Expanded view of the absolute LF (black) and HF (blue) values.
- (d) LF (black) and HF (blue) in normalized units.
- (e) LF/HF ratio.

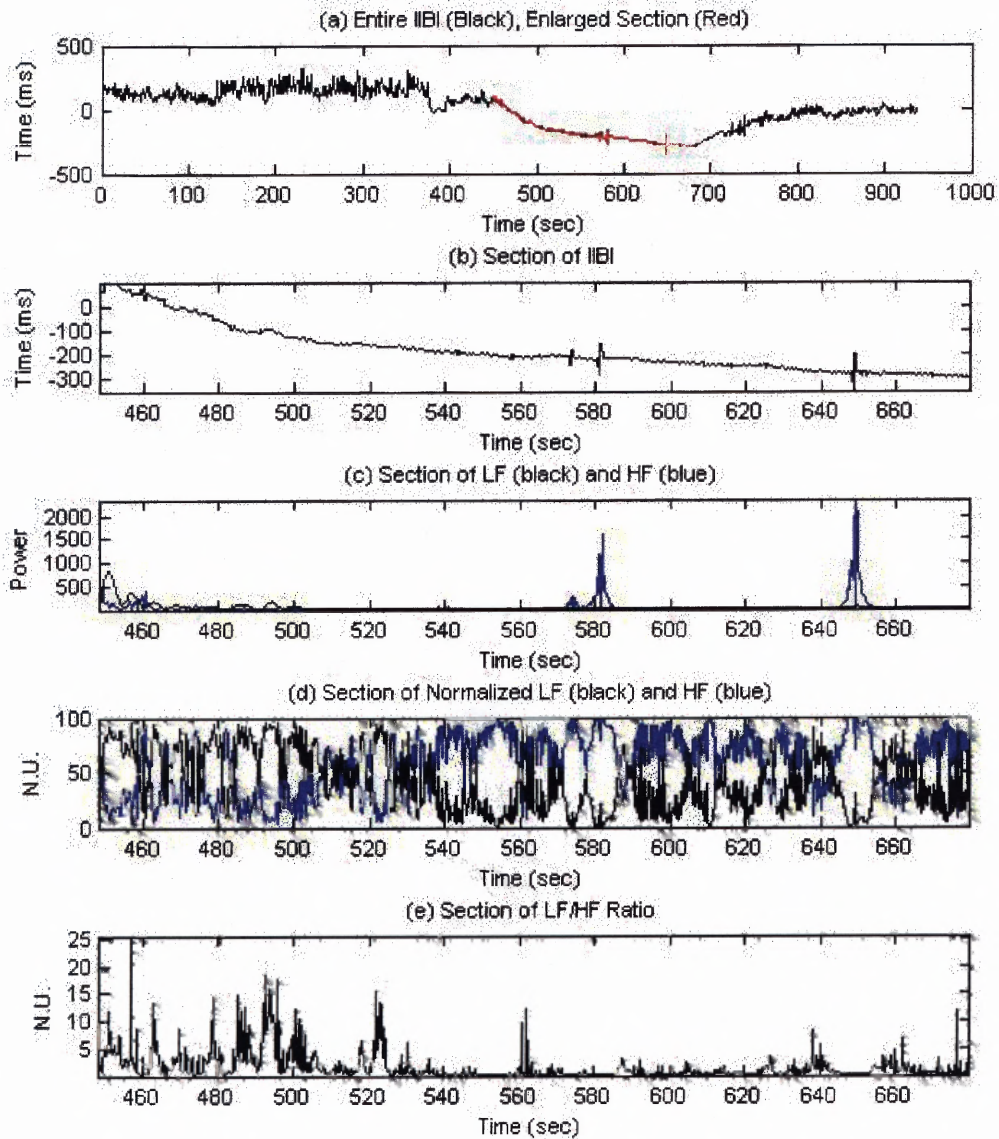


Figure 4.11 WT output for the exercise portion of the experiment.
 (a) IIBI of the entire collection period (black), exercise IIBI section (red).
 (b) Expanded view of the exercise IIBI.
 (c) Expanded view of the absolute LF (black) and HF (blue) values.
 (d) LF (black) and HF (blue) in normalized units.
 (e) LF/HF ratio.

The recovery portion presented in Figure 4.12 and Figure 4.13 surprisingly has similar characteristics to that of the exercise portion. Figure 4.12c through Figure 4.12e show the LF as the dominant frequency range at the start of recovery, where it also increases until it peaks, followed by rapid attenuation until it equalizes with the HF. This is most apparent in the LF/HF ratio where there was a spike at the start of recovery in 12 and 11 of the of the STFT and WT plots, respectively. Another important feature noticed is that the LF starts its recovery before the HF does. This indicates an initially large sympathetic activity with the parasympathetic activity inhibited which should prevent the heart rate recovery and is contrary to what was expected.

There are a few possibilities to explain this result. There could be an effect of a change in respiration where the person automatically reduced their breathing frequency initially to be contained within the LF range. There may also be an effect of the sympathetic system going out of saturation as it transitions from exercise to recovery. Another theory is that having an increased parasympathetic activity may saturate the HRV response [12,32,33]. A more detailed explanation will be discussed later.

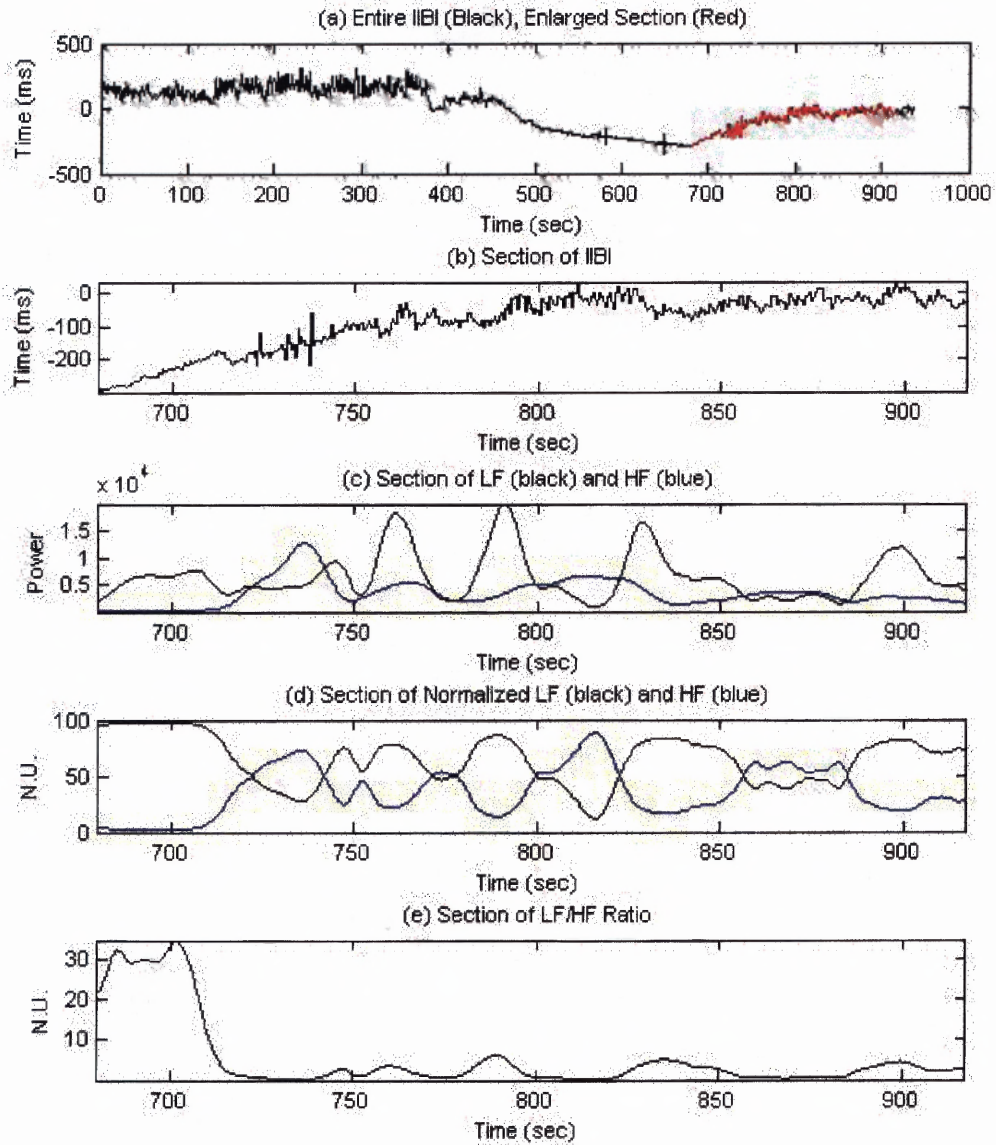


Figure 4.12 STFT output for the recovery portion of the experiment. (a) IIBI of the entire collection period (black), recovery IIBI section (red). (b) Expanded view of the recovery IIBI. (c) Expanded view of the absolute LF (black) and HF (blue) values. (d) LF (black) and HF (blue) in normalized units. (e) LF/HF ratio.

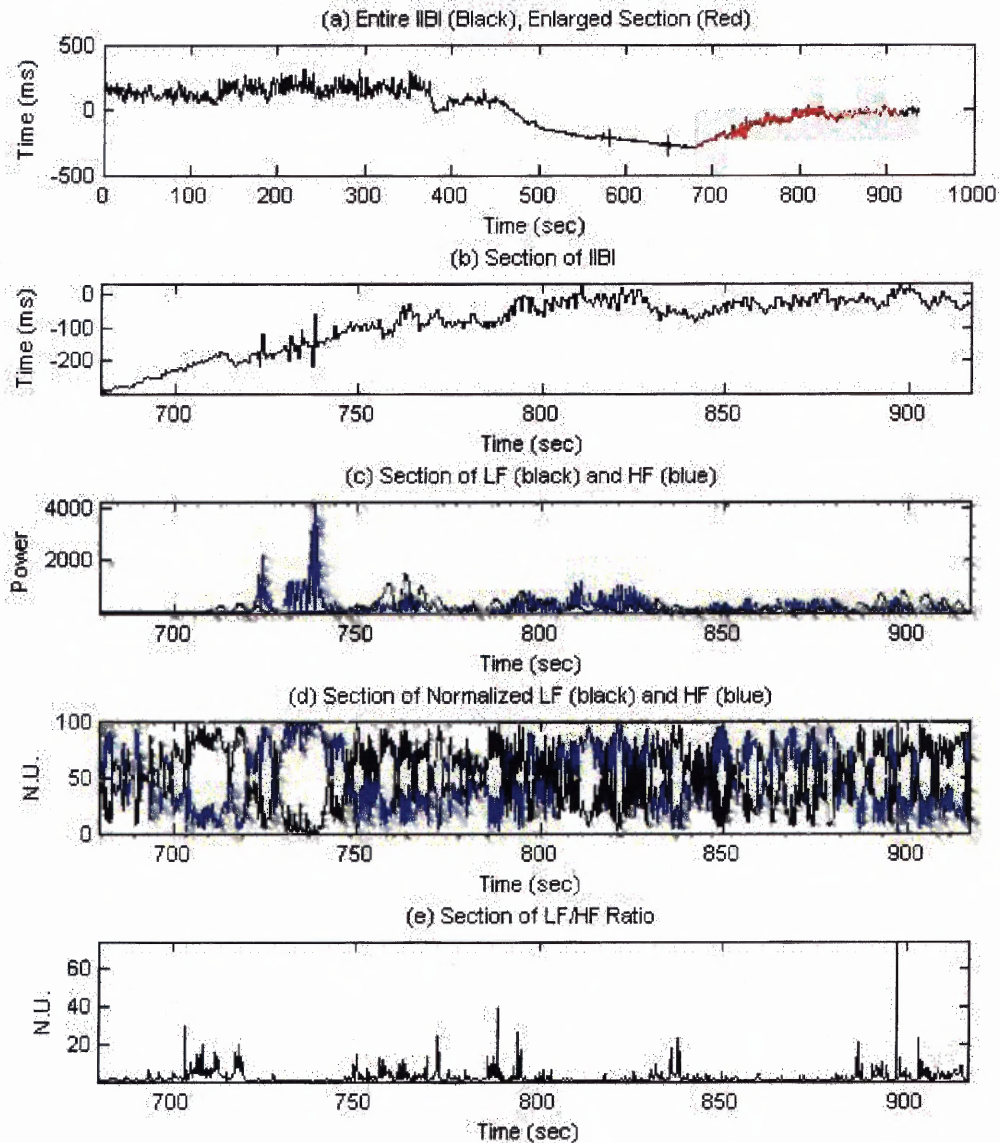


Figure 4.13 WT output for the recovery portion of the experiment.
 (a) IBI of the entire collection period (black), recovery IBI section (red).
 (b) Expanded view of the recovery IBI.
 (c) Expanded view of the absolute LF (black) and HF (blue) values.
 (d) LF (black) and HF (blue) in normalized units.
 (e) LF/HF ratio.

4.5 Results for Test B

Figure 4.14 represents the output for the single participant of Test B with an extended recovery period. This person rested for close to 6 minutes, then started to run for about 8 minutes and then sat down quietly during his recovery for 30 minutes. The important difference between this experiment and Test A is the extended recovery period. This would allow us to view the changes occurring throughout the entire recovery period. The acquired IIBI data was analyzed using both the STFT and WT programs, and the result of this analysis is shown in Figure 4.14 and Figure 4.15, respectively. Since these outputs are also similar they will be presented in parallel, in a similar manner to section 4.2.

Figure 4.14a and Figure 4.15a, show the same acquired IIBI for the subject. From this plot it is discernable that the resting, exercise and recovery stages are easily distinguished from one another. The resting stage is indicated by a plateau in the graph, the exercise stage by the following negative slope, and the recovery by a final positive slope.

The subsequent graphs, Figure 4.14b and Figure 4.15b, show the LF/HF ratio for the same subject. These plots exhibit little difference between the LF and HF values during the baseline resting period of Test B similar to the paced breathing phase of Test A. However, once the subject started exercising there was a significant drop in this ratio. Once the subject finished exercising and was seated the increase in this ratio was far greater than what was observed during resting but as time passed it slowly started to resume resting values.

Figure 4.14c and Figure 4.15c represents the absolute values of the LF and HF. This graph indicates first an equal mixture of LF and HF during rest, a subsequent

significant drop in the amplitude of these two variables during exercise, then finally, an approach to baseline values once the subject has stopped exercising and is seated. This graph also indicates that even 30 minutes of rest is not enough time to bring these values back to baseline level.

Figure 4.14d and Figure 4.15d represents the LF and HF in normalized units. They show the LF and HF as a percentage of their activation. It is difficult to see what exactly is happening with the normalized LF and HF values, therefore they have been expanded into different sections represented in Figure 4.16 through Figure 4.21, which will be discussed in detail later.

Figure 4.14e and Figure 4.14f both show how the frequencies change with time over the entire testing session; however, they are illustrated differently. The mesh plot of Figure 4.14e has a clearer view of the change in amplitudes of each frequency component contained in the signal, while the contour plot of Figure 4.14f better reveals which frequencies become active throughout the testing session.

Figure 4.15e and Figure 4.15f also show how the frequencies change with time in a similar fashion as Figure 4.14e. These graphs are both contour plots in which Figure 4.15e represents how the scales change with time and Figure 4.15f represents how the converted frequencies change with time.

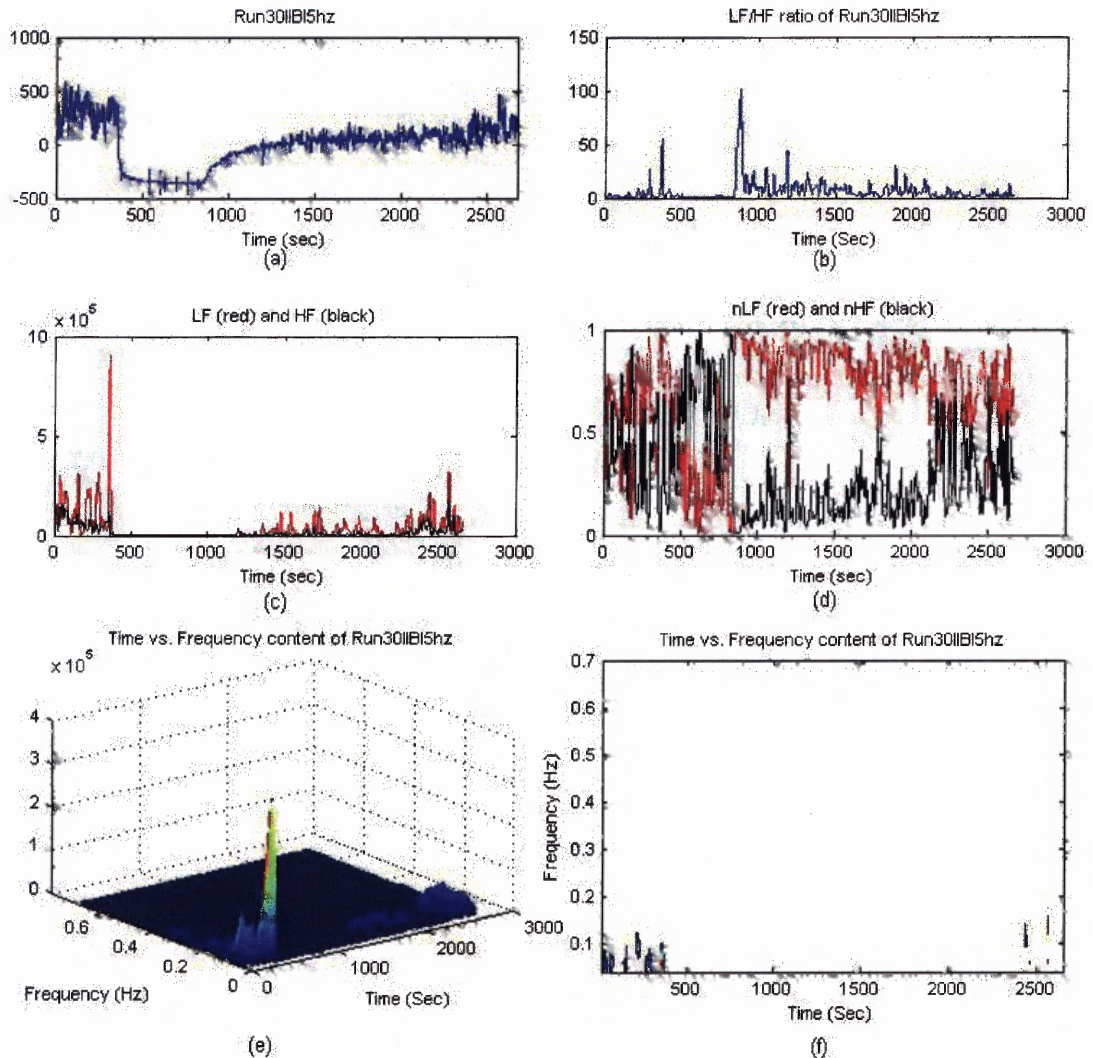


Figure 4.14 Output from the STFT program running a file with an extended 30 minute recovery period.

- (a) IIBI with the mean removed.
- (b) LF/HF ratio .
- (c) Absolute values of the LF and HF.
- (d) LF and HF in normalized units.
- (e) 3D representations of the frequency data as a mesh.
- (f) 3D representations of the frequency data contour plot.

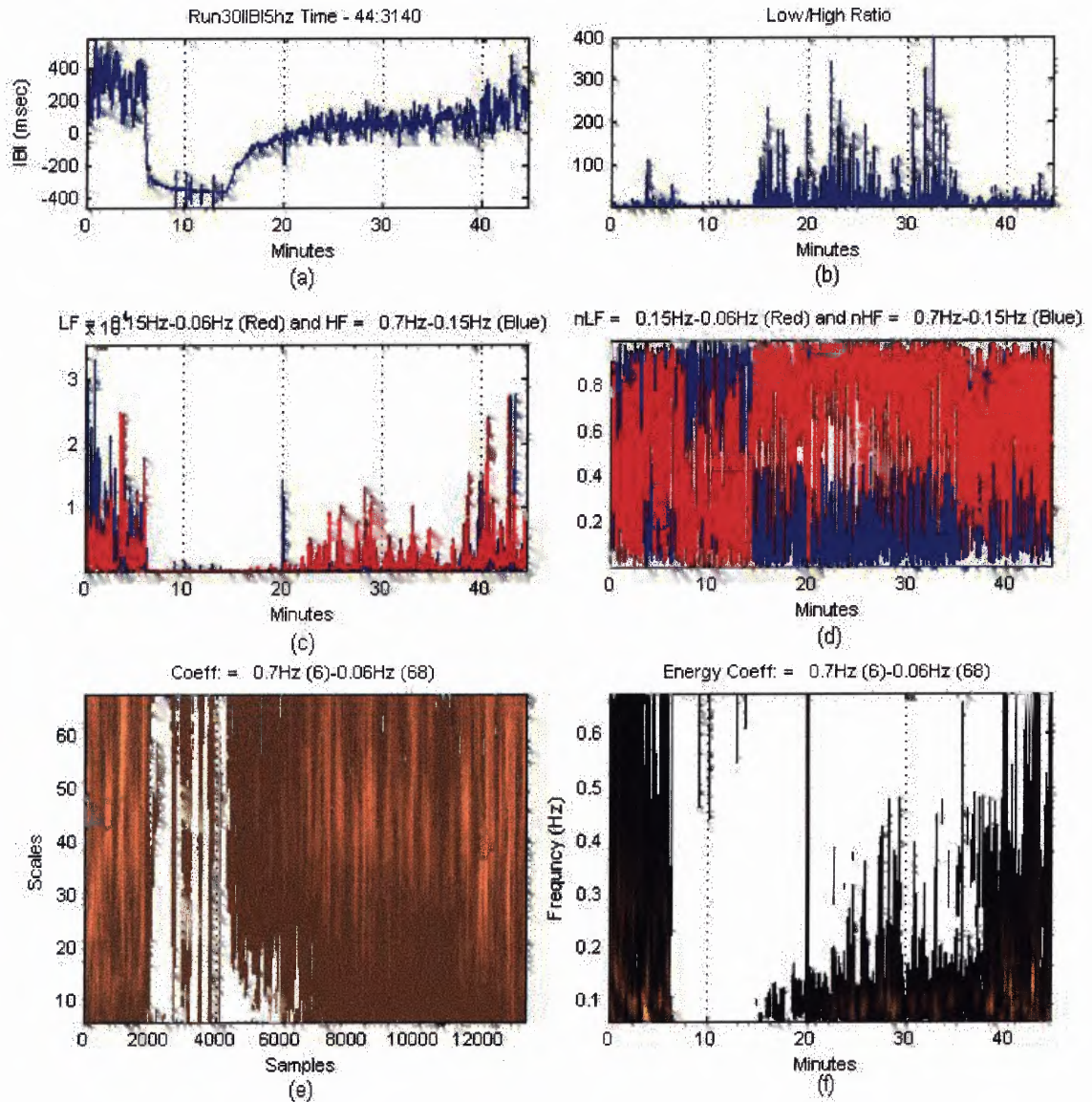


Figure 4.15 Output from the WT program running a file with an extended 30 minute recovery period.

- (a) IIBI with the mean removed.
- (b) LF/HF ratio.
- (c) Absolute values of the LF and HF.
- (d) LF and HF in normalized units.
- (e) 3D representations of the frequency data as a mesh.
- (f) 3D representations of the frequency data contour plot.

The STFT output for the resting baseline portion of the data can be seen below in Figure 4.16 while Figure 4.17 exhibits the WT. The entire IIBI data collected is plotted in Figure 4.16a and Figure 4.17a. The current area of interest, resting baseline, is highlighted in red. This section is expanded in Figure 4.16b and Figure 4.17b, with the subsequent plots corresponding to the same time line, in order to give a clearer view of how the data behaves. The resting IIBI is level with oscillations mainly due to the effects of the ANS and respiration. The results shown in Figure 4.16c through Figure 4.16e and Figure 4.17c through Figure 4.17e exhibit the LF and HF values at similar levels.

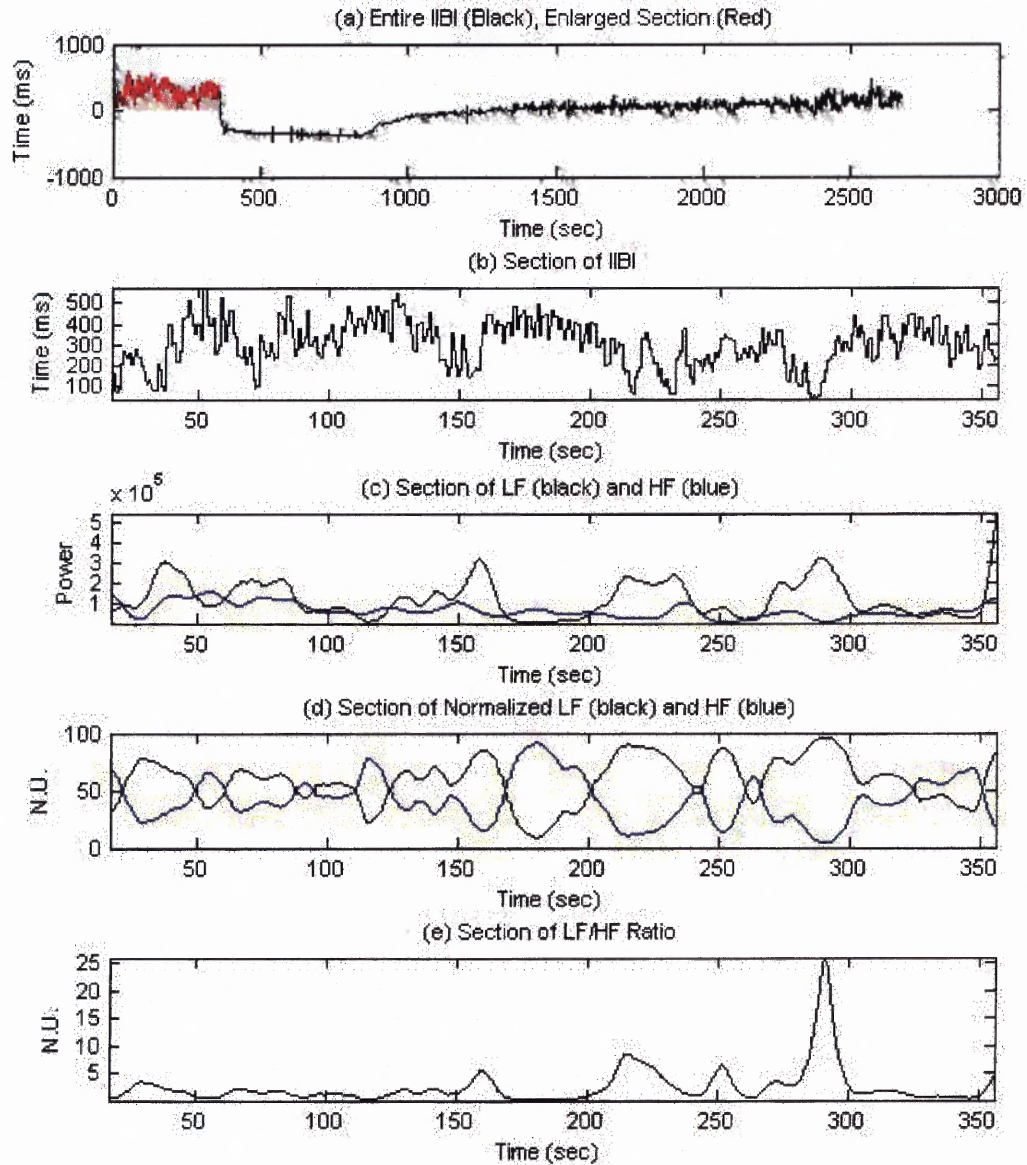


Figure 4.16 STFT output for the resting portion of the experiment.
 (a) IBI of the entire collection period (black), resting IBI section (red).
 (b) Expanded view of the resting IBI.
 (c) Expanded view of the absolute LF (black) and HF (blue) values.
 (d) LF (black) and HF (blue) in normalized units.
 (e) LF/HF ratio.

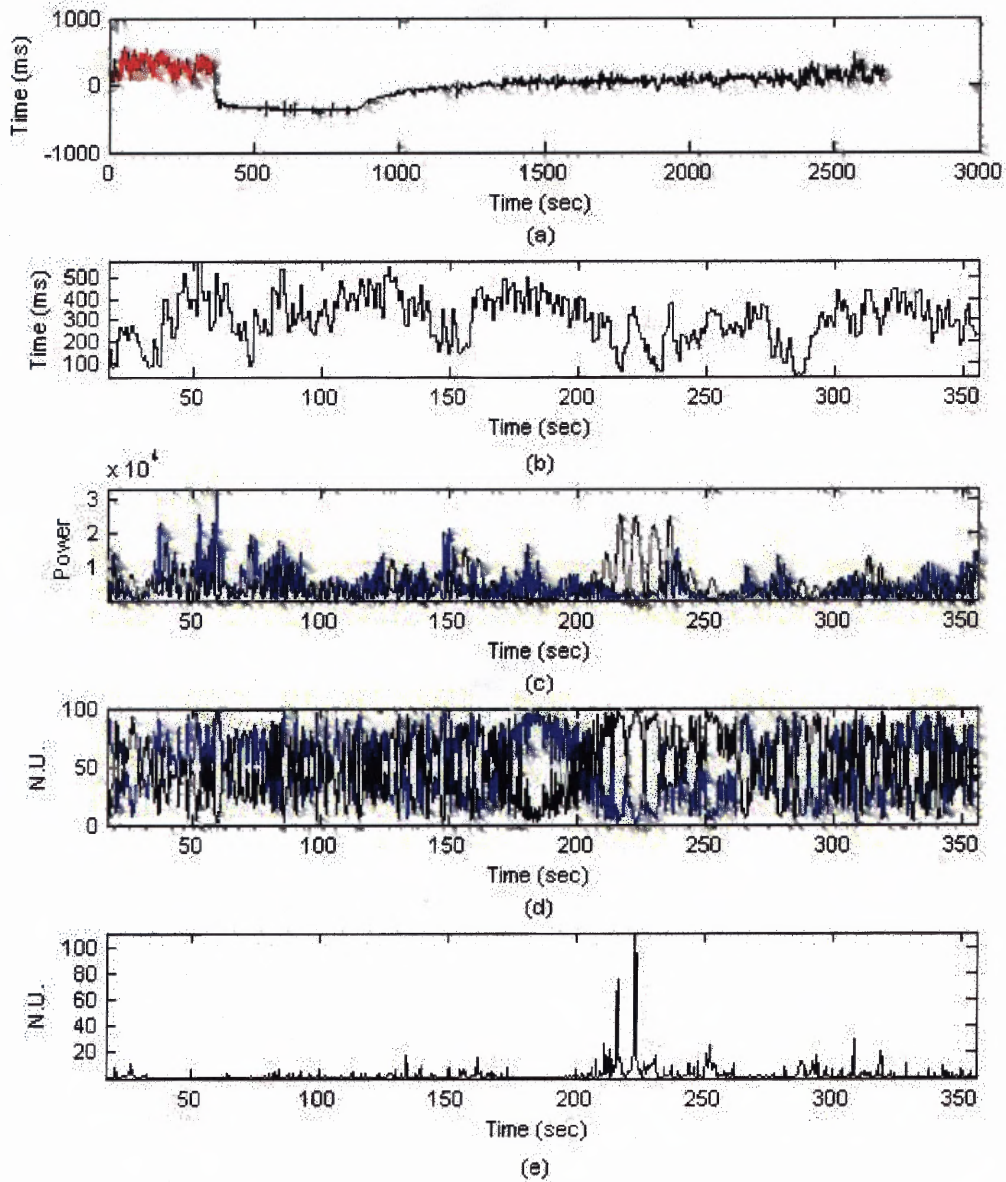


Figure 4.17 WT output for the resting portion of the experiment.
 (a) IBI of the entire collection period (black), resting IBI section (red).
 (b) Expanded view of the resting IBI.
 (c) Expanded view of the absolute LF (black) and HF (blue) values.
 (d) LF (black) and HF (blue) in normalized units.
 (e) LF/HF ratio.

Figure 4.18 and Figure 4.19 represent the exercise portion of the experiment, which took place immediately after the resting portion. This person did not stand up and wait a few minutes before starting to exercise which is why there is no drop in the IIBI between this section and the resting breathing as there was with some of the Test A data. Figure 4.18c through Figure 4.18e and Figure 4.19c through Figure 4.19e indicate that the LF is dominant for a very brief period, consistent with what was obtained with the Test A data. This portion of time corresponds to the period in which the IIBI is decreasing at a rapid rate. Surprisingly, once the IIBI starts to level off the HF starts to become the dominant frequency range.

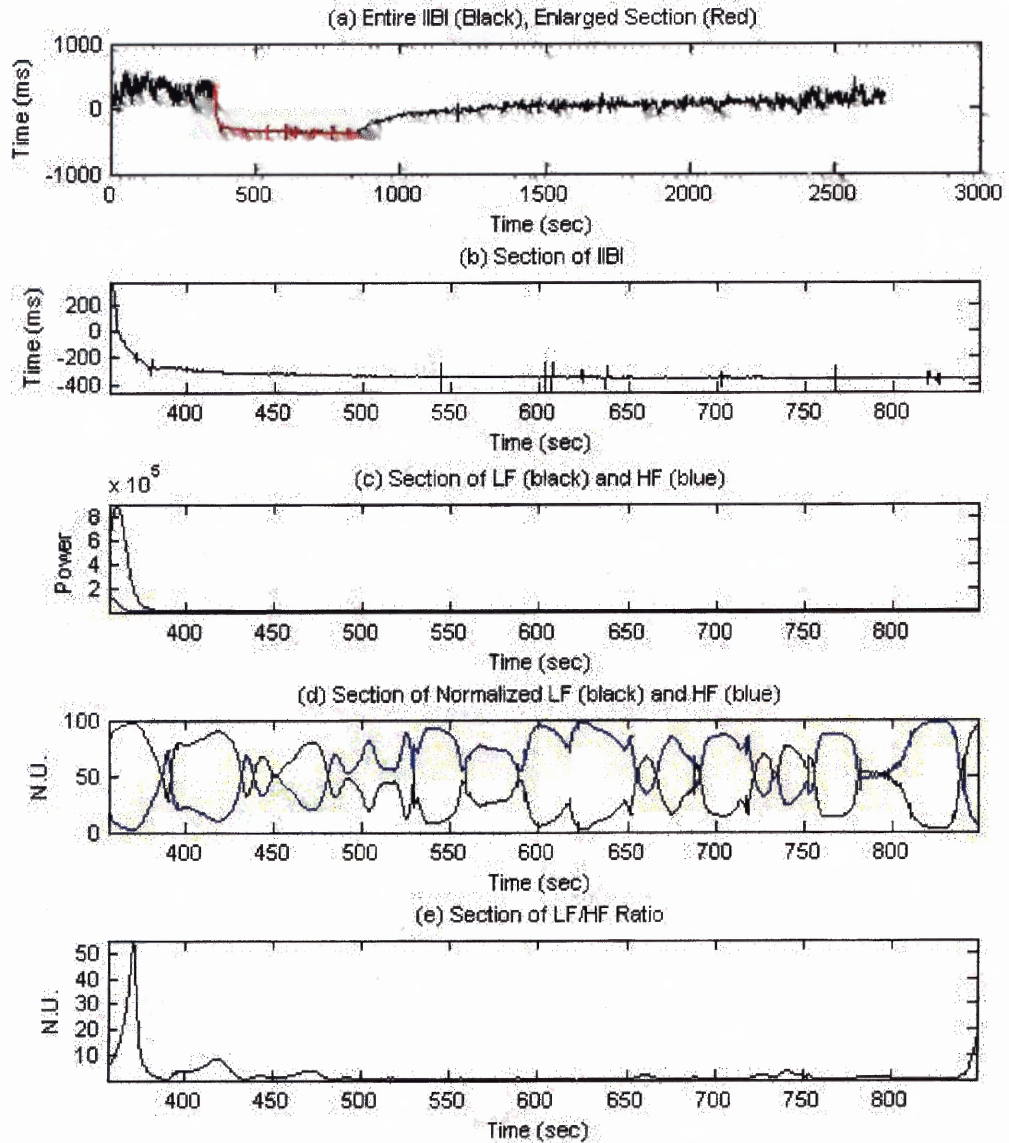


Figure 4.18 STFT output for the exercise portion of the experiment.

- (a) IIBI of the entire collection period (black), exercise IIBI section (red).
- (b) Expanded view of the exercise IIBI.
- (c) Expanded view of the absolute LF (black) and HF (blue) values.
- (d) LF (black) and HF (blue) in normalized units.
- (e) LF/HF ratio.

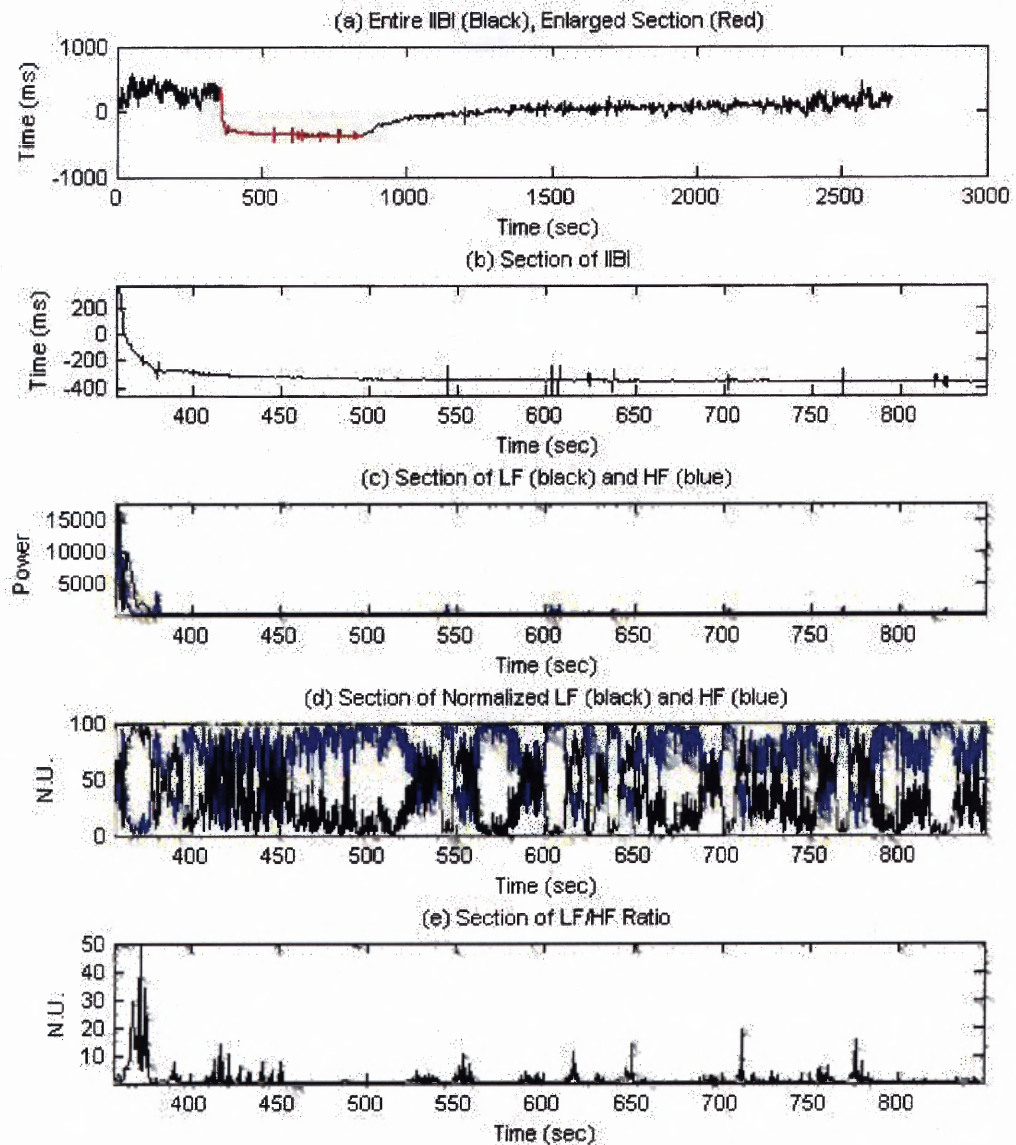


Figure 4.19 WT output for the exercise portion of the experiment.
 (a) IBI of the entire collection period (black), exercise IBI section (red).
 (b) Expanded view of the exercise IBI.
 (c) Expanded view of the absolute LF (black) and HF (blue) values.
 (d) LF (black) and HF (blue) in normalized units.
 (e) LF/HF ratio.

The output for the recovery of the STFT and WT is presented in Figure 4.20 and Figure 4.21, respectively. The LF range is the dominant frequency range throughout this time period, as indicated by Figure 4.20c through Figure 4.20e and Figure 4.21c through Figure 4.21e. However, the results obtained from the STFT shows that at the start of recovery, there is an increase in LF followed by a rapid drop but the LF still remains as the dominant frequency range. This increase is most apparent within the LF/HF ratio plot. The result from the WT does not show this initial spike but it does show a significant increase in the LF. Both methods of analysis indicated that as time passed the signal started to slowly attenuate until the LF equalized with the HF. However, this data indicates the LF was always more elevated and for longer period of time then what was revealed in the Test A experiment. This suggests that the parasympathetic nervous system is still inhibited with predominance within the sympathetic division.

Even though HRV has been shown to be reliable and reproducible [34], the results seem to contradict other reports [35,36,39]. However, there is other research done [37] that produced similar results to what was obtained for Test B. They tested normal subjects at different intensities of exertion also using a polar heart rate monitor for data acquisition. They not only recorded IBI but also obtained respiration as well. Their results were similar to what was obtained in Test B where the HF in normalized units increased as exercise continued and that it was always significantly higher then the LF. Their explanation for this phenomenon is to the intensification of respiratory sinus arrhythmia.

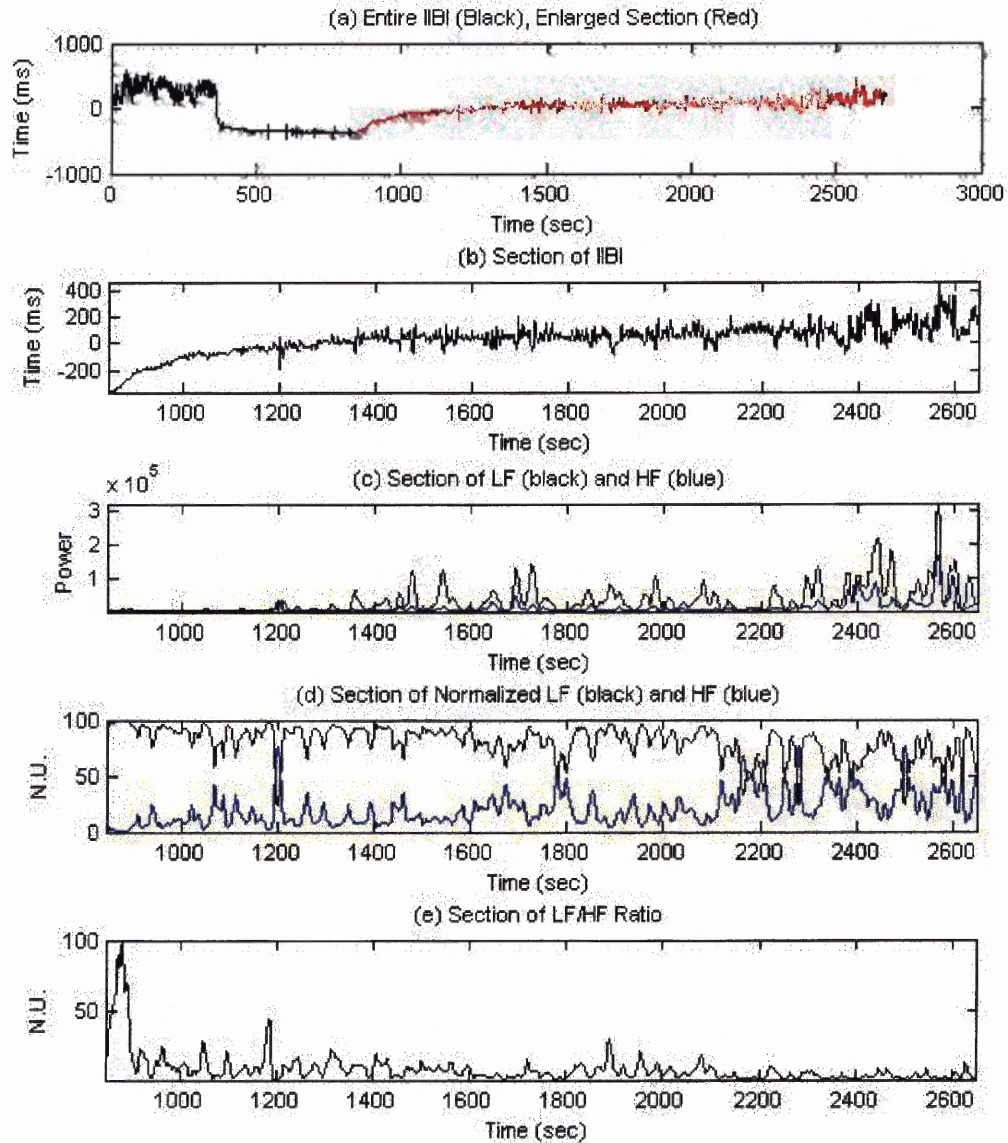


Figure 4.20 STFT output for the recovery portion of the experiment.
 (a) IIBI of the entire collection period (black), recovery IIBI section (red).
 (b) Expanded view of the recovery IIBI.
 (c) Expanded view of the absolute LF (black) and HF (blue) values.
 (d) LF (black) and HF (blue) in normalized units.
 (e) LF/HF ratio.

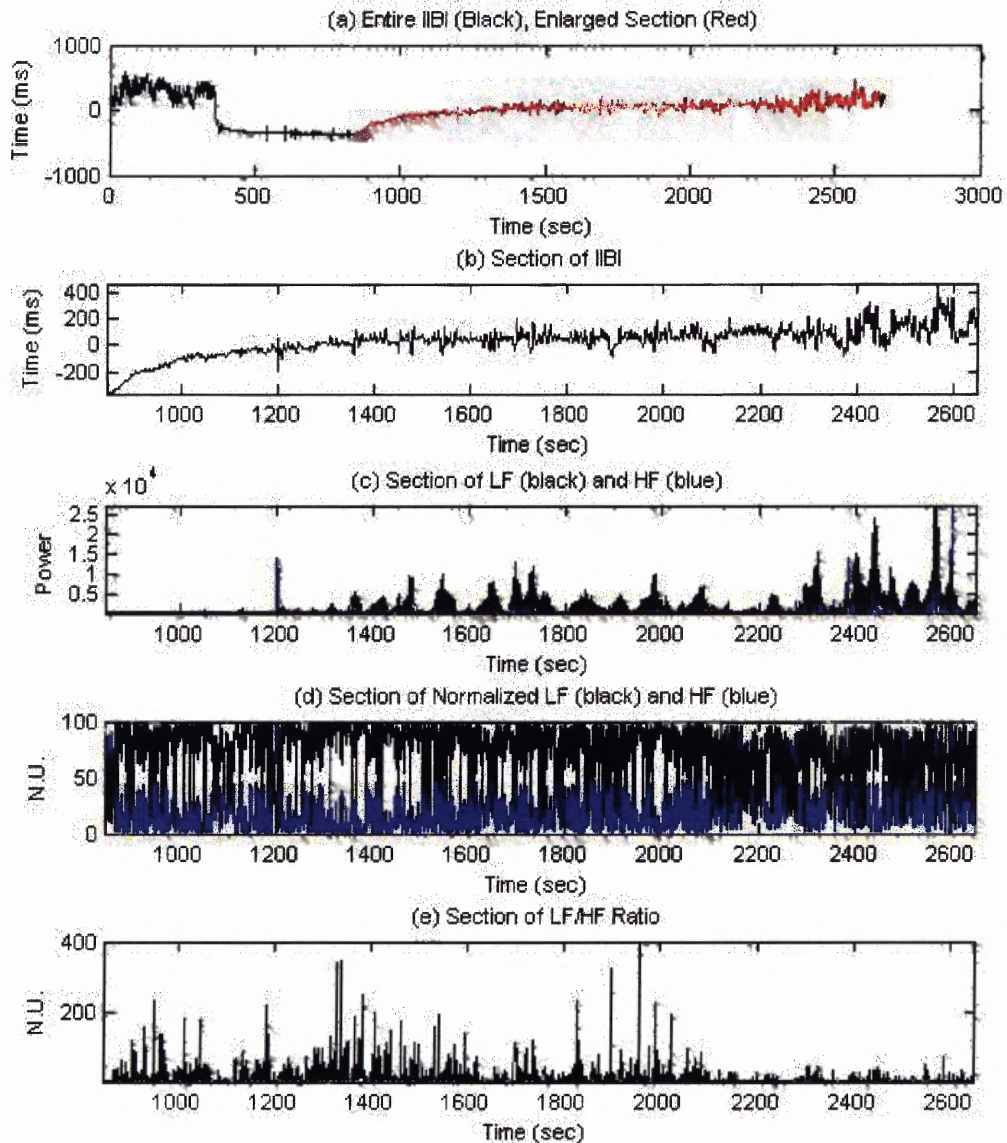


Figure 4.21 WT output for the recovery portion of the experiment.
 (a) IIBI of the entire collection period (black), recovery IIBI section (red).
 (b) Expanded view of the recovery IIBI.
 (c) Expanded view of the absolute LF (black) and HF (blue) values.
 (d) LF (black) and HF (blue) in normalized units.
 (e) LF/HF ratio.

As exercise increases so does the breathing frequency and the depth of breathing. Amara obtained HRV results from normal participants breathing at a rate of 12 breaths/min and 16 breaths/min and indicated no significant difference for all spectral parameters [34]. However, the depth of breathing effects the energy contained at the breathing frequency in the IIBI power spectrum in such a way that the deeper the breath the more energy is added to the HRV frequency spectrum [38]. Since the depth of breathing during exercise is heavier and the breathing frequency is in the HF range this would explain why the HF dominates during the exercise phase of Test B. Nevertheless, it would not explain the sudden increase in the LF during the recovery phase. Although a person could automatically decrease their breathing rate after exercise causing the energy derived from respiration to be contained within the LF range, it is unlikely to occur for the entire recovery period.

The large activation found within the HF during the exercise phase of Test B and the large LF dominance during the subsequent recovery phase could also be due to variability introduced by the heart rate monitor used to acquire the data. The variability could have been introduced by the algorithm that the heart rate monitor used for heart beat detection. This algorithm may have miss detected the heart beat in such a way that it added energy in to the HF during exercise and LF during recovery. This method of acquiring an IBI did not allow for correcting any improperly detected beats such as what was available with the Test A data. Therefore this method of collecting data may need to be reevaluated.

There are some researchers such as Arai [39] that have obtained the expected results by normalizing the HF according to the respiration power. They conducted a

similar experiment which compared results obtained from three populations: normal, heart failure, and heart transplant. This group rationalized this decision since the variations in the heart rate are dependent on the frequency and amplitude of respiration. They found the HF to progressively decrease during exercise and then increase post exercise. This however contradicts their finding that the LF/HF ratio increased significantly during the recovery stage compared to exercise. This shows that the results due to exercise and recovery may partially be affected by the respiration.

Another theory, presented by Goldberger, was that increased parasympathetic activity may saturate the HRV response [32,33]. He performed a pharmacological study consisting of ten normal volunteers where he increased parasympathetic tone by activating the baroreflex using phenylephrine [33]. His results showed a decrease in both frequency and time domain measures of HRV which are an indication of parasympathetic activity.

Another explanation for the spike in the LF data at the start of recovery could be the effect of the sympathetic branch of the ANS coming out of saturation. This theory is based on another presumption which justifies the low levels of LF energy during exercise as an indication of sympathetic saturation [40]. Therefore, when the person stops exercising it may be possible the sympathetic division would come out of saturation producing the increase in the LF.

CHAPTER 5

CONCLUSION AND FUTURE WORK

Since the HRV method is an indirect measure of analyzing the ANS, there may be some other mechanisms that dampen the effects of the ANS. In order to form a conclusion on what exactly occurs to the heart from the ANS during exercise and recovery, more testing would be needed. Other tests regarding the effects of the respiratory sinus arrhythmia, or chemical changes in the body may be needed to further explain the presented results.

The main drawback to this study was that respiration was not recorded. This parameter would have been very useful in order to determine how much effect the respiration had on the HRV throughout the experiment. It could also have been potentially used to normalize the data according to the respiration. Before the respiration could be used for normalization, a linear relationship between the depth of breathing and energy added to the frequency spectrum would have to be determined.

Since every person has different levels of HRV even though their health may be the same, it would be interesting to be able to form a relationship between actual parasympathetic activity and the HF. Perhaps this could be accomplished by recording resting baseline HF of healthy participants and record parasympathetic activity directly. This may help show more significance within the relationship of HF and the recovery time constant, since there may be different things causing every individual's heart to be more variable.

Other work that may help form a more significant correlation coefficient in the HF verses the recovery time constant would be to keep the time and level of exertion

constant. It may be possible that the more time spent active the more time the heart will take to recover back to baseline values. Even though this study used a stress test which is supposed to represent maximal exercise it would be better if a slightly lower level of exertion be used in order to achieve consistent exercise duration.

APPENDIX A

PEAK DETECTOR

The ECG signal was filtered with a second order band pass Butterworth filter in the frequency range of 0.5-40Hz, providing a smoother cleaner ECG signal. The derivative of the filtered signal was then computed and the result was then squared which suppressed other segments of the ECG and made the R-wave more prominent. The signal was then divided into a series of 2 second intervals where the maximum values are found for these 2 second blocks. Afterward, the signal was clipped to be between zero and the median value from the array of maximum values. Next a threshold was set indicating that the peak value of the R-waves is greater than 30 percent of the median value from the array of maximum values. Then an array of indexes was formed indicating where the program started looking for an R-wave by finding where the points in the data start to exceed the threshold. The program then uses these values and extends the search window out for 150ms to find where the maximum occurred. The program filled another array of approximated R-wave locations with the index value of where the maximum occurred. Finally the actual array of R-wave locations was found by taking the assumed location of the R-waves and look for the maximum value in the range starting at 60ms before and ending at 60ms after the assumed index location from the initial raw ECG array. Once the array of actual peak locations was acquired, the times between the occurrence of successive beats or IBI was derived using the sampling rate.

APPENDIX B

POWER SPECTRUM NORMALIZATION

During the analysis an issue was discovered with the off the shelf LabView program that performs the power spectral analysis called 'Power Spectrum.vi'. The problem was noticed when looking at the same signals but taking samples of different time duration. The output after the processing would still produce greater power output then the longer signal. For example a 5 min signal was taken and the power it contained was obtained. Then the power was obtained for the first 2.5 min found the power was not half of that which was in the 5 min signal. Then the power was obtained from the last 2.5 min and added to the first power of the first half of the signal. The result still did not match what was obtained from the total 5 min signal.

In order to resolve this problem the first step taken was analyzing the algorithm which calculates the power spectrum. In doing so it was noticed that the method of calculation followed the following equation

$$S_{xx}(f) = \frac{|F\{X\}|^2}{n^2} \quad (\text{B.1})$$

Where $S_{xx}(f)$ is the power spectrum output, n is the sample size, and $F\{X\}$ is the fast Fourier transform (FFT) when the sample size is a power of 2 or the discrete Fourier transform (DFT) for other sample sizes. The division by the sample size squared essentially normalizes the power of the signal so that no matter how long of a signal is taken the same power would be attained. For example if a 0.2 Hz sine wave lasting 1 minute and another lasting 10 minutes was entered into the power spectrum program, the

output would be the same value. The expected result would be to have the 10 minute signal produce an output that is 10 minute times that of the 1 min signal.

Further analysis was then done by breaking down the Power Spectrum.vi algorithm. In order to break down the program into more basic components the first process was to just perform a FFT with the Labview FFT.vi block. This still did not produce what was expected.

Then it was noticed that the program added some zero padding the signal input into the FFT.vi. The zero padding was there in order to use the FFT algorithm as apposed to the DFT. The only difference between the two algorithms is the processing time associated with the two. Theoretically the zero's added at the end of the signal should not effect the power contained within the zero padding should be zero. After testing the signal with different amounts of zero padding it was noticed that the output power would increase. We then looked at how the spectrum was changing with the different amounts of zeros added. It appeared that there was a spreading affect caused by the zero padded signal. A Hanning window was then added to the padded signal in order to reduce the spreading and it was noticed that the program would then get values similar to what you would get with a signal that did not have any zero padding.

The final outcome of these discoveries was to eliminate the zero padding and let the program use the DFT algorithm. In addition the use of the Power Spectrum.vi was eliminated and a program was written to perform this function. Although the numbers produced were tremendously larger in value then that which was obtained from the Power Spectrum.vi, it was clearer exactly what the program was doing.

APPENDIX C

WAVELET TRANSFORM PROGRAM CODE

This appendix presents the code for the Matlab program used to perform the wavelet transform

C.1 Main Program

```
%waveletAnalysisPierre05.m

%this will bring a window so that you can tell the program which file that
%you want to load

[File, Path, FILTERINDEX] = uigetfile('\HEALTHY\*. *', 'import IIBI for PBR');
iibiWhole1=load([Path File]);

samplerate=5;

%y=round(1000/round(max(max(testdata1(iibiWhole1)))))/samplerate);
y=1;
iibi=iibiWhole1(1:y:length(iibiWhole1));

[hf,lf,curvehf,curvelf,coeff]=iibiplots10(samplerate,.7,.15,.15,.06,iibi,File,0,'OFF');

fl=length(File);
File=File(1:(fl-4));
saveas(figure(gcf),[Path, 'Plots\',File, '.fig'],'fig');
save([Path, 'Output\',File, 'HF.txt'], 'hf','-ascii')
save([Path, 'Output\',File, 'LF.txt'], 'lf','-ascii')
save([Path, 'Output\',File, 'CurveHF.m'], 'curvehf')
save([Path, 'Output\',File, 'CurveLF.m'], 'curvelf')
```

C.2 Main Sub Function

```
%iibiplots10.m

function [hf,lf,curvehf,curvelf,
coeff]=iibiplots10(samplrate,upperhf,lowerhf,upperlf,lowerlf,iibi,file,y,curves)
% This function calculates the Continuous Wavelet coefficients using a Morlet wavelet
```

```

% Inputs:
% samprate: data stream sample rate in samples per second - numerical constant
% upperhf: upper frequency point of the high frequency band to be
% calculated in Hz - numerical constant
% lowerhf: lower frequency point of the high frequency band to be
% calculated in Hz - numerical constant
% upperlf: upper frequency point of the low frequency band to be
% calculated in Hz - numerical constant
% lowerlf: lower frequency point of the low frequency band to be
% calculated in Hz - numerical constant
% iibi: the data stream whose CWT coefficients are to be calculated. -
% numerical array
% file: name of the iibi file - string.
% y: the factor to descimate the padding, if y=0 then no padding.
% curves: curve fit model - text.

```

```

% Outputs:
% The plot of iibi
% The plot of the CWT coefficients of iibi as a function of scale and
% sample point
% The plot of the CWT coefficients squared as a function of scale and
% sample point
% The plot of the CWT coefficients squared in the high frequency band as a
% function of sample point with a smoothed and curve fitted
% The plot of the CWT coefficients squared in the low frequency band as a
% function of sample point
% The plot of the ratio of the CWT coefficients squared of the low
% frequency band to the CWT coefficients squared of the high frequency
% band as a function of sample point
% Outputs the hf, high frequency band, and lf, low frequency band, data
% streams numerical array
% Outputs the curve fit parameters for the hf and lf bands. - structured
% array

```

```

%This section calculates basic parameters

```

```

%curves='poly2';
curves='OFF';
wavelets='morl';
centre=centfrq(wavelets);

```

```

%This section converts the frequency limits to scale for the CWT
%calculation
upperhfscale=scalefind(upperhf,samprate,centre);
lowerhfscale=scalefind(lowerhf,samprate,centre);

```

```

upperlfscale=scalefind(upperlf,samprate,centre);
lowerlfscale=scalefind(lowerlf,samprate,centre);

% remove the average value
iibix=filterdc(iibi);

%Pad the iibi file with 60000/60/1000 = 1 min of data at the beginning and
%end
if y > 0;
    iibix=[ones(1,60000/y)*iibix(1), iibix, ones(1,60000/y)*iibix(length(iibix))];
end;

%calculate the wavelet coefficients with the padded file
coeff=cwt(iibix,upperhfscale:lowerlfscale,wavelets);

%Unpad the wavelet coefficients and iibi file
if y > 0;
    coeff=coeff(:,(60000/y)+1:(length(coeff)-60000/y));
    iibix=iibix((60000/y)+1:(length(iibix)-60000/y));
end;

%normalize the coefficients
%coeff=coeff/max(max(coeff));

%length of the iibi file
Liibi1 = length(iibix);
Liibi = [0 Liibi1];

%calculates the time of the IBI
timeMin = (Liibi(2)/samprate)/60;
timeSec= floor((timeMin-floor(timeMin))*60*100);
timeMin=floor(timeMin);

%calculates the span of time for data streams
timemax=(Liibi(2)-1)/samprate/60;
time=[0:1/samprate/60:timemax];

%calculates the span of time for plots
xlimit=[0 timemax];

%Plot the iibi data stream without removing the dc
plots(time, iibi, 0, [0.075 .8 .4 .15], xlimit, [file,' Time - ', num2str(timeMin),
':',num2str(timeSec)], 'IBI (msec)', 'Minutes',0);

```

```

%plot the wavelet coefficients
plots3D([0.075 .08 .4 .29],['Coeff: = ',num2str(upperhf),'Hz (' ,num2str(upperhfscale),')-
',num2str(lowerlf),'Hz (' ,num2str(lowerlfscale),')'], 'Scales','Samples',[0 Liibi1],0:Liibi1-
1,upperhfscale:lowerlfscale,coeff);

% calculate the frequency band
freqBand = scal2frq(upperhfscale:lowerlfscale,wavelets,1/samprate);

% Square the coefficients
%coeff=coeff.^2;
coeff=abs(coeff);

%plot the energy coefficients
plots3D([0.55 .08 .4 .29],['Energy Coeff: = ',num2str(upperhf),'Hz
(' ,num2str(upperhfscale),')- ',num2str(lowerlf),'Hz (' ,num2str(lowerlfscale),')'], 'Frequency
(Hz)', 'Minutes',xlimit,time,freqBand,coeff);

%This section calculates the frequency band and ration plots
[hf,lf,r]=freqbandcalc(samprate,centre,coeff,upperhfscale,lowerhfscale,upperlfscale,lowe
rlfscale);

nhf=hf./(hf+lf);
nlf=lf./(hf+lf);

% find the maximum of the high and/or low frequency band to plot this bands using the
same vertical scale
maxhf=max(max(hf,lf));

%plot the hf bands
[curvehf]=plotband([0.075 .44 .4 .29],['HF = ',num2str(upperhf),'Hz-
',num2str(lowerhf),'Hz '], 'Minutes',xlimit,time,hf,curves,'b');

hold on
%plot the lf band
[curvelf]=plotband([0.075 .44 .4 .29],['LF = ',num2str(upperlf),'Hz-
',num2str(lowerlf),'Hz HF = ',num2str(upperhf),'Hz-',num2str(lowerhf),'Hz
'], 'Minutes',xlimit,time,lf,curves,'r');
hold off

%plot the nhf bands
[curvehf]=plotband([0.55 .44 .4 .29],['HF = ',num2str(upperhf),'Hz-
',num2str(lowerhf),'Hz '], 'Minutes',xlimit,time,nhf,curves, 'b');

hold on

```

```

%plot the nlf band
[curvelf]=plotband([0.55 .44 .4 .29],[ 'LF = ',num2str(upperlf),'Hz-',num2str(lowerlf),'Hz
'],'Minutes',xlimit,time,nlf,curves,'r');
hold off

% plot the lf/hf ratio
plotband([0.55 .8 .4 .15],'Low/High Ratio','Minutes',xlimit,time,r,curves,'b');

set(gcf,'position', [5 36 646 662]);

```

C.3 Format the Scale

```

%scalefind.m

function scale = scalefind(freq,samprate,centre);
scale=round(centre*samprate/freq);

```

C.4 Removing Mean

```

function x = filterdc(x);
y=mean(x)*ones(size(x));x=x-y;

```

C.5 Format Plotting

```

% plotts.m

function x=plotts(x, y, z, plotposition, xlimit, plottitle, plotylabel,
plotxlabel,linetype,linewidth,size)

% x: x coordinate - numerical array
% y: y coordinate - numerical array
% z: z coordinate - numerical array
% plotposition: subplot position - numerical array
% xlimit x coordinate limit - 2 element array
% plottitle: title of plot - string array
% plotylabel: label of y axis - string array
% plotxlabel: label of x axis - string array
% linetype: string
% linewidth parameter: string
% size: numerical constant

```



```

fontsize=7;

subplot('position',plotposition);
if x==0
    if linetype==0;
        plot(y);
    else;
        plot(y,linetype);
    end;
else;
    if z==0;
        if linetype==0;
            plot(x,y);
        else;
            plot(x,y,linetype,linewidth,size);
        end;
    else;
        contour(x,y,z,15);
        %mesh(x,y,z);
        colormap(copper); % Set up the colormap
        view(2); % Set up the 2D view
    end;
end;
axis('tight');
set(gca,'XLim',xlim);
title(plottitle,'FontSize',fontsize);
ylabel(plotylabel,'FontSize',fontsize);
xlabel(plotxlabel,'FontSize',fontsize);
set(gca,'FontSize',fontsize,'XGrid','on');

```

C.6 Format 3D Plots

```

% plotts3D.m

function x=plotts3D(plotposition,plottitle,plotylabel,plotxlabel,xlimit,x,y,z)

[TIMES,SCALES]=meshgrid(x,y);

plotts(TIMES, SCALES, z, plotposition, xlim, plottitle, plotylabel, plotxlabel,0);

```

C.7 Calculating Power Contained in Frequency

```
% freqbandcalc.m

function [hf,lf,r] =
freqbandcalc(samprate,centre,coeff,upperhfscale,lowerhfscale,upperlfscale,lowerlfscale)

m=size(coeff); %m(2) is the size of the data stream

for i=1:m(2)
    hf(i)=0;

    for j=upperhfscale:lowerhfscale;
        hf(i)=(coeff(j-upperhfscale+1,i)^2)/(j*(j+1))*centre*samprate+hf(i);
    end;

    lf(i)=0;

    for j=upperlfscale:lowerlfscale;
        lf(i)=(coeff(j-upperhfscale+1,i)^2)/(j*(j+1))*centre*samprate+lf(i);
    end;

    r(i)=lf(i)/hf(i);
end
```

C.8 Sets the Plotting Environment for Output Graph

```
%plotband.m

function [curve]=
plotband(plotposition,plottitle,plotylabel,plotxlabel,xlimit,x,y,curvefit,linetype)

%plot raw data
if strcmp(curvefit,'OFF')
    plotts(x, y, 0, plotposition, xlimit, plottitle, plotylabel,
plotxlabel,linetype,'LineWidth',1);
    curve='OFF';
else;
    plotts(x, y, 0, plotposition, xlimit, " ", plotxlabel,0);

%plot on top the smoothed curve

hold on;
```

```
plots(x, filtfilt(hamming(100),50,y), 0, plotposition, xlabel, ylabel, plotlabel, 'r-  
'LineWidth',2);
```

```
%plot on top the fitted curve
```

```
%curve fit data
```

```
curve=fit(x',y',curvefit);  
p1=num2str(curve.p1);  
decp1=strfind(p1, '.');  
p2=num2str(curve.p2);  
decp2=strfind(p2, '.');  
p3=num2str(curve.p3);  
decp3=strfind(p3, '.');
```

```
plots(0, curve, 0, plotposition, xlabel, [plottitle, ' p1: ',p1([1:2+decp1]),' p2:  
'p2([1:2+decp2])], ylabel, plotlabel, 'k.');
```

```
hold off;  
end
```

APPENDIX D

SHORT TIME FOURIER TRANSFORM PROGRAM CODE

This appendix presents the code for the Matlab program used to perform the short time Fourier Transform (STFT)

D.1 STFT Matlab Program Code

```
%STFTpa05.m

clear
%This will open a browser window to choose which file to load
[File, Path, FILTERINDEX] = uigetfile('*.wav', 'Choose the data file you wish to process');
rawSignal=load([Path File]);

%Set up the time scale for a 5hz interpolated signal
fs=5;
dtime=1/fs;
time=length(rawSignal)*dtime;
t=[0:dtime:time-dtime];

%this will set up the window length
winSizeSec=30;
winSizeSample=winSizeSec*(1/dtime);

winCent=ceil(winSizeSample/2);

%sets up the DFT with the length of segLength
%makes the fft frequency spike sharper
%since it is a power of 2 this will make the FFT go faster
segLength=2^8;

h = waitbar(0,'Processing FFT...'); %Sets up the %complete

%this will do how much over lap will be with the windowing
%the more overlap the slower the program runs but the better the time vs
%frequency will be
overlap=.9;
skip=round(winSizeSample*(1-overlap));
```

```

skip=1;

%performs the fft on a the set window with 100% overlap
for i=1:skip:length(t)-winSizeSample
    i=(i-1+skip)/skip;    %this will readjust the counter
    winSig=rawSignal(i:i+winSizeSample-1);
    winSig=winSig-mean(winSig);
    winSig=winSig.*hanning(winSizeSample); %adds a hanning window
    winSigMat(i,[1:winSizeSample])=winSig; %constructs a matrix with windowed
signals
    waitbar(i/(round((length(t)-winSizeSample)*2)/skip))    %Marks the Progress of
%complete
end
close(h)    %will close the %done window

%computes the fourier transform of the signal
WINSIGMAT = fft(winSigMat',segLength);

h = waitbar(0,'Processing Power Spectrum...');    %Sets up the %complete
[r,c]=size(WINSIGMAT)
for i=1:c
    %converts the signal to it measure of power at various frequencies
    Pow([1:segLength],i)= WINSIGMAT([1:segLength],i).*
conj(WINSIGMAT([1:segLength],i)) / segLength;
    % Pow= WINSIGMAT.* conj(WINSIGMAT) / segLength;
    waitbar(i/c)    %Marks the Progress of %complete
end
close(h)    %will close the %done window

%this will calculate the frequency energy
lowLF=0.04;
lowLF=round(lowLF*segLength*dtime);
highLF=0.15;
highLF=round(highLF*segLength*dtime);
lowHF=highLF;
highHF=.7;
highHF=round(highHF*segLength*dtime);

%does the sum for the frequency calculation
LF=sum(Pow(lowLF:highLF,:))';
HF=sum(Pow(lowHF:highHF,:))';

%does the normalization
nLF=LF./(LF+HF);
nHF=HF./(LF+HF);

```

```
%does the LF/HF ratio
LFHFratio=LF./HF;
```

```
%adds padding to since the windowing cuts off some of the time data
time=winSizeSec/2*fs; %15 seconds of time with a sampling rate of 5 hz
pad=zeros(time,1);
LF=[pad;LF;pad];
HF=[pad;HF;pad];
nLF=[pad;nLF;pad];
nHF=[pad;nHF;pad];
LFHFratio=[pad;LFHFratio;pad];
```

```
%%%%%%%%%%this section does all the
plotting%%%%%%%%%
```

```
f = 1/dtime*(lowLF:highHF)/segLength; %this will normalize and adjust the frequency
in the proper range
adjTime=t(winCent+1:skip:length(t)-winCent); %this will crop the time due to the
windowing spacing for the first and last spectrum analysis. this could potentially be
resolved with padding.
```

```
startData=length(pad)+1;
endData=startData+length(adjTime)-1;
```

```
%Plotting the original signal
subplot('position',[0.075 .8 .4 .15]),plot(t,rawSignal);
title(File,'FontSize',7);
xlabel('Time (sec)','FontSize',7);
set(gca,'XLim',[0 time],'FontSize',7);
```

```
%this does the LF/Hf ratio plot
subplot('position',[0.55 .8 .4 .15]),plot(adjTime,LFHFratio(startData:endData));
title(['LF/HF ratio of ', File],'FontSize',7)
% ylabel('Frequency (Hz)','FontSize',7)
xlabel('Time (Sec)','FontSize',7)
set(gca,'FontSize',7)
```

```
%this does the contour plot
subplot('position',[0.55 .08 .4 .29]),contour(adjTime,f,Pow(lowLF:highHF,:))
title(['Time vs. Frequency content of ', File],'FontSize',7)
ylabel('Frequency (Hz)','FontSize',7)
xlabel('Time (Sec)','FontSize',7)
set(gca,'FontSize',7)
```

```
%Plot of the total power in the LF and HF ranges
```

```

subplot('position',[0.075 .44 .4 .29]),
plot(adjTime,LF(startData:endData),'r',adjTime,HF(startData:endData),'k')
title('LF (red) and HF (black)','FontSize',7)
xlabel('Time (sec)','FontSize',7)
set(gca,'FontSize',7)

%Plot of the normalized power of the LF and HF ranges
subplot('position',[0.55 .44 .4 .29]),
plot(adjTime,nLF(startData:endData),'r',adjTime,nHF(startData:endData),'k')
title('nLF (red) and nHF (black)','FontSize',7)
xlabel('Time (sec)','FontSize',7)
set(gca,'FontSize',7)

subplot('position',[0.075 .08 .4 .29]), mesh(adjTime,f,Pow(lowLF:highHF,:))
title(['Time vs. Frequency content of ', File],'FontSize',7)
ylabel('Frequency (Hz)','FontSize',7)
xlabel('Time (Sec)','FontSize',7)
set(gca,'FontSize',7)

set(gcf,'position', [5 36 646 662]);

position = findstr('.', File)
if position>=0
File=File(1:position);
end

saveas(figure(gcf),[Path, 'stftPlots\',File, '.fig'],'fig');
save([Path, 'stftOutput\',File, 'HF.txt'], 'HF','-ascii')
save([Path, 'stftOutput\',File, 'LF.txt'], 'LF','-ascii')
save([Path, 'stftOutput\',File, 'Power.txt'], 'Pow','-ascii')

```

APPENDIX E

EXPANDING PROGRAM

This appendix presents the front panel and block diagrams for the Labview programs used to expand sections of the data. This program loaded an IIBI and the corresponding LF and HF data. Then the user can focus on a section of the IIBI data and the program will expand the view of the LF, HF, normalized LF, normalized HF, and the LF/HF ratio. This program will also indicate if the mean LF or HF is greater in that particular section of the data and how significant it is. Once everything is set the program will plot the graphs in Matlab so that they can be saved and viewed later.

E.1 Labview Front Panel and Block Diagrams



Figure E.1 Front panel of the main program used to expand data view.

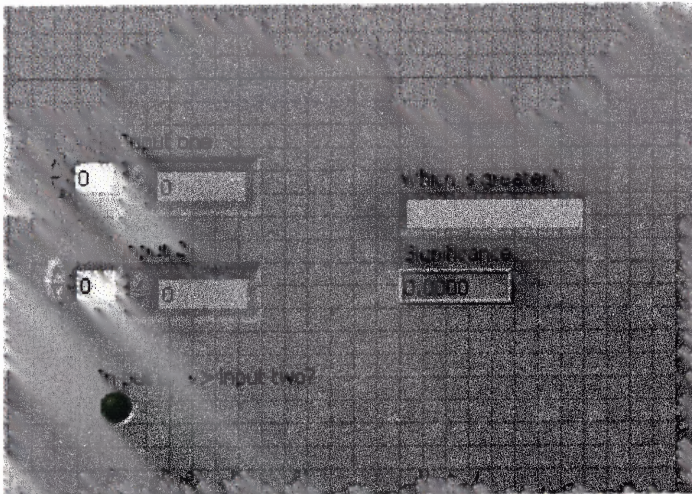


Figure E.3 Front panel of sub program that will calculate the significance of one group being greater then the other.

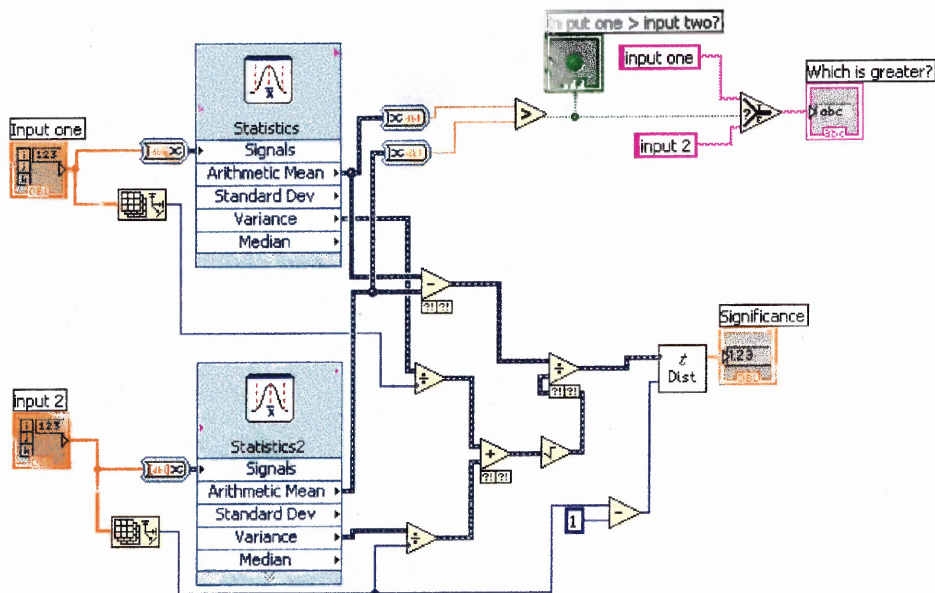


Figure E.4 Block Diagram of sub program that will calculate the significance of one group being greater then the other.

E.2 Matlab Script Used for Plotting

```

l=length(IIBI);
partL=length(IIBIsection);
time=1/5:1/5:1/5
endL=start+partL;
partTime=start/5:1/5:(endL/5-1/5)

subplot(5,1,1),plot(time,IIBI,'k',partTime,IIBIsection,'r')
title(['(a) Entire IIBI (Black), Enlarged Section (Red)'],'FontSize',8)
ylabel('Time (ms)','FontSize',8)
xlabel('Time (sec)','FontSize',8)
set(gca,'FontSize',8)

subplot(5,1,2),plot(partTime,IIBIsection,'k')
title('(b) Section of IIBI','FontSize',8)
axis tight
%title('(a)')
ylabel('Time (ms)','FontSize',8)
xlabel('Time (sec)','FontSize',8)
set(gca,'XLim',[start/5 (endL/5-1/5)],'FontSize',8)

subplot(5,1,3),plot(partTime,HF,'b',partTime,LF,'k')
title('(c) Section of LF (black) and HF (blue)','FontSize',8)
%title('(b)')
axis tight
ylabel('Power','FontSize',8)
xlabel('Time (sec)','FontSize',8)
set(gca,'XLim',[start/5 (endL/5-1/5)],'FontSize',8)

subplot(5,1,4),plot(partTime,nHF,'b',partTime,nLF,'k')
title('(d) Section of Normalized LF (black) and HF (blue)','FontSize',8)
%title('(c)')
ylabel('N.U.','FontSize',8)
xlabel('Time (sec)','FontSize',8)
set(gca,'XLim',[start/5 (endL/5-1/5)],'FontSize',8)

subplot(5,1,5),plot(partTime,LFHF,'k')
title('(e) Section of LF/HF Ratio','FontSize',8)
axis tight
%title('(d)')
ylabel('N.U.','FontSize',8)
xlabel('Time (sec)','FontSize',8)
set(gca,'XLim',[start/5 (endL/5-1/5)],'FontSize',8)

```

APPENDIX F

PEAK DETECTOR PROGRAM

This program was developed by Dr. Ronald Rockland and was used to detect the R-waves from the acquired ECG signal.

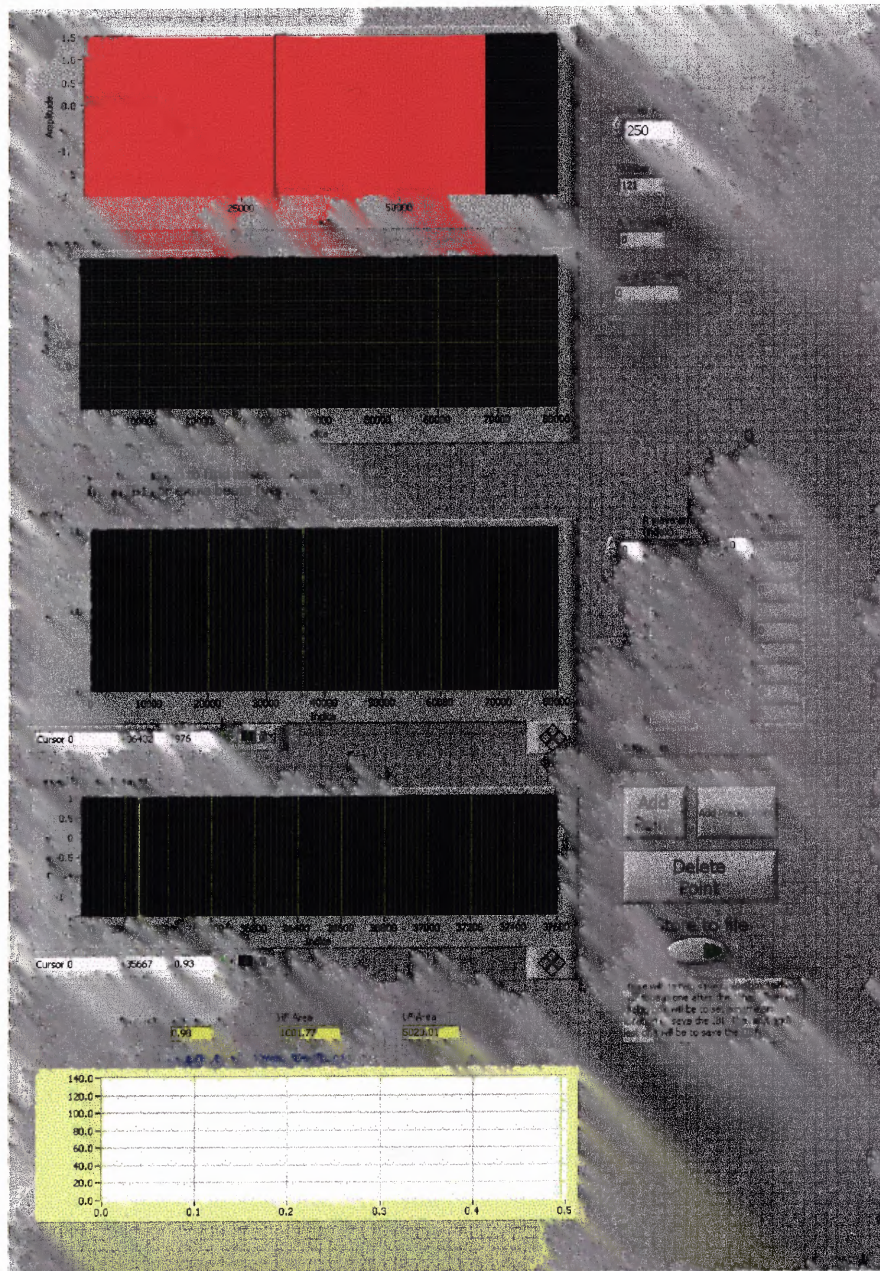


Figure F.1 Main program for peak detection front panel.

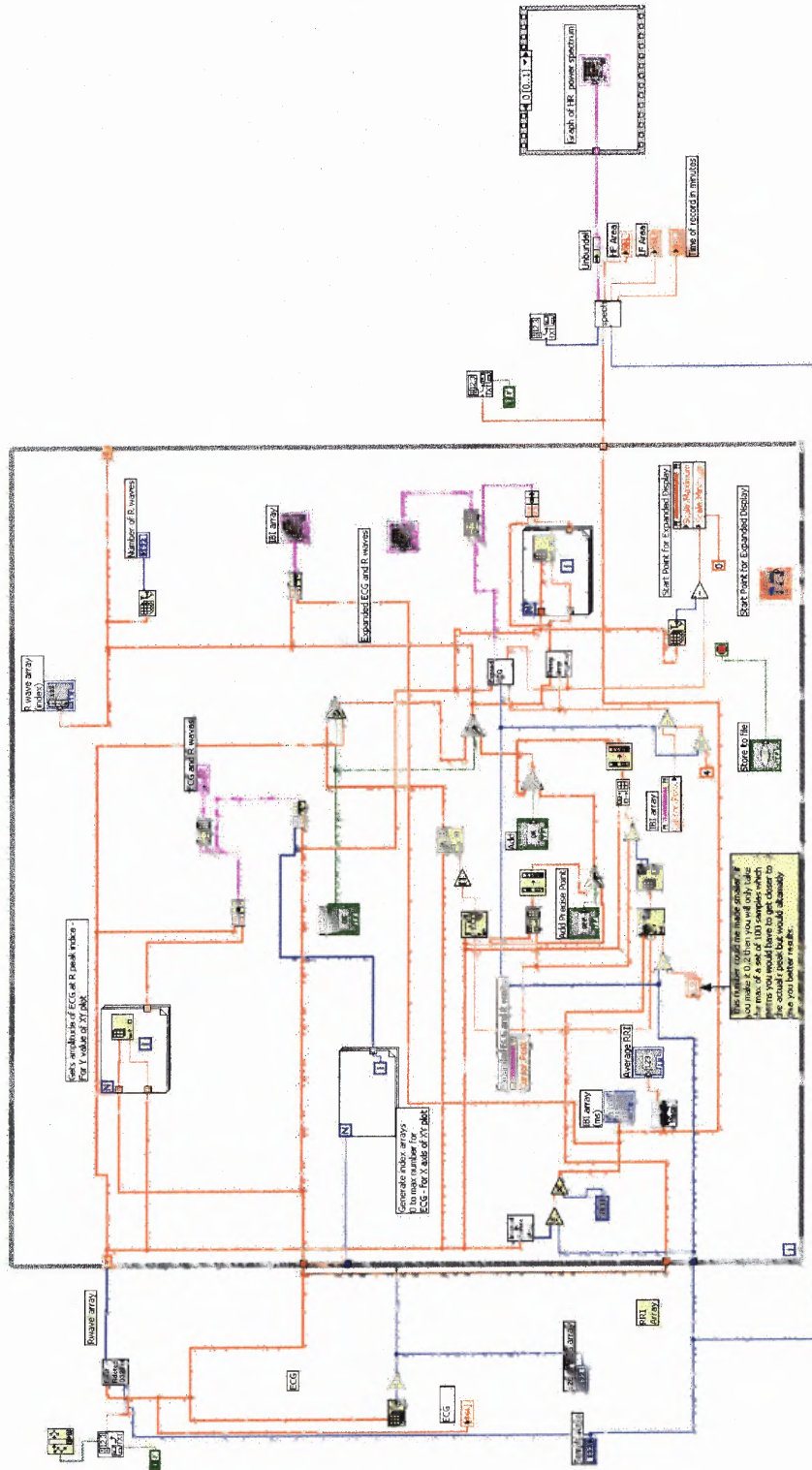


Figure F.2 Main program for peak detection block diagram.

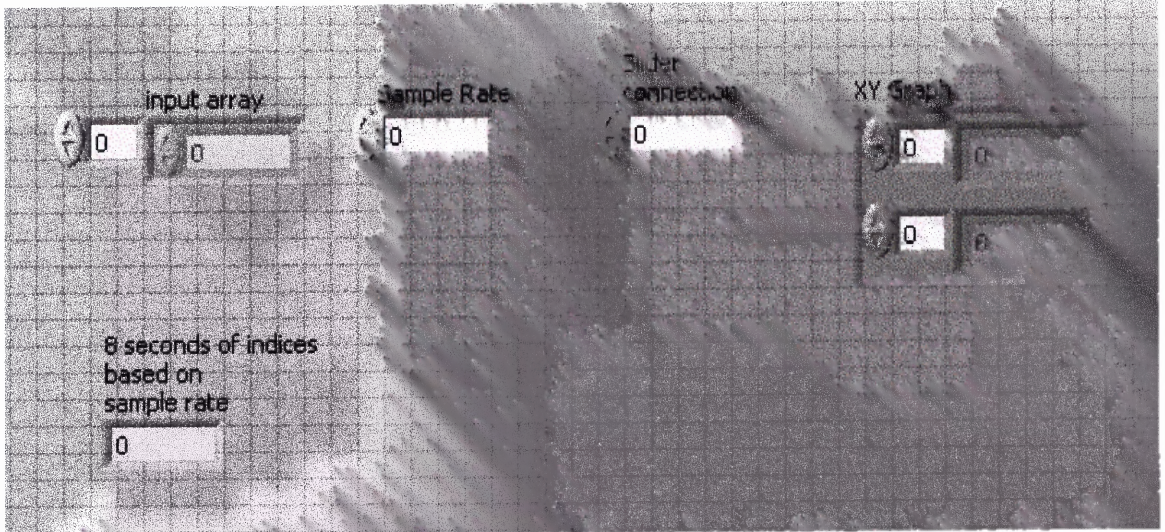


Figure F.3 Expand ECG front panel.

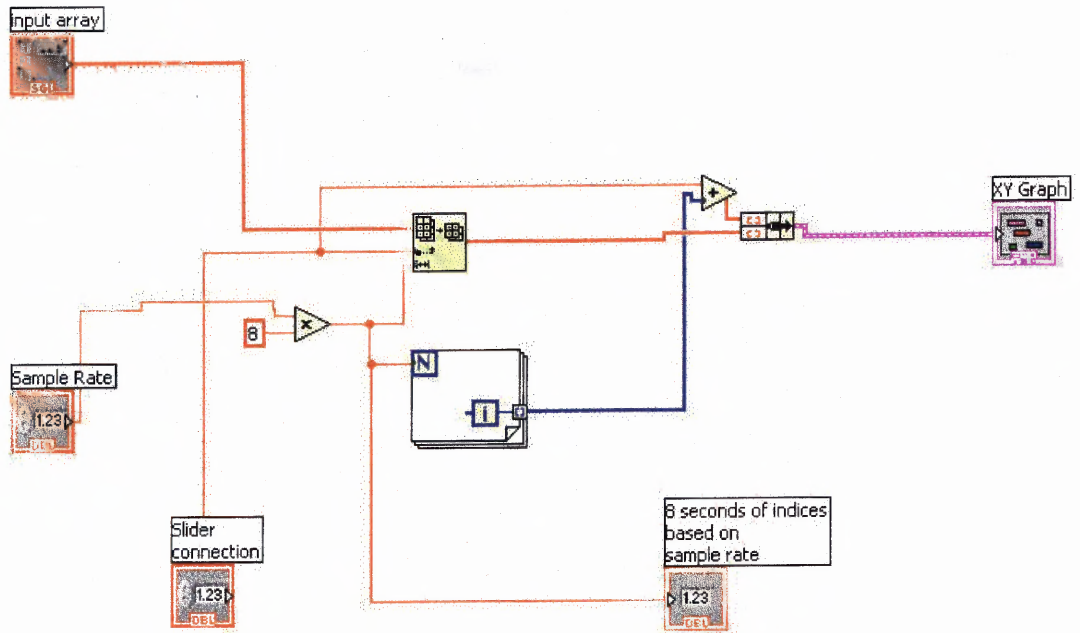


Figure F.4 Expand ECG block diagram.

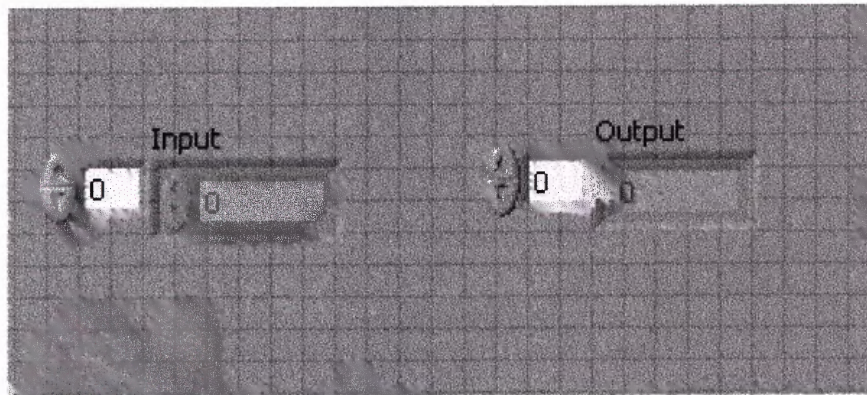


Figure F.5 Interval Rwave array front panel.

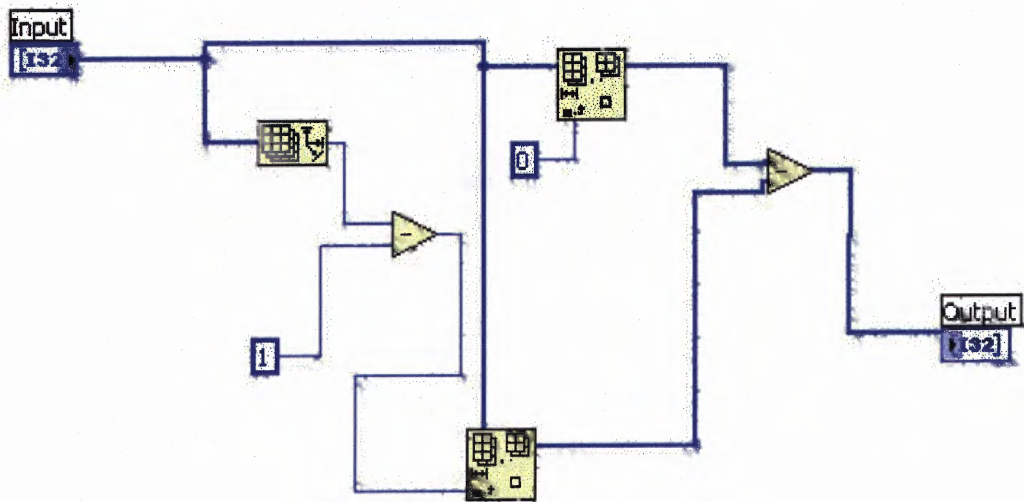


Figure F.6 Interval Rwave array block diagram.

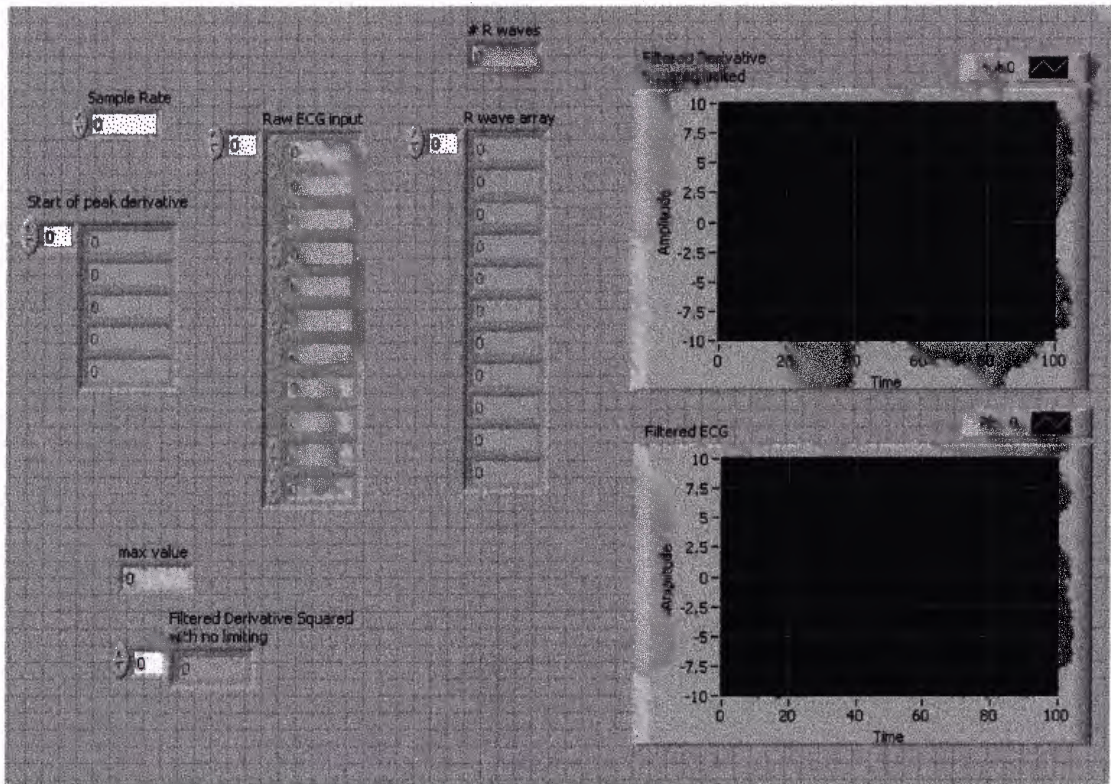


Figure F.7 Final Rdetect 032704 front panel.

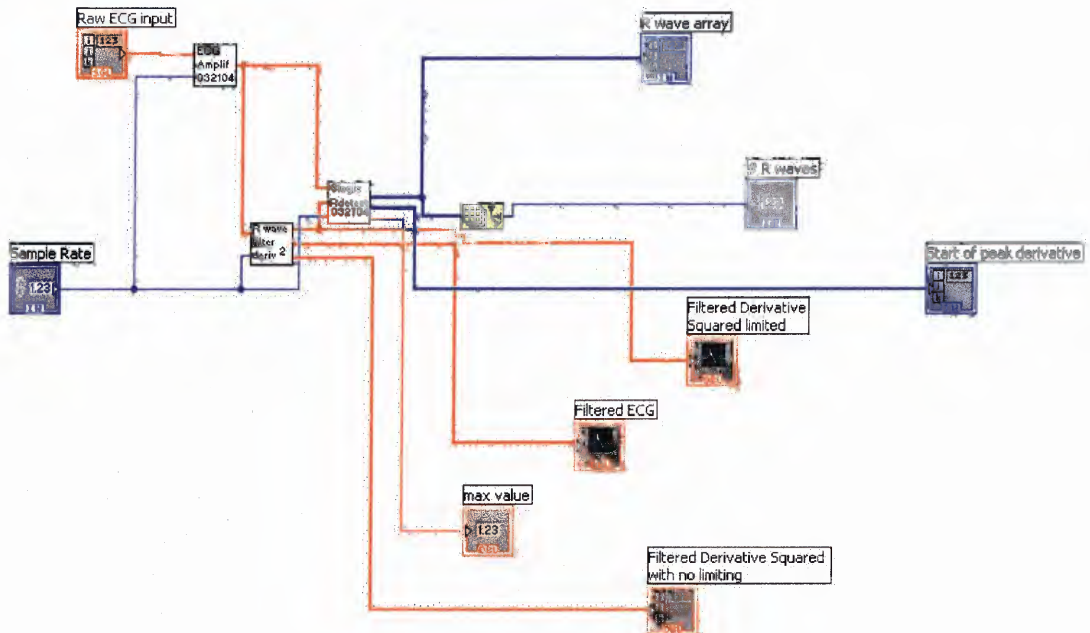


Figure F.8 Final Rdetect 032704 block diagram.

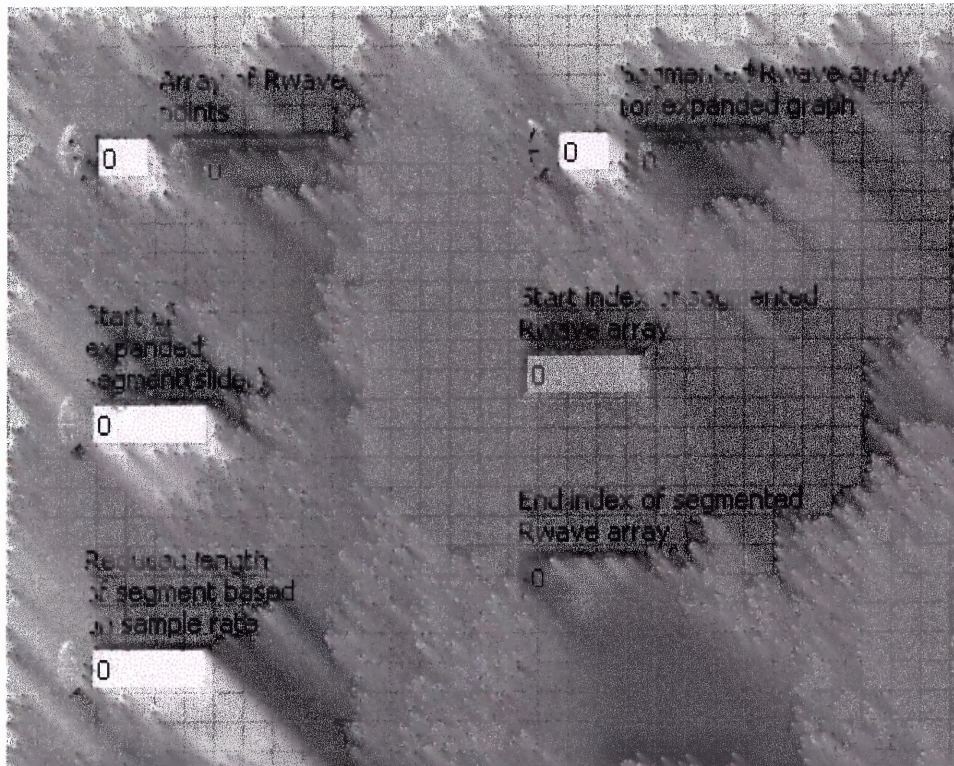


Figure F.9 Rwave array segment front panel.

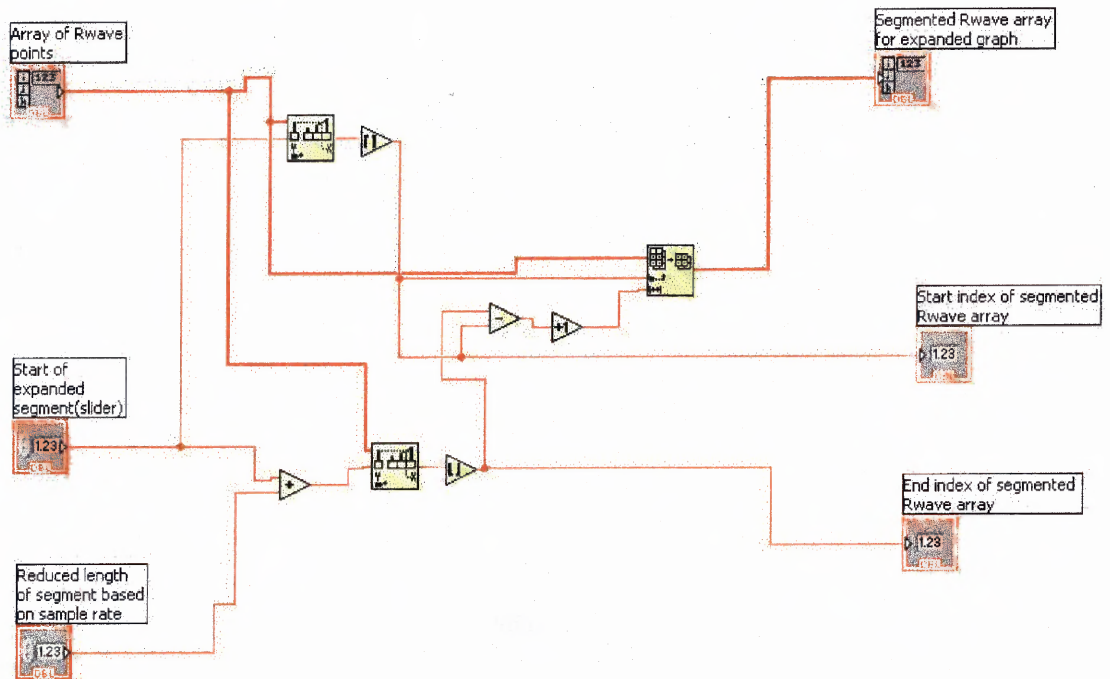


Figure F.10 Rwave array segment block diagram.

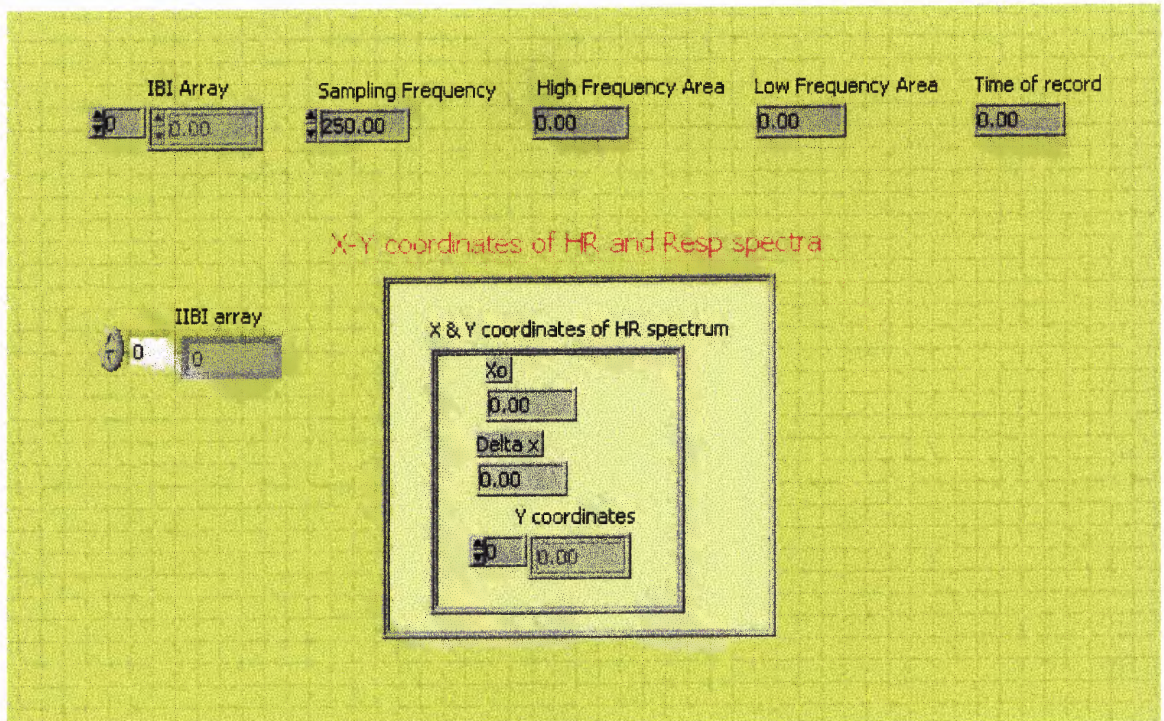


Figure F.11 Spectrum front panel.

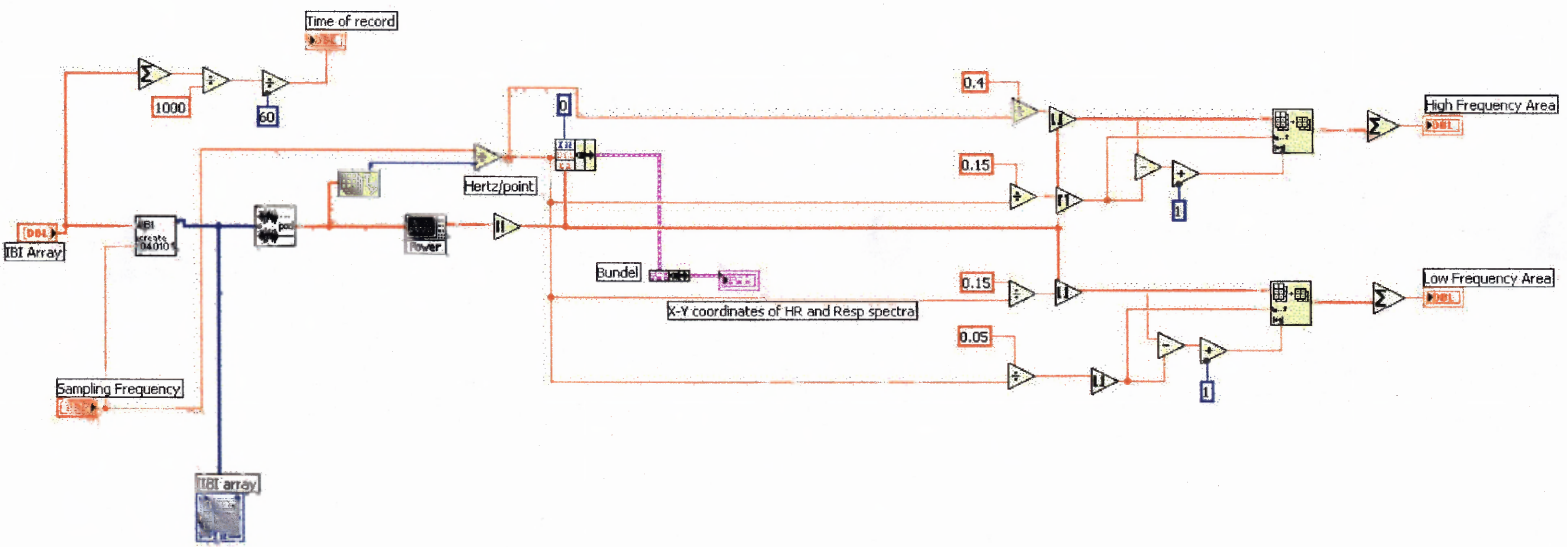


Figure F.12 Spectrum block diagram.

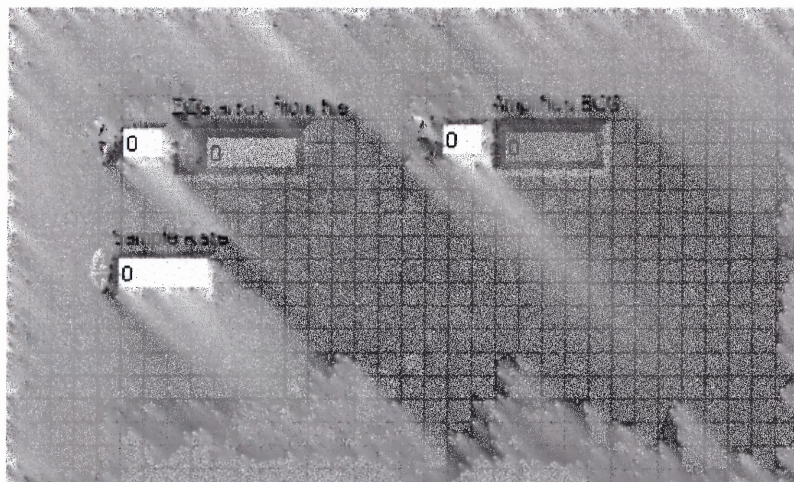


Figure F.13 EGG amplif 032104 front panel.

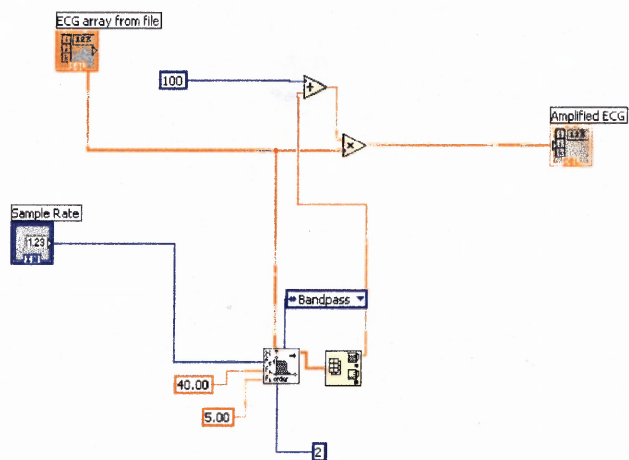


Figure F.14 EGG amplif 032104 block diagram.

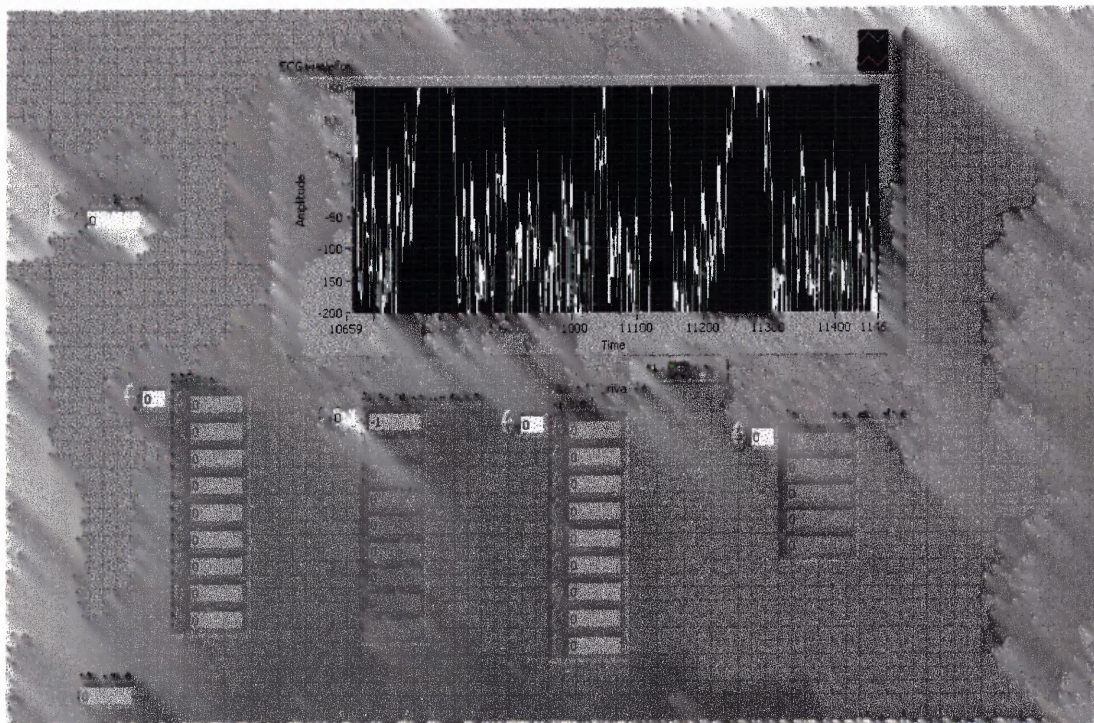


Figure F.15 Single Rdetect 032704 front panel.

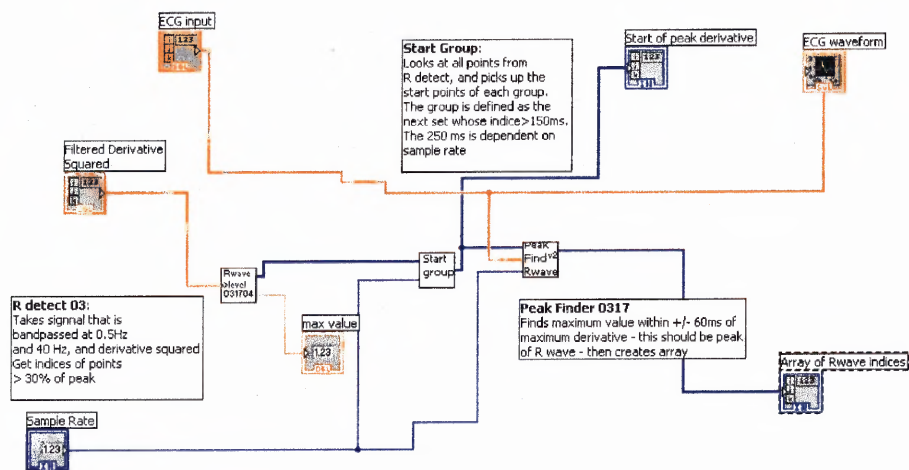


Figure F.16 Single Rdetect 032704 block diagram.

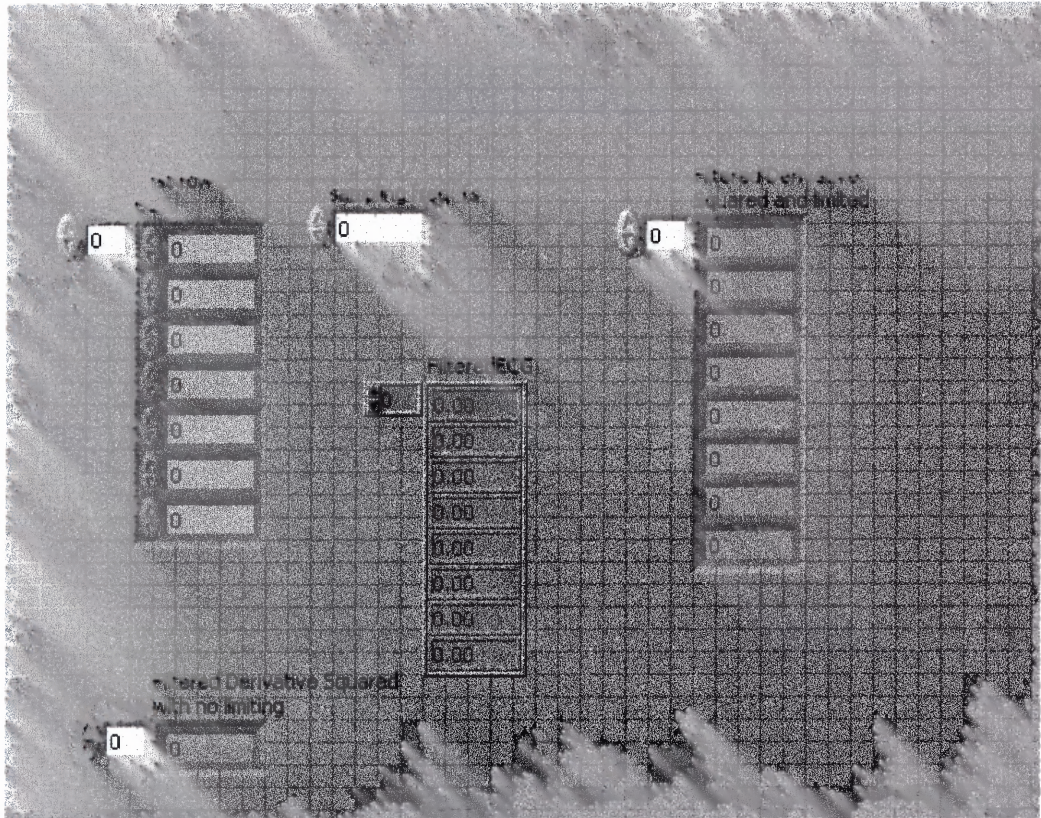


Figure F.17 R wave filter deriv 2 front panel.

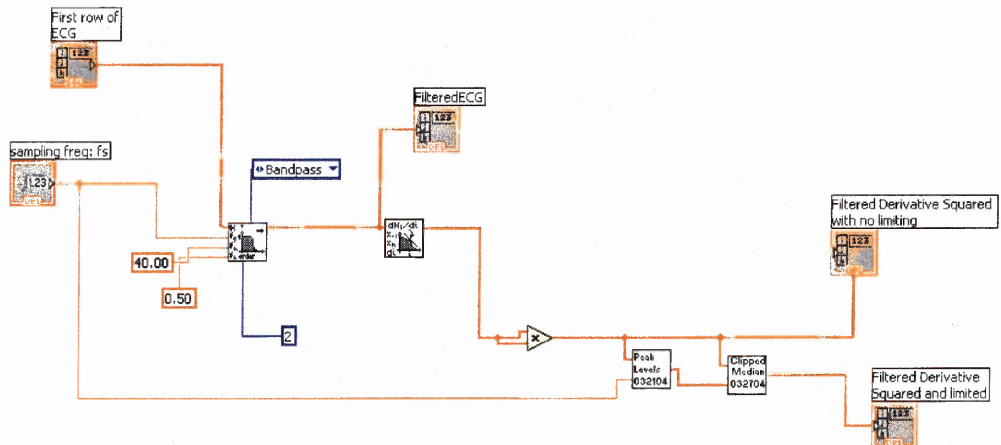


Figure F.18 R wave filter deriv 2 block diagram.

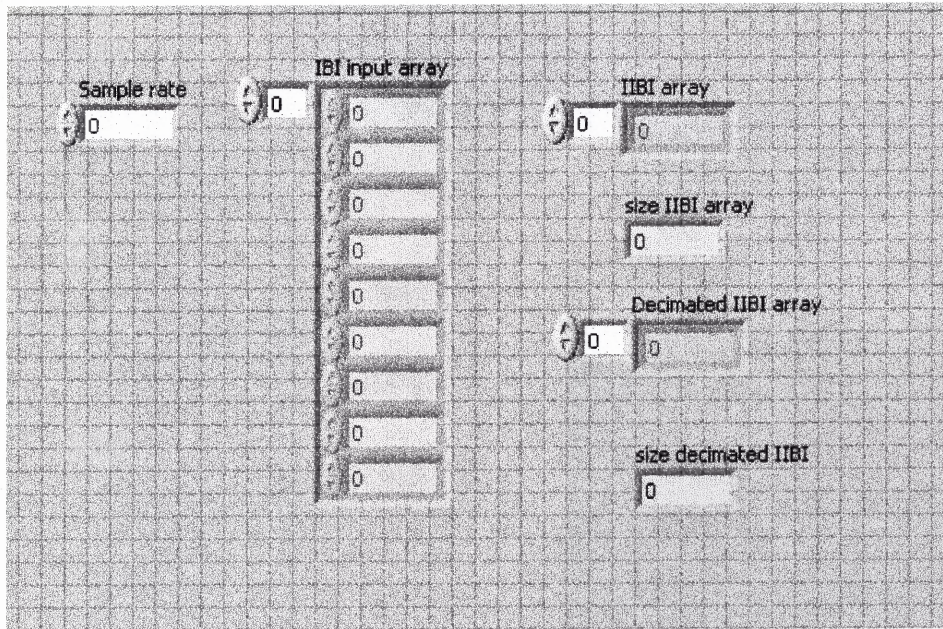


Figure F.19 IIBI create 040104 front panel.

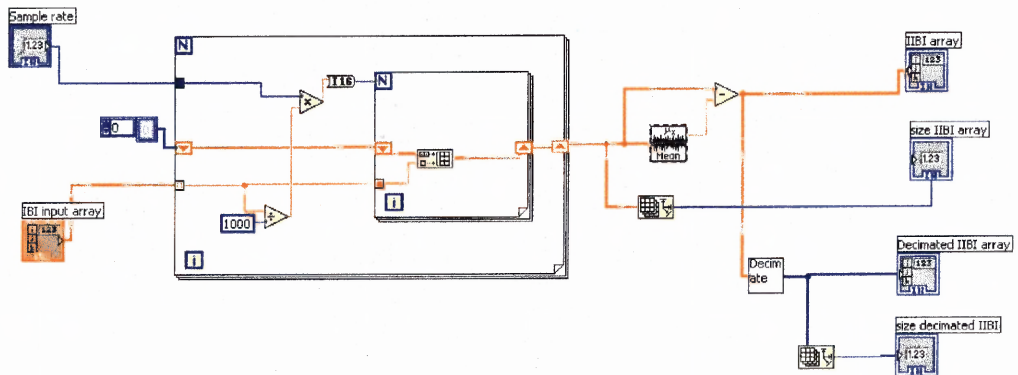


Figure F.20 IIBI create 040104 block diagram.

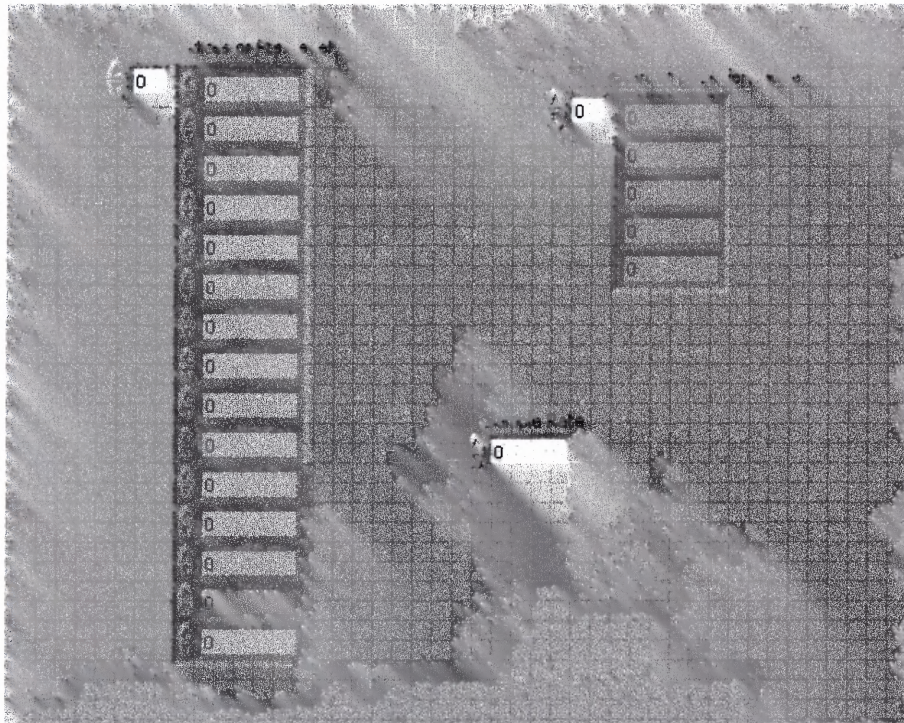


Figure F.21 Start group front panel.

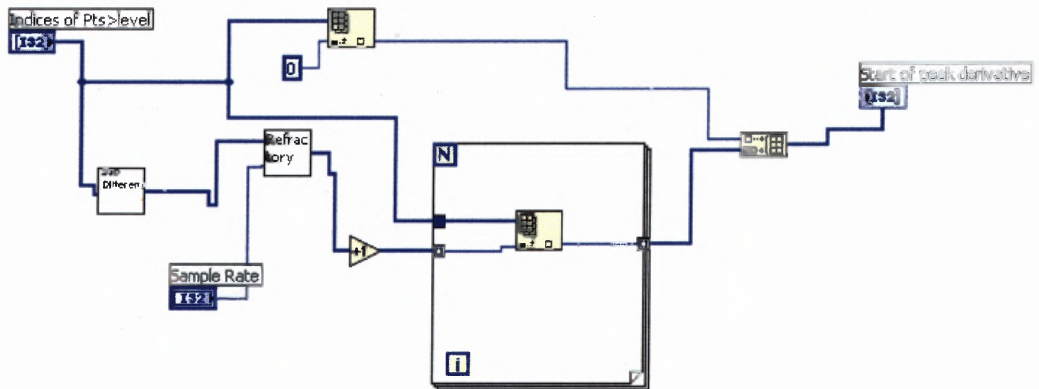


Figure F.22 Start group block diagram.

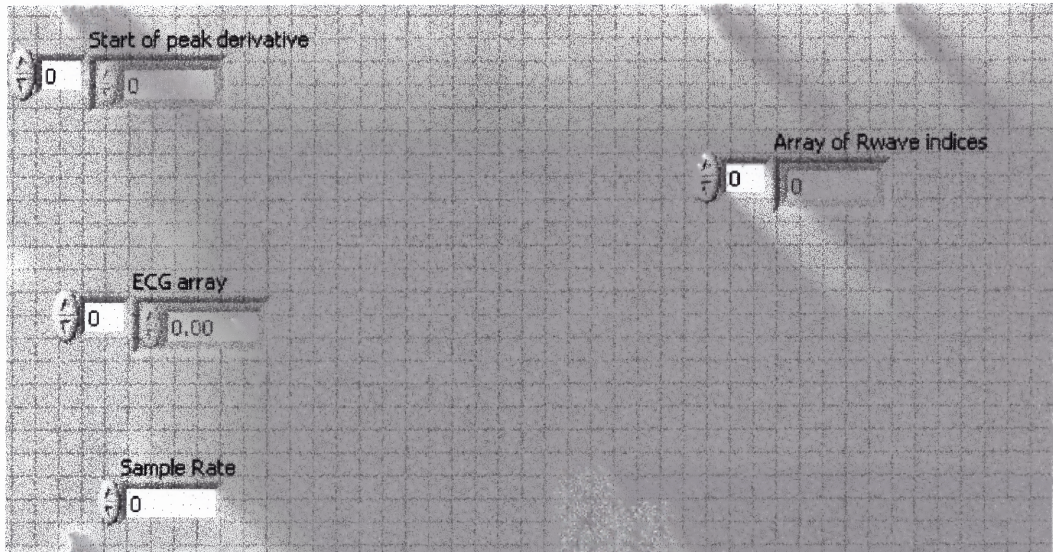


Figure F.23 Peak find v2 Rwave front panel.

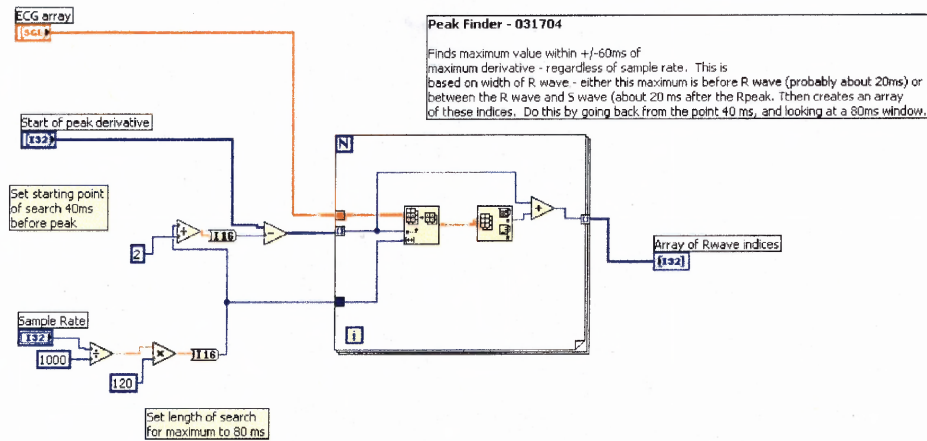


Figure F.24 Peak find v2 Rwave block diagram.

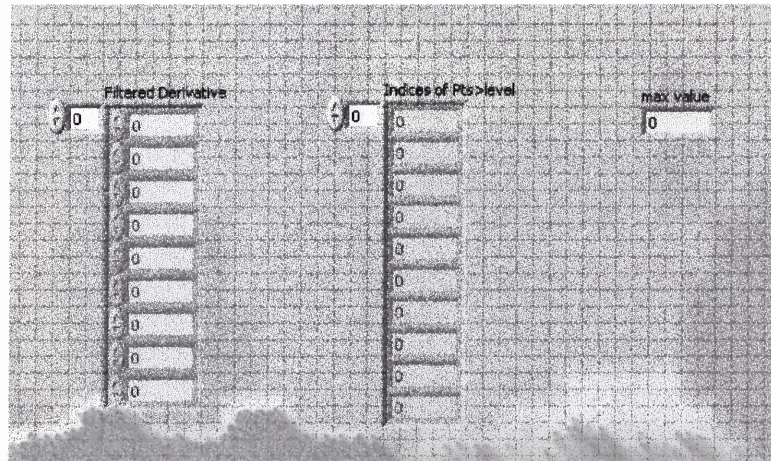


Figure F.25 Rwave >level 031704 front panel.

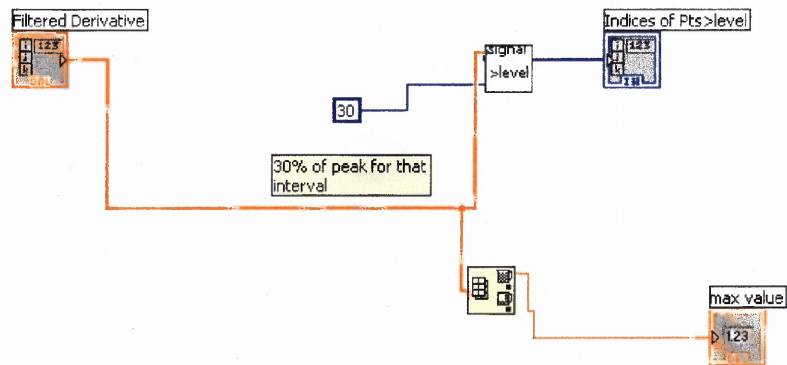


Figure F.26 Rwave >level 031704 block diagram.

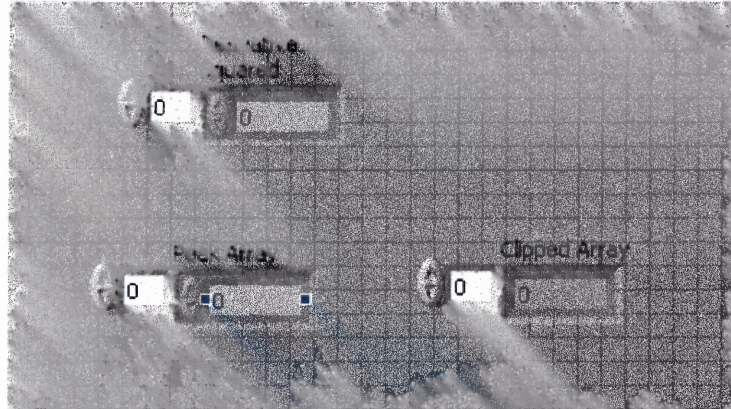


Figure F.27 Clipped median 032704 front panel.

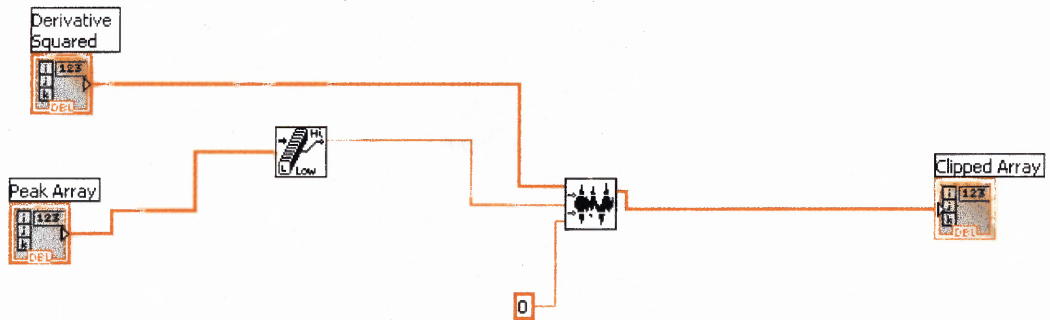


Figure F.28 Clipped median 032704 block diagram.

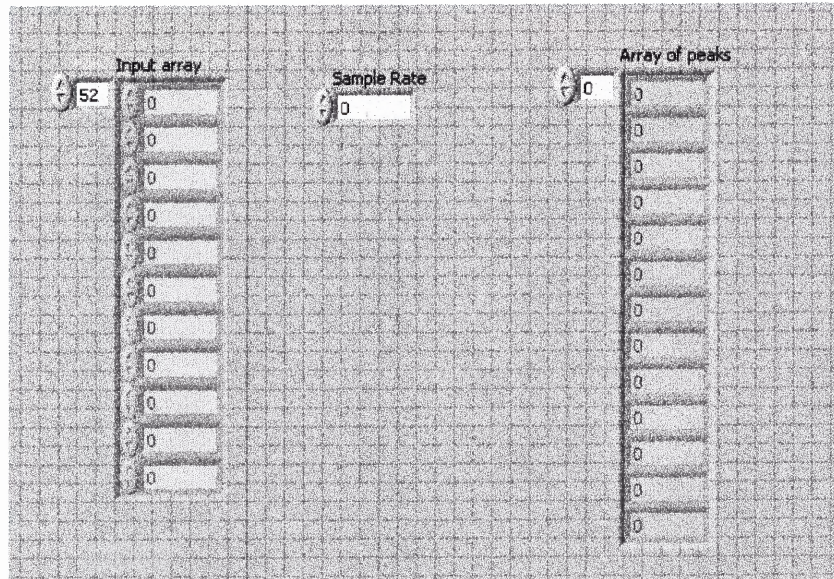


Figure F.29 Peak levels 032104 front panel.

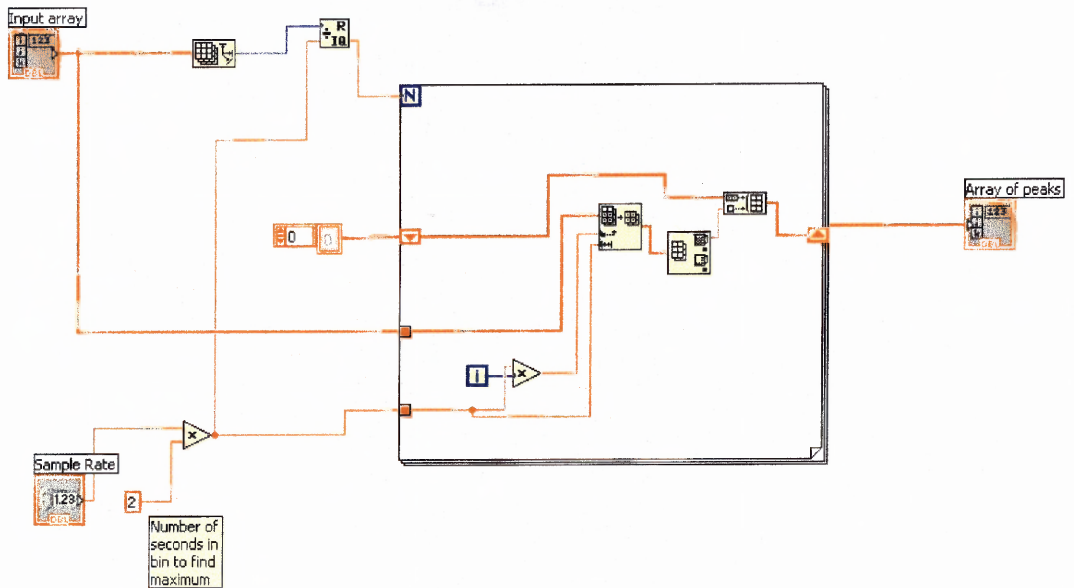


Figure F.30 Peak levels 032104 block diagram.



Figure F.31 Decimate front panel.

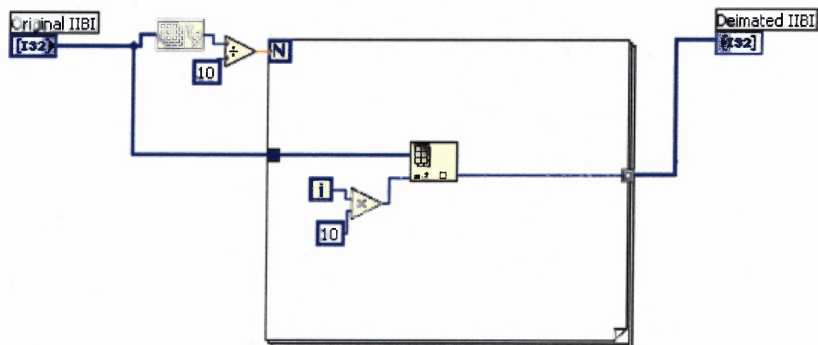


Figure F.32 Decimate block diagram.

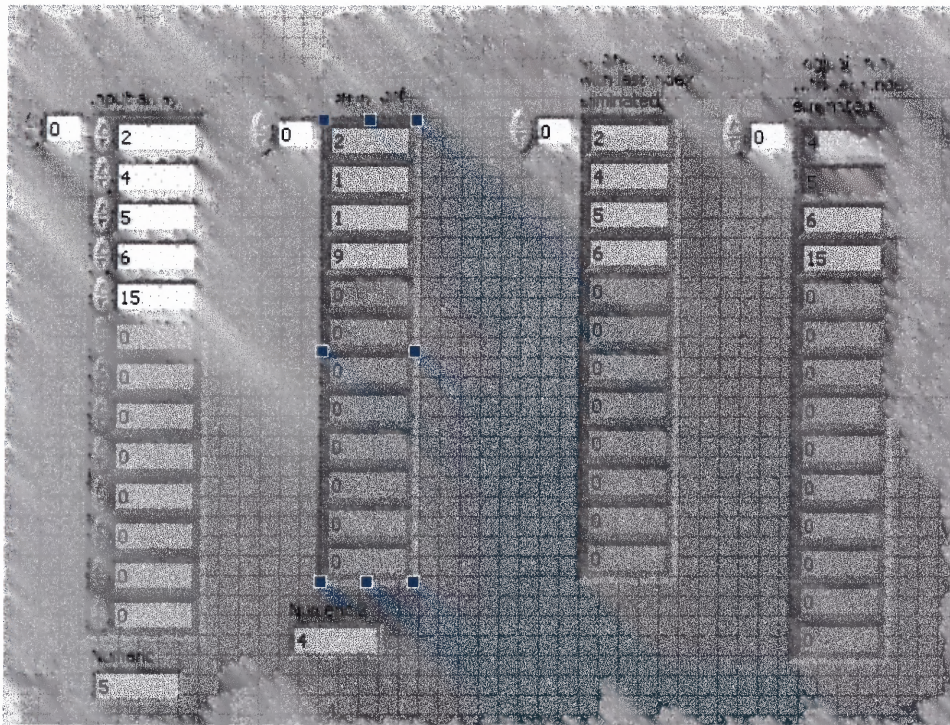


Figure F.33 Sub difference front panel.

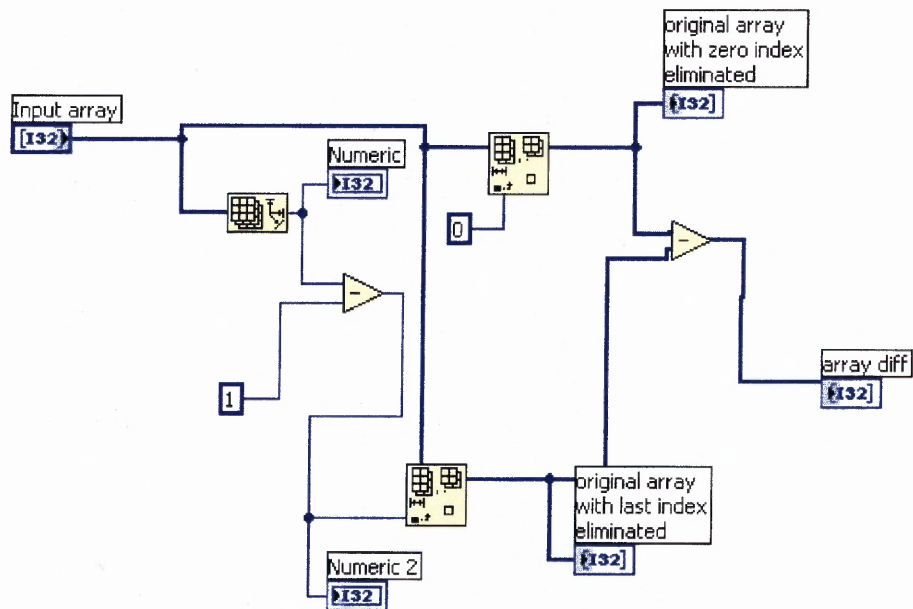


Figure F.34 Sub difference block diagram.

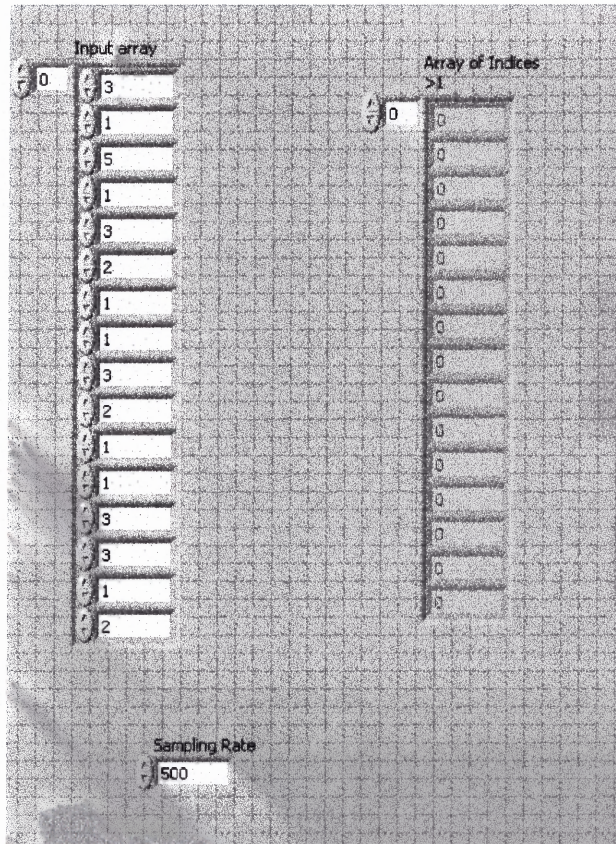


Figure F.35 Refractory front panel.

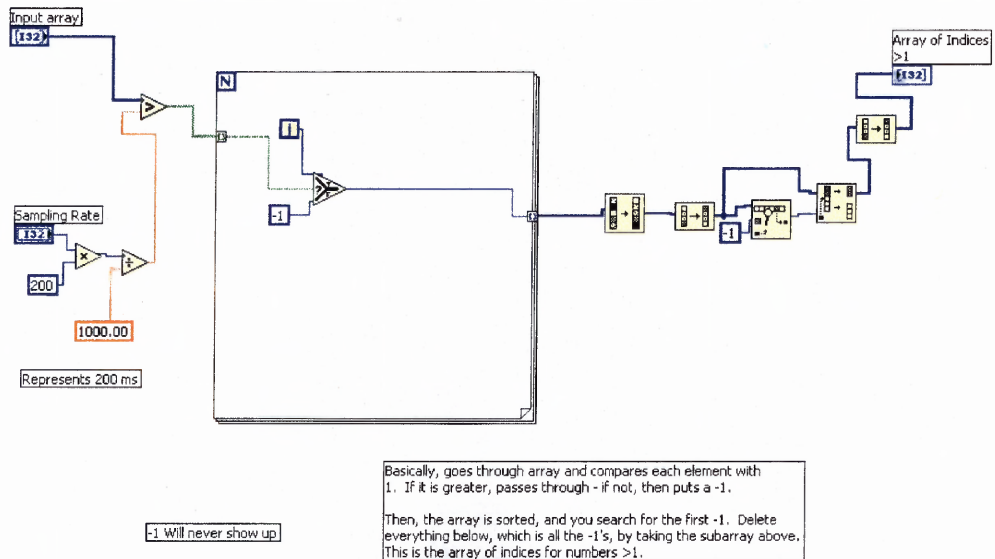


Figure F.36 Refractory block diagram.

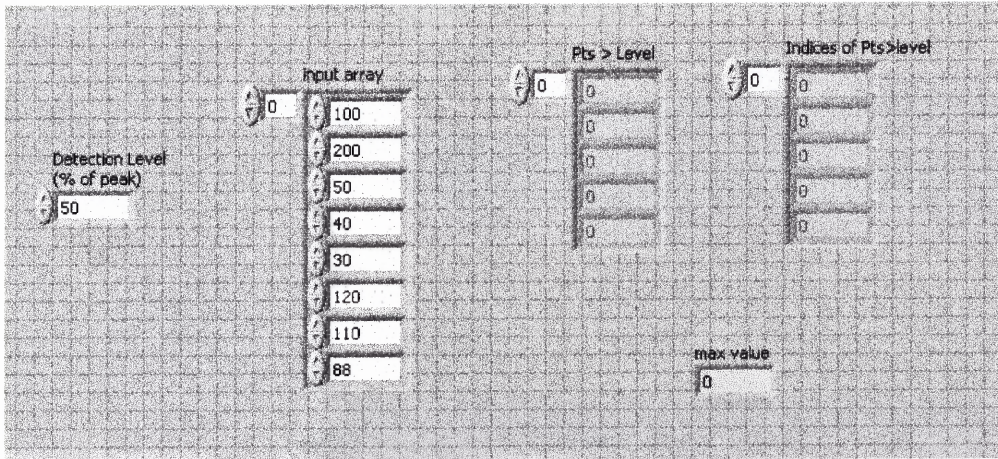


Figure F.37 Signal greater than level front panel.

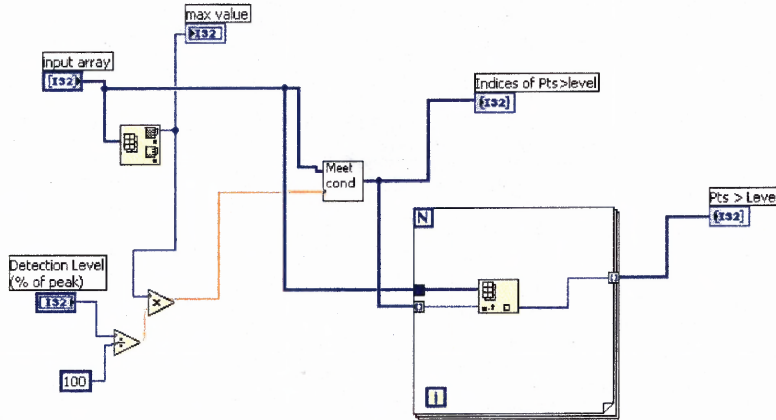


Figure F.38 Signal greater than level block diagram.

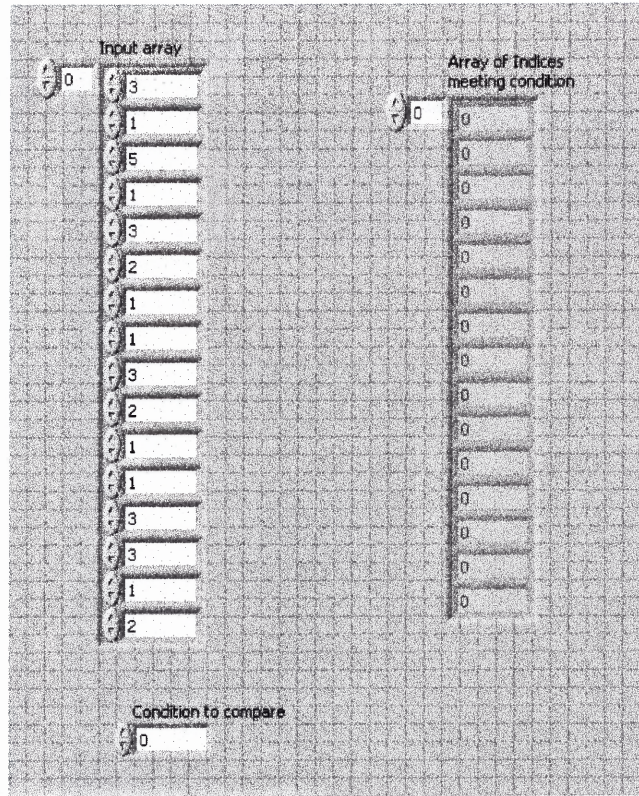


Figure F.39 Meet conditions front panel.

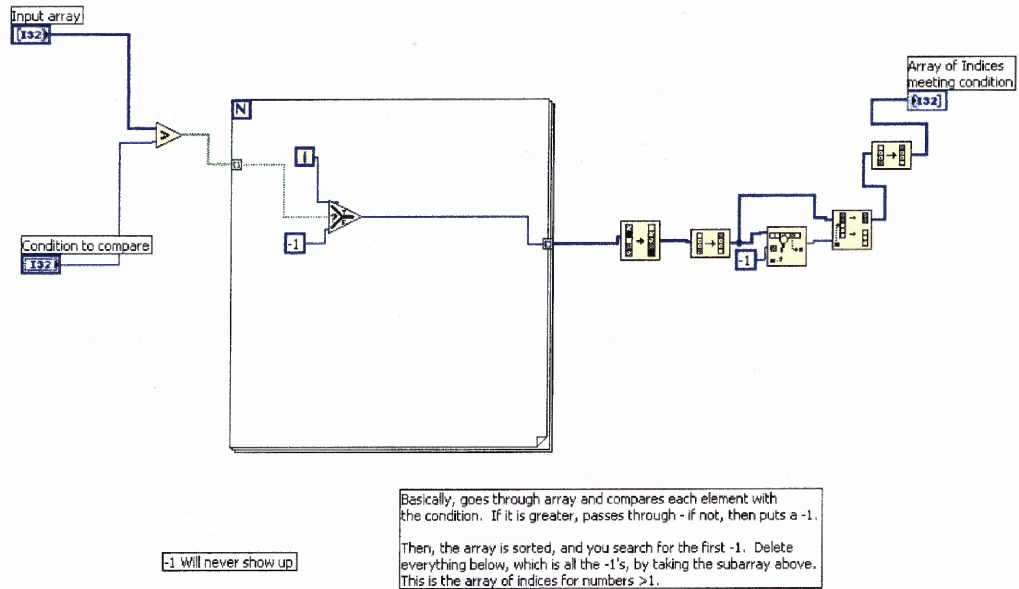


Figure F.40 Meet conditions block diagram.

APPENDIX G

IBI FILTERING PROGRAM

This appendix presents the Matlab code used to filter the data obtained from the Polar S810 heart rate monitor.

```
for i=5:length(Data)
    test = Data(i)/mean(Data(i-4:i-1));
    if test > 1.7
        % DataPoint = 3718
        temp = Data(i)/round(test);
        DataTemp=Data(1:(i-1));
        for j=1:round(test)
            DataTemp=[DataTemp; temp];
        end
        Data=[DataTemp; Data((i+1):length(Data))];
    end
    % if test < .75

end
```

APPENDIX H

PLOTS FROM TIME FREQUENCY ANALYSIS

This appendix presents the outputs for all participant data that was analyzed using both the STFT and the wavelet transform, time-frequency methods.

H.1 STFT Results

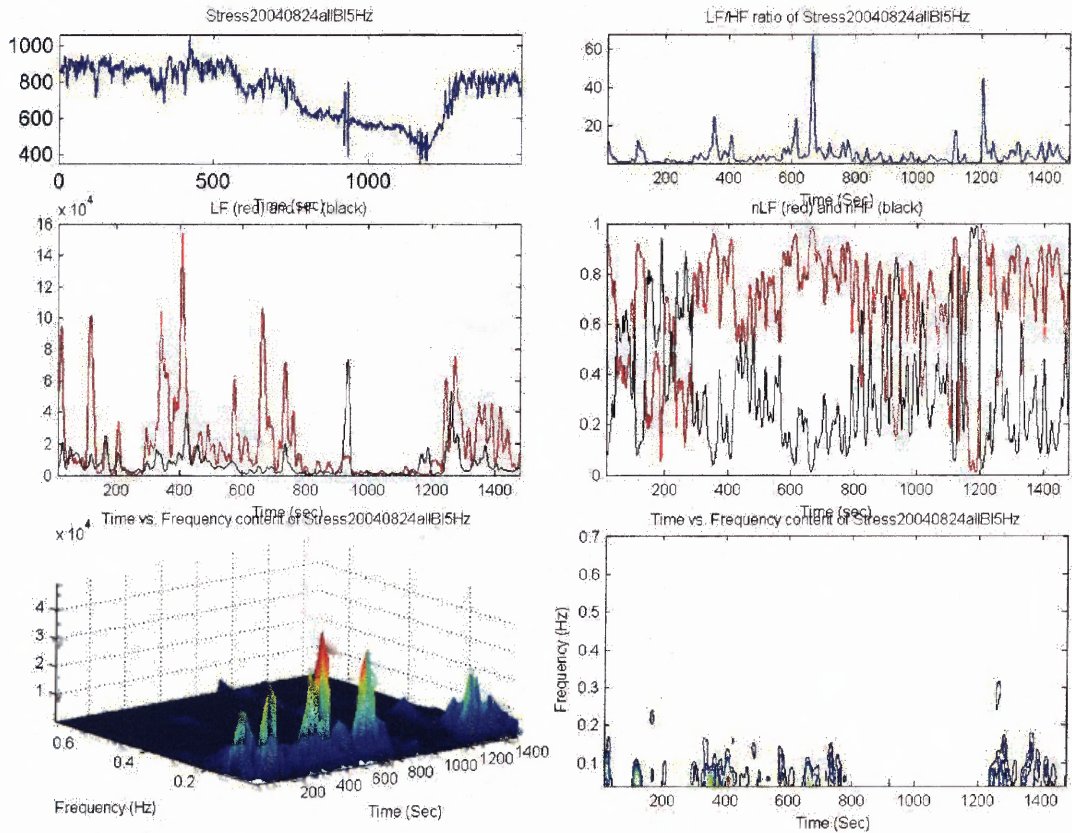


Figure H.1 STFT output for subject 1.

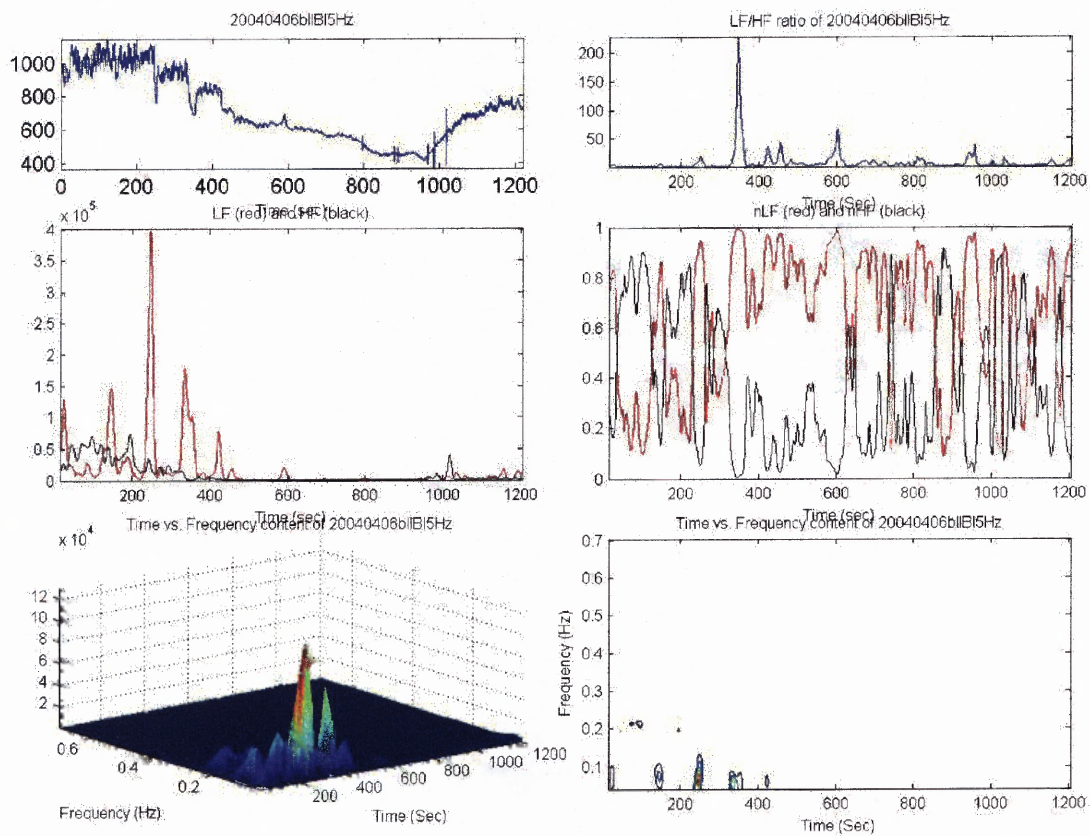


Figure H.2 STFT output for subject 2.

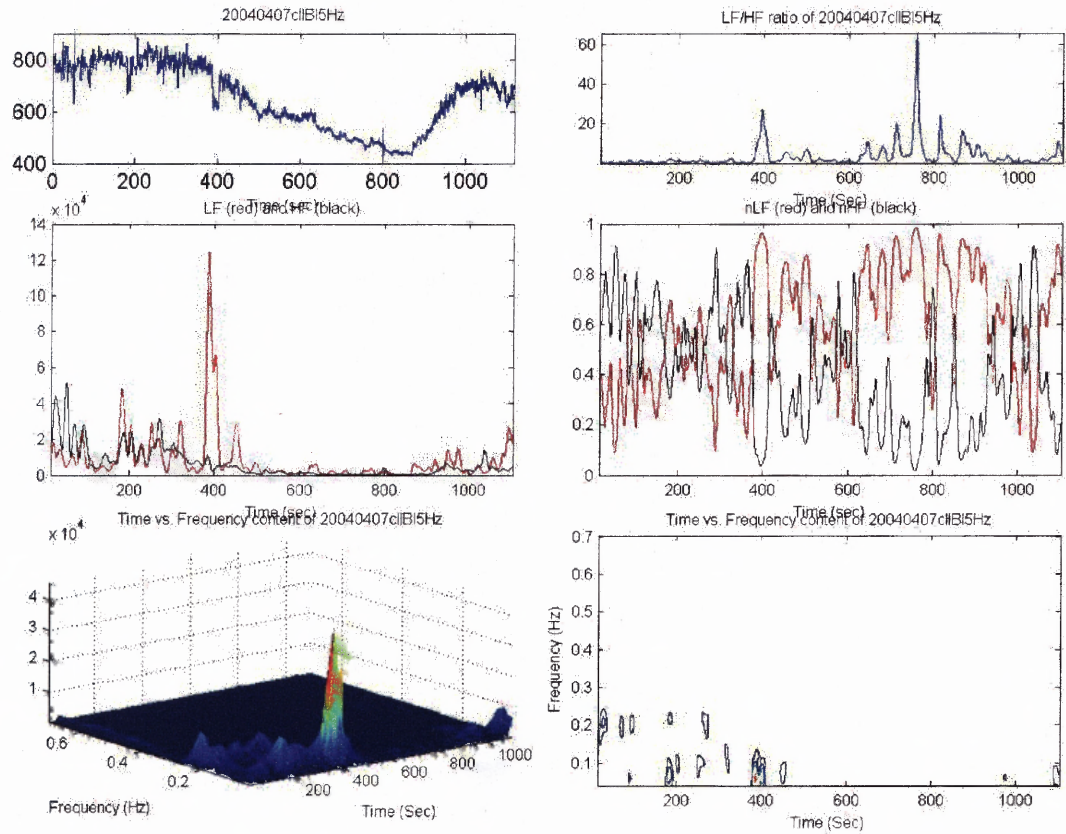


Figure H.3 STFT output for subject 3.

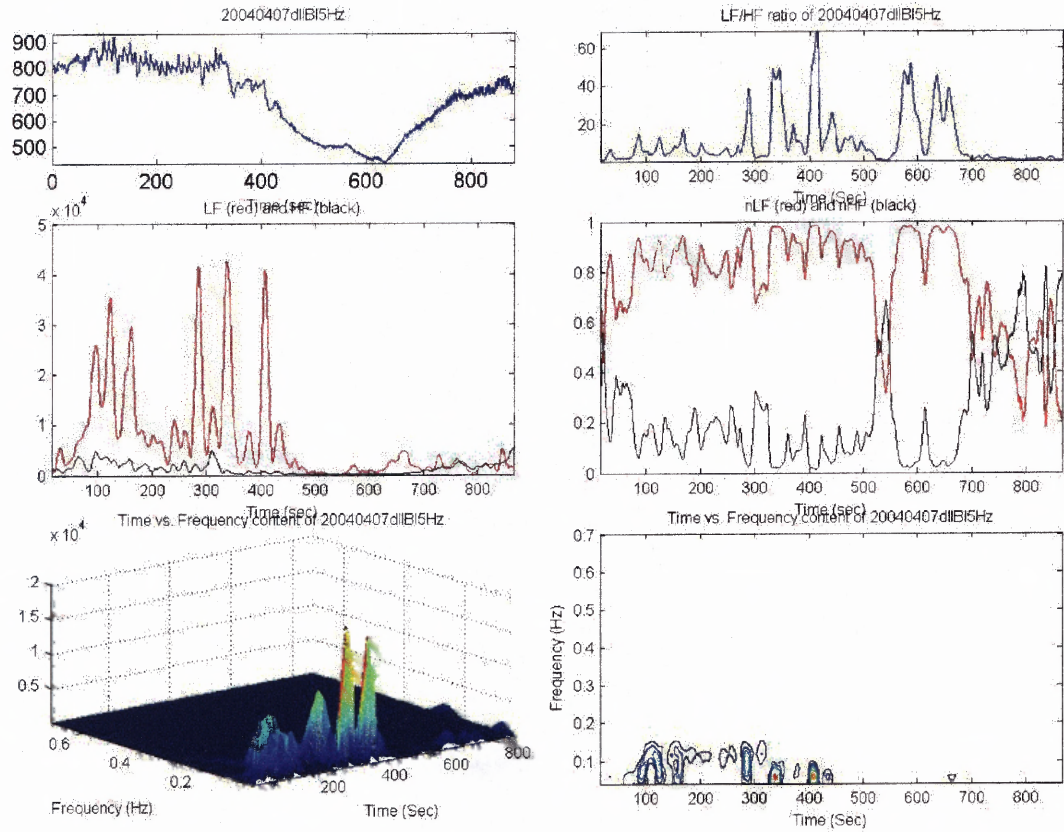


Figure H.4 STFT output for subject 4.

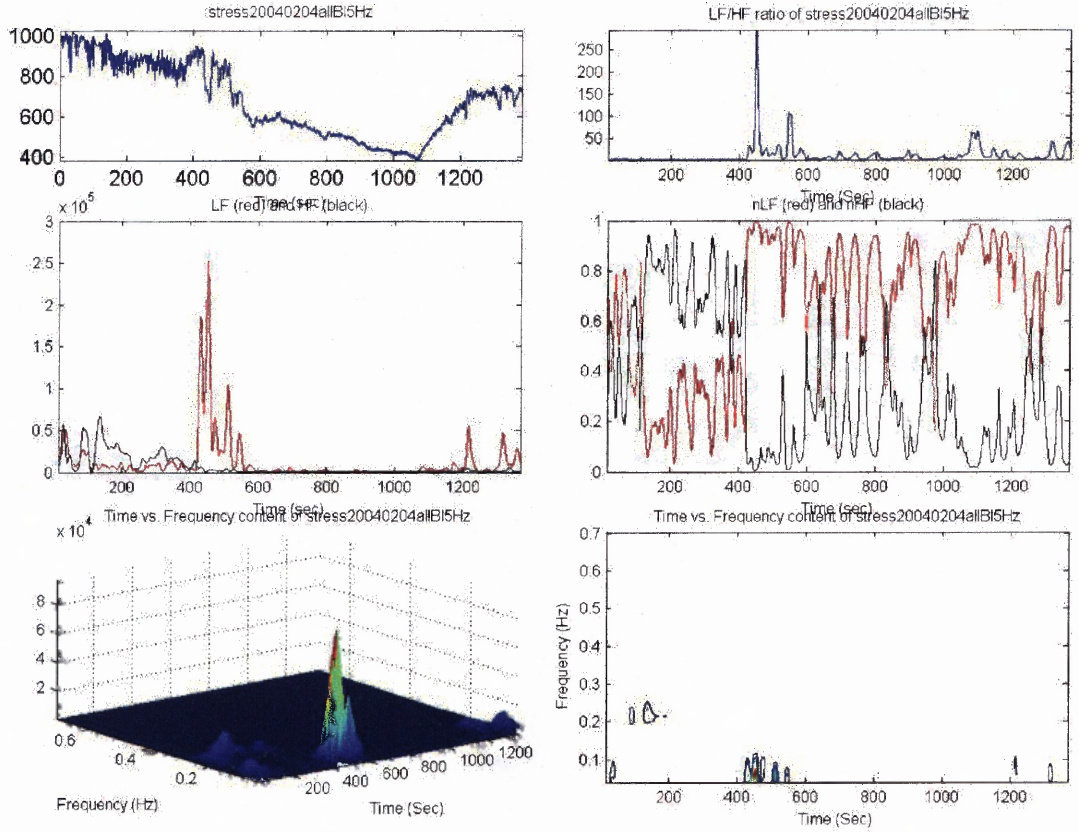


Figure H.5 STFT output for subject 5.

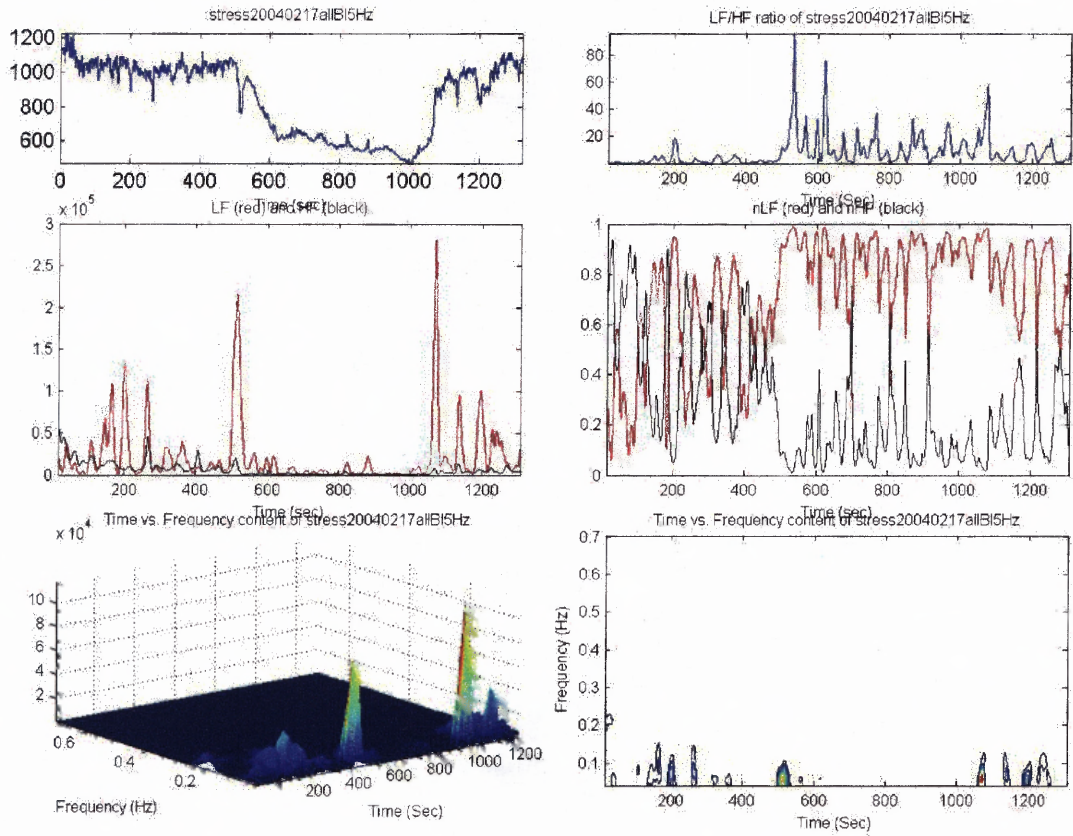


Figure H.6 STFT output for subject 6.

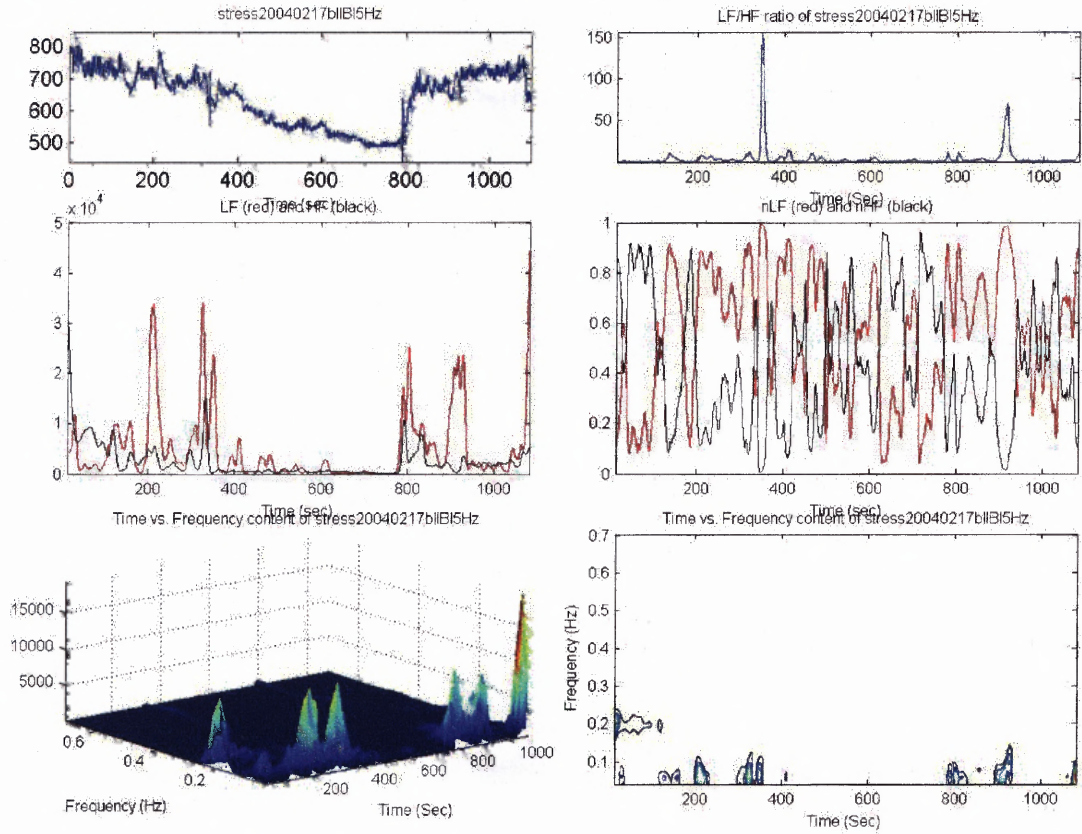


Figure H.7 STFT output for subject 7.

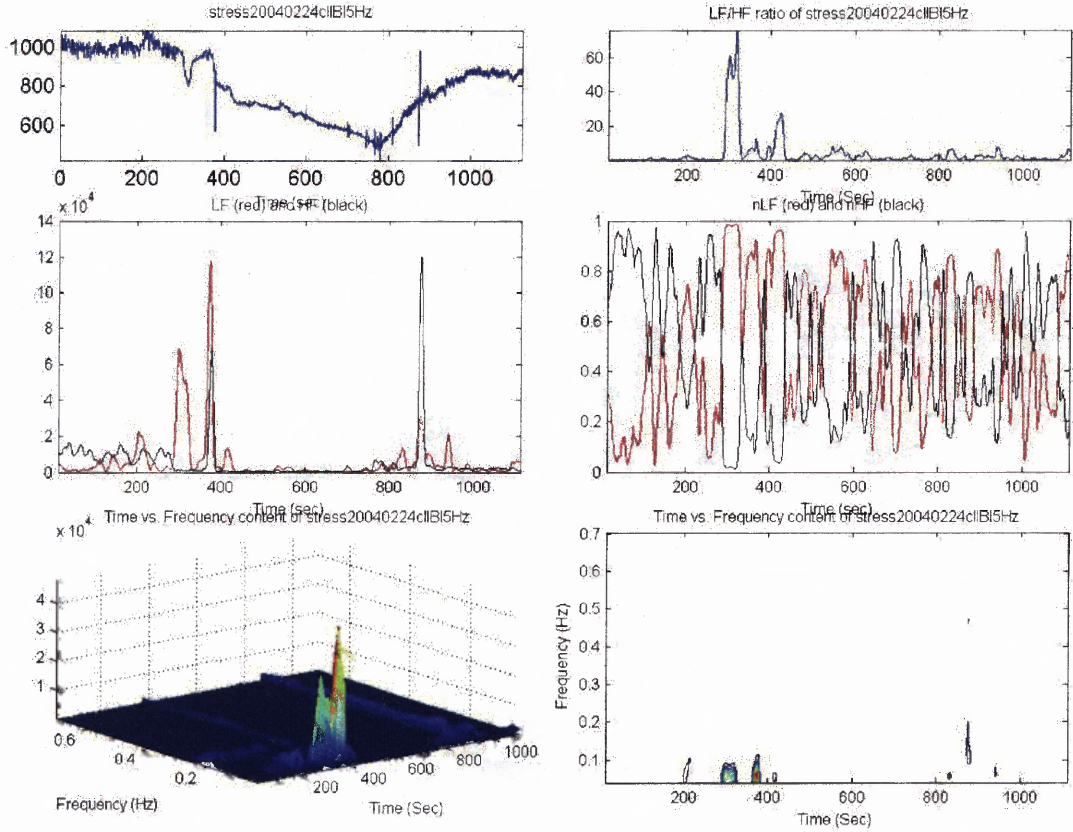


Figure H.8 STFT output for subject 8.

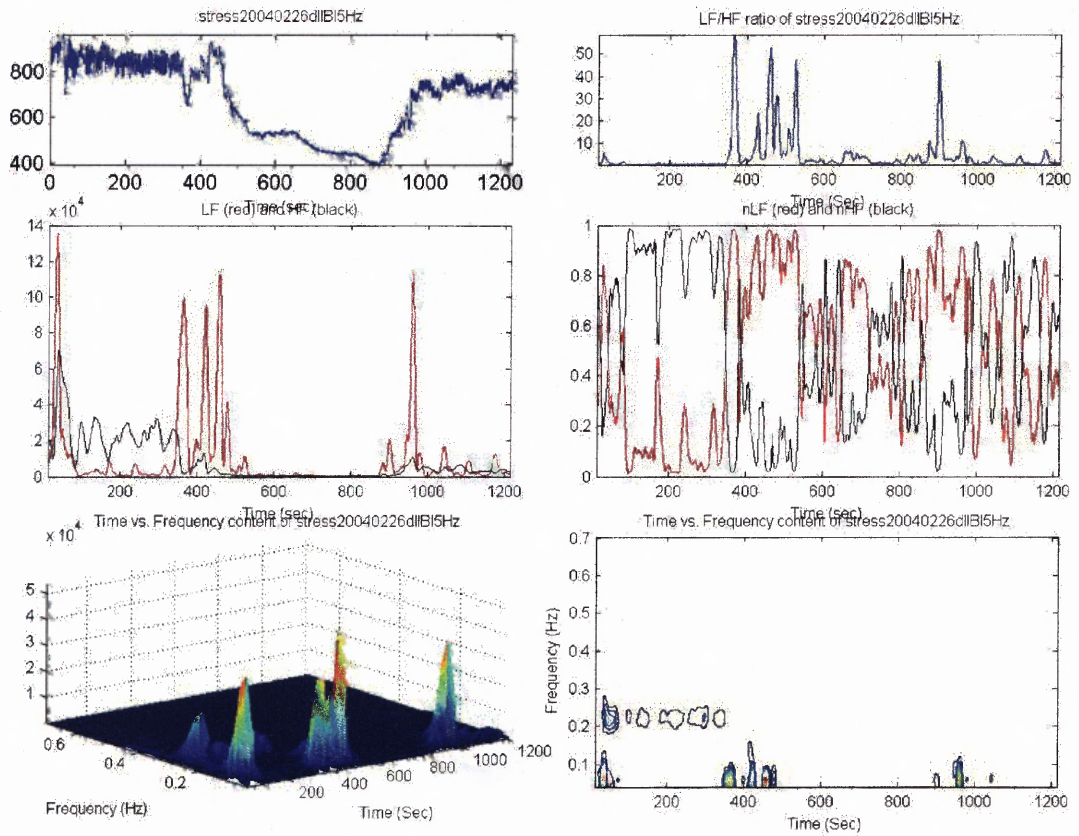


Figure H.9 STFT output for subject 9.

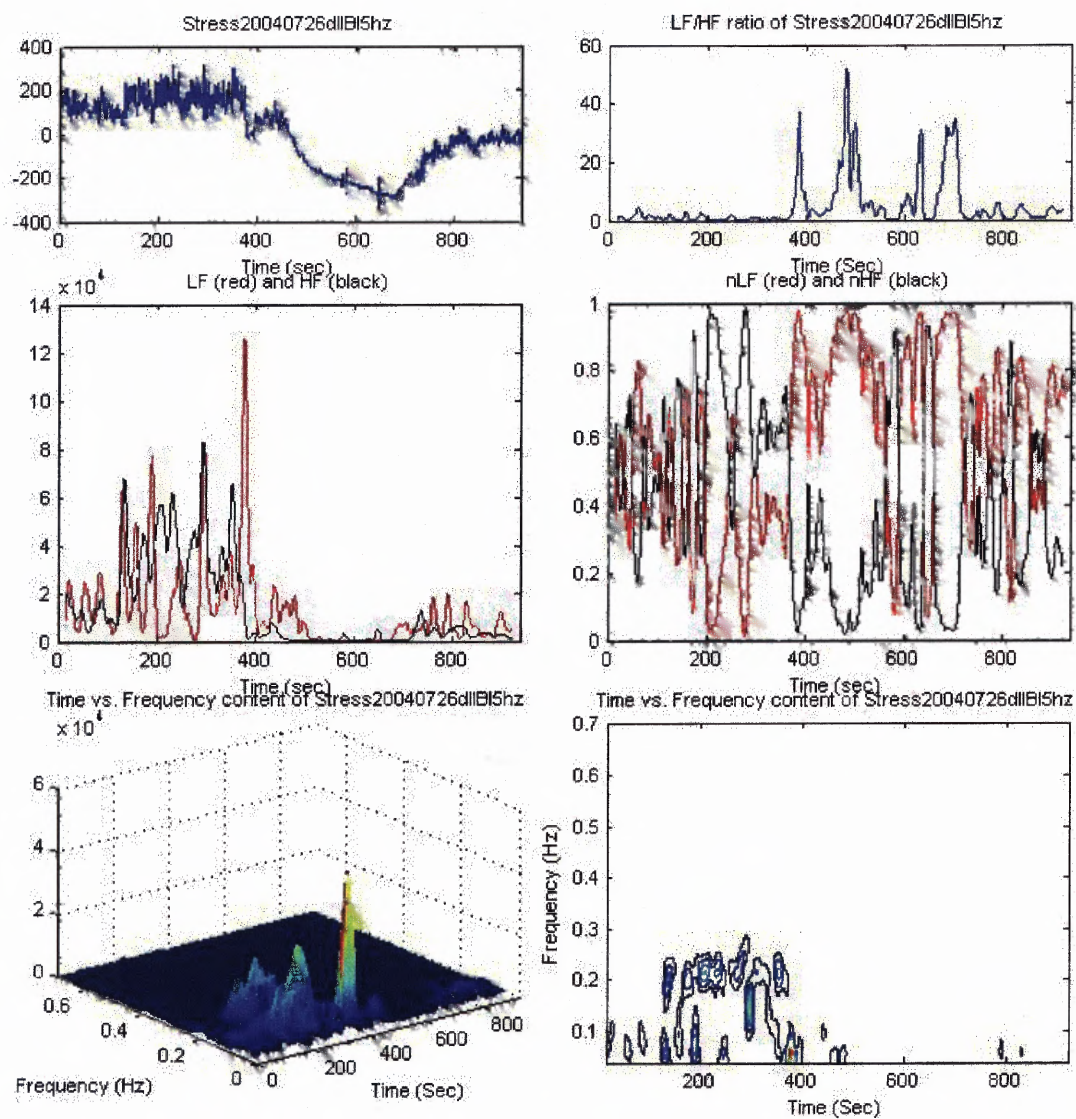


Figure H.10 STFT output for subject 10.

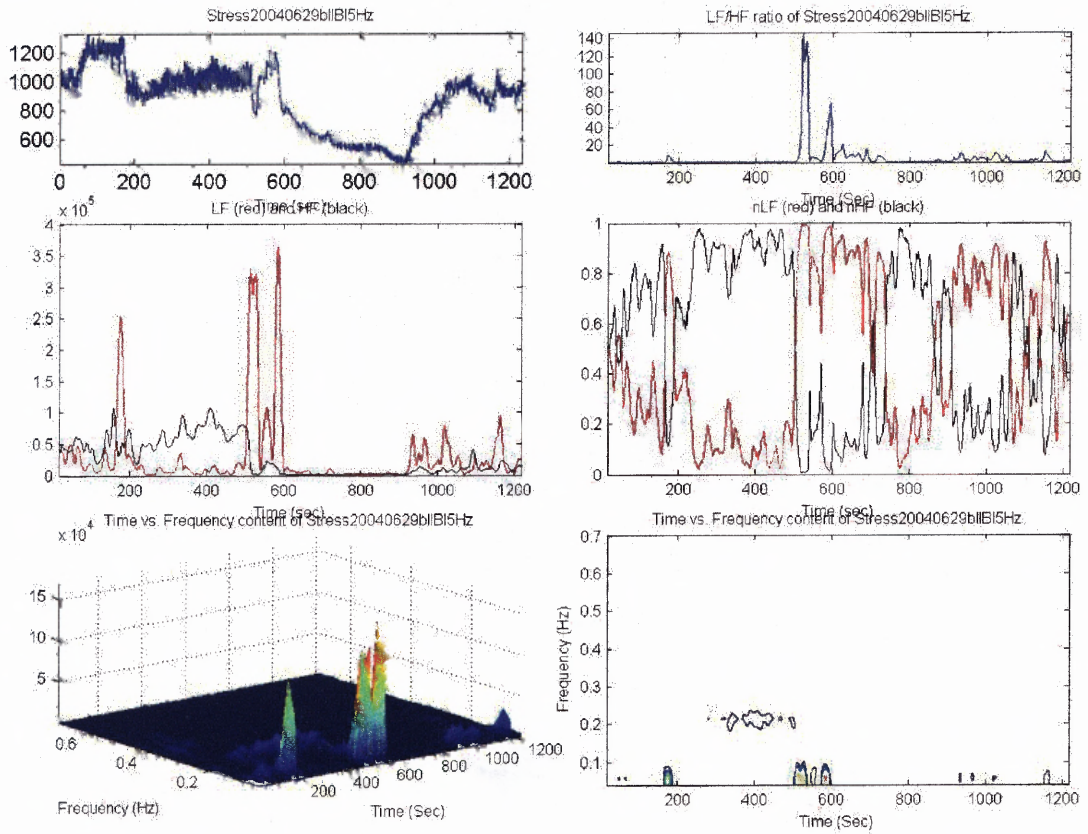


Figure H.11 STFT output for subject 11.

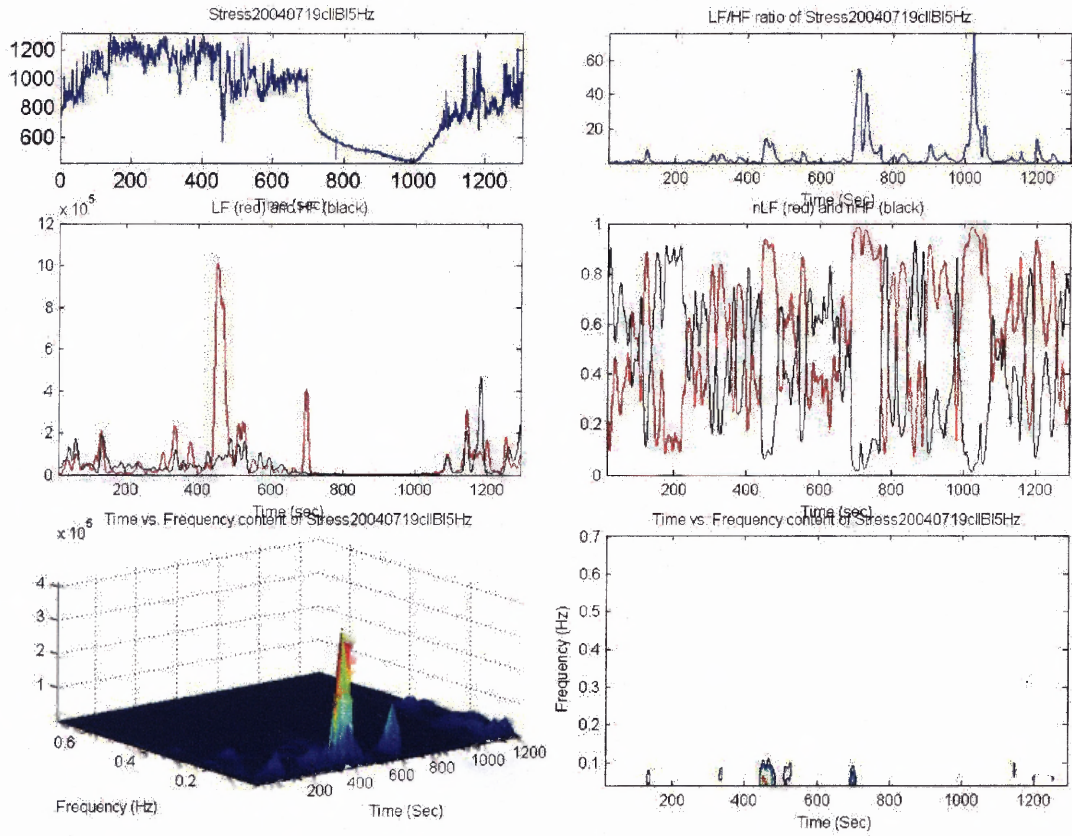


Figure H.12 STFT output for subject 12.

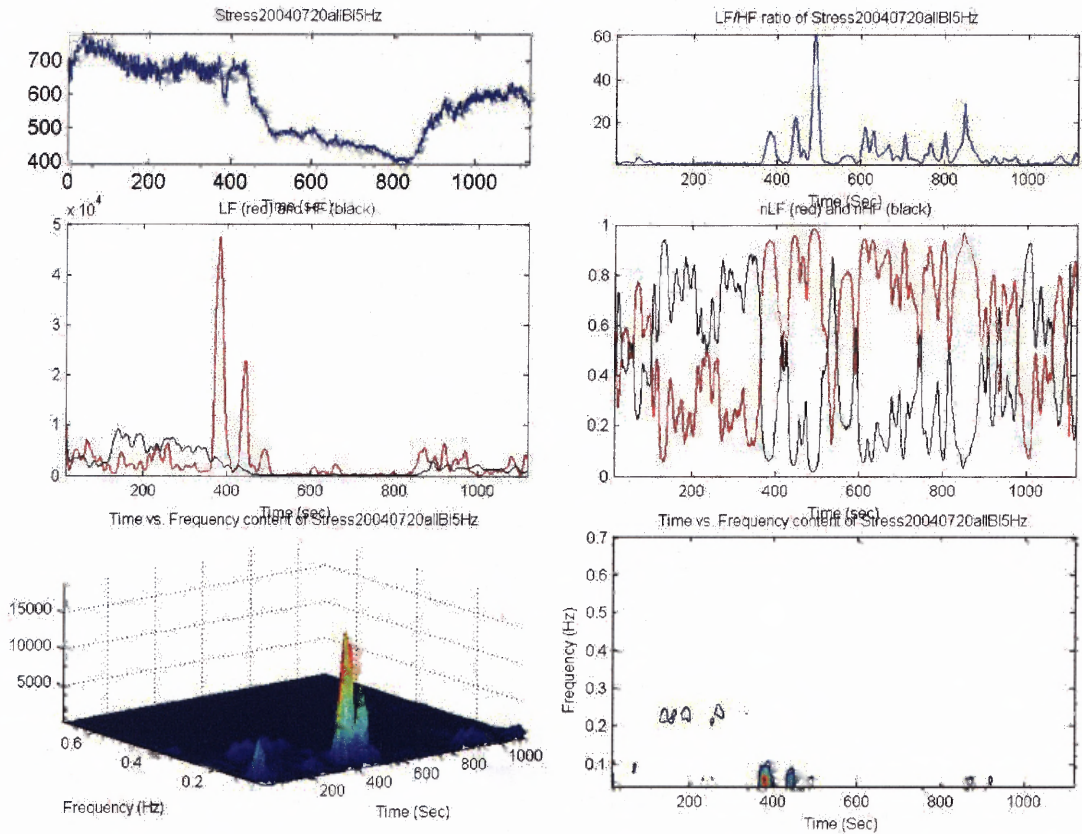


Figure H.13 STFT output for subject 13.

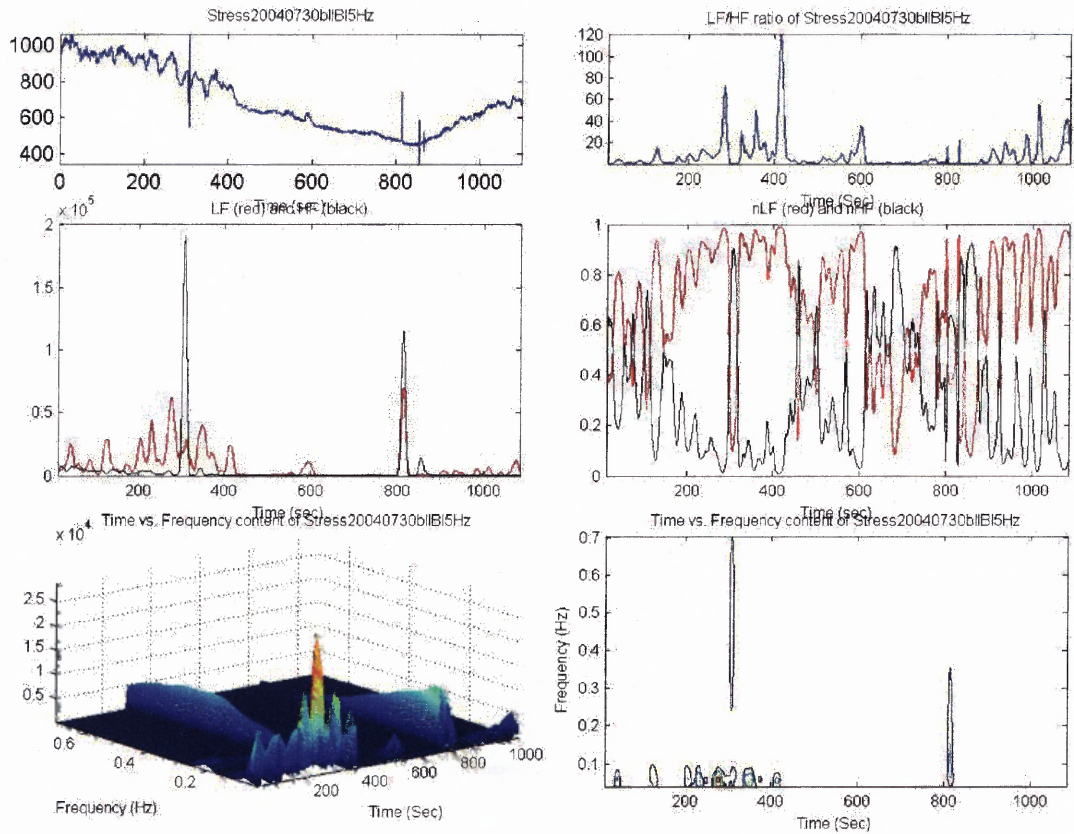


Figure H.14 STFT output for subject 14.

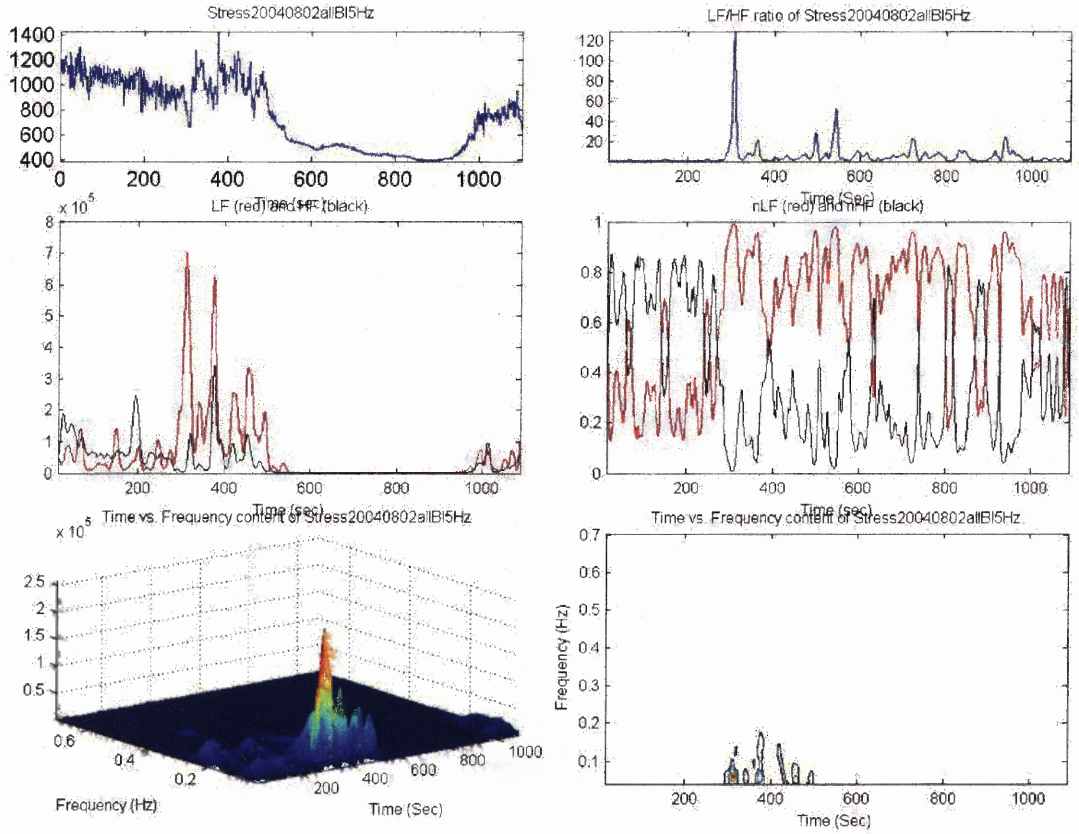


Figure H.15 STFT output for subject 15.

H.2 Wavelet Results

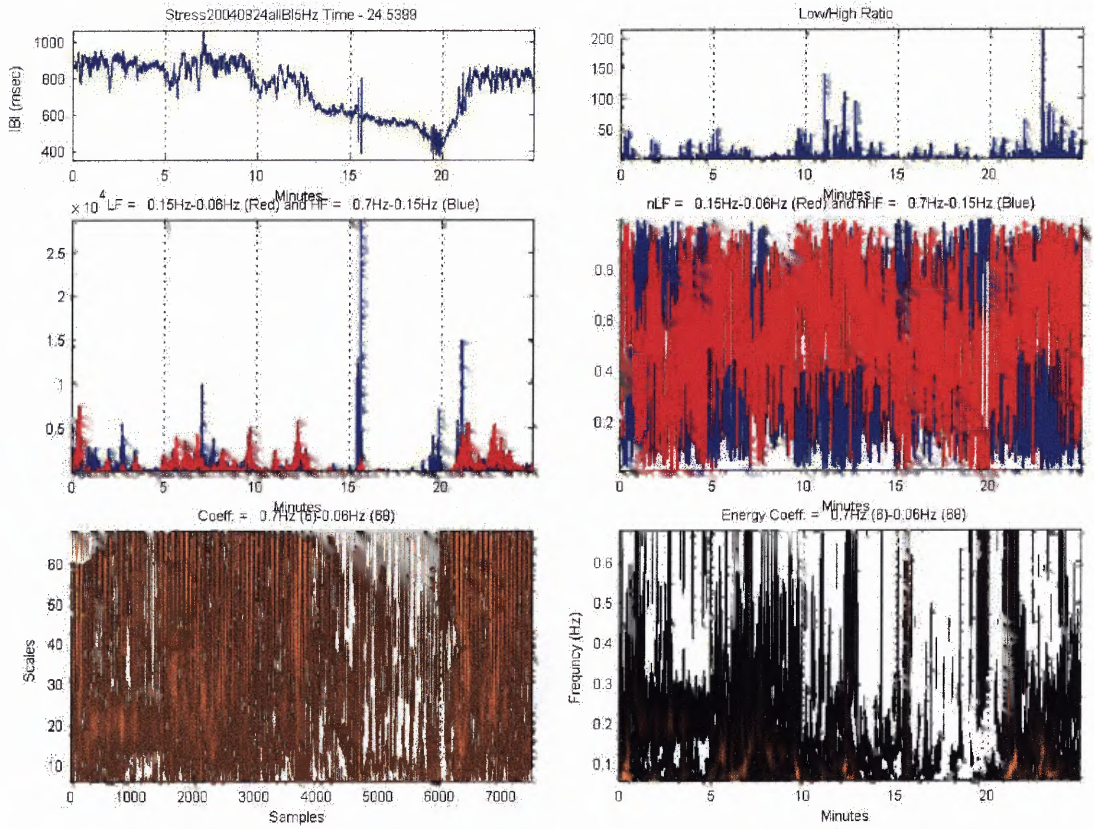


Figure H.16 STFT output for subject 16.

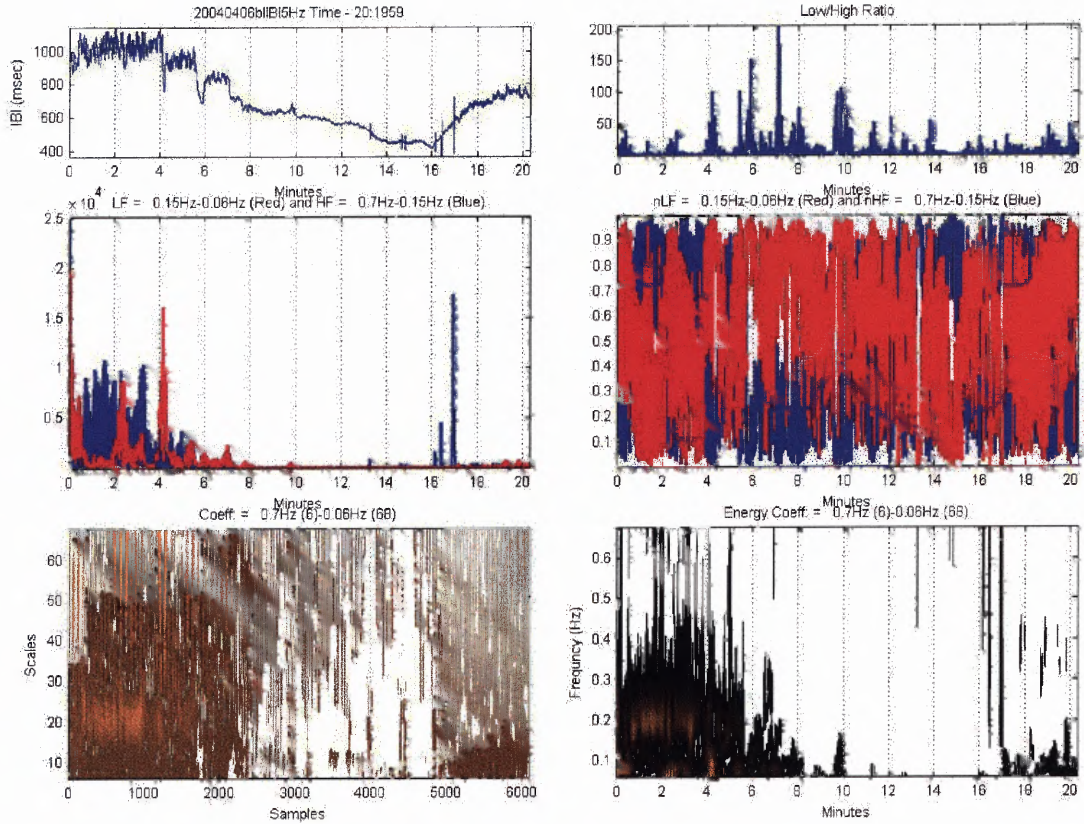


Figure H.17 STFT output for subject 17.

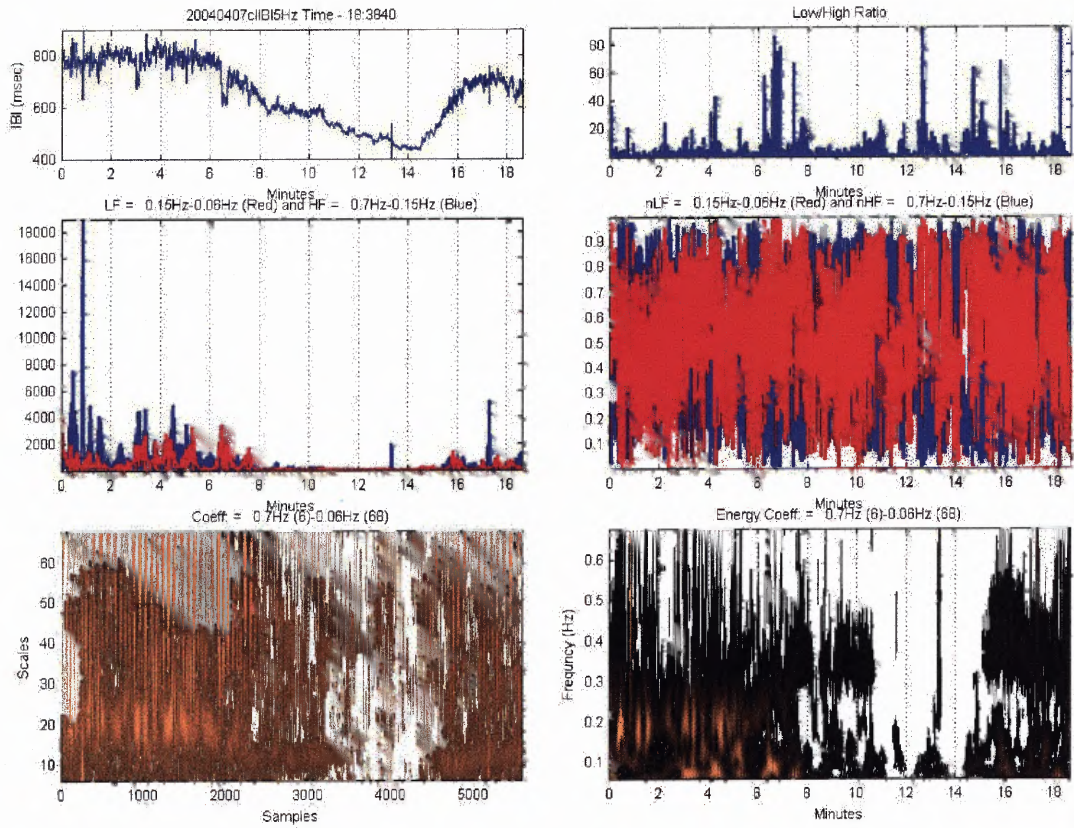


Figure H.18 STFT output for subject 18.

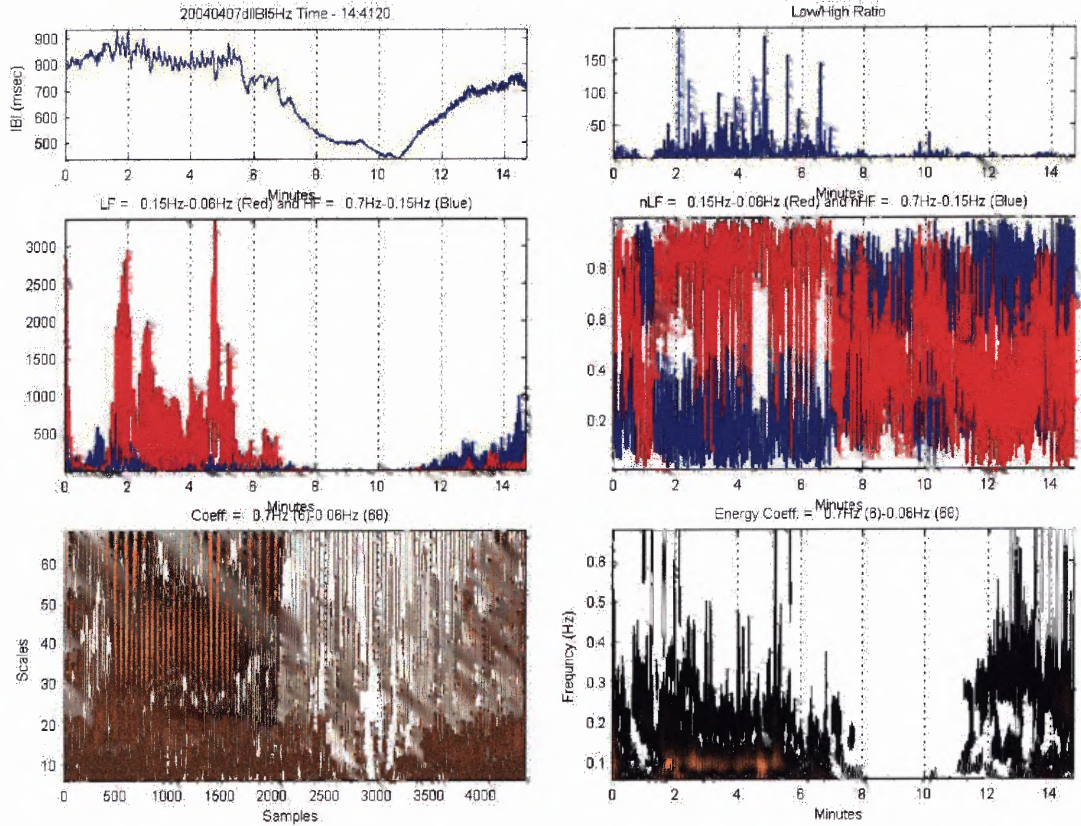


Figure H.19 STFT output for subject 19.

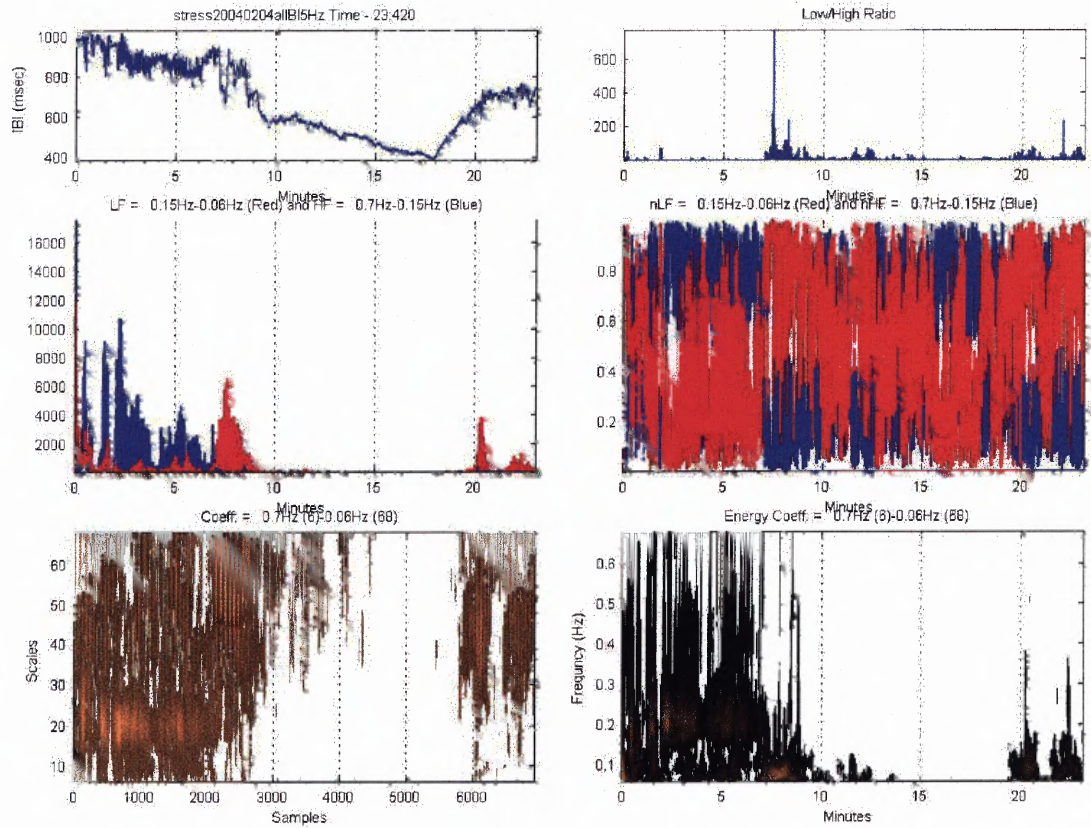


Figure H.20 STFT output for subject 20.

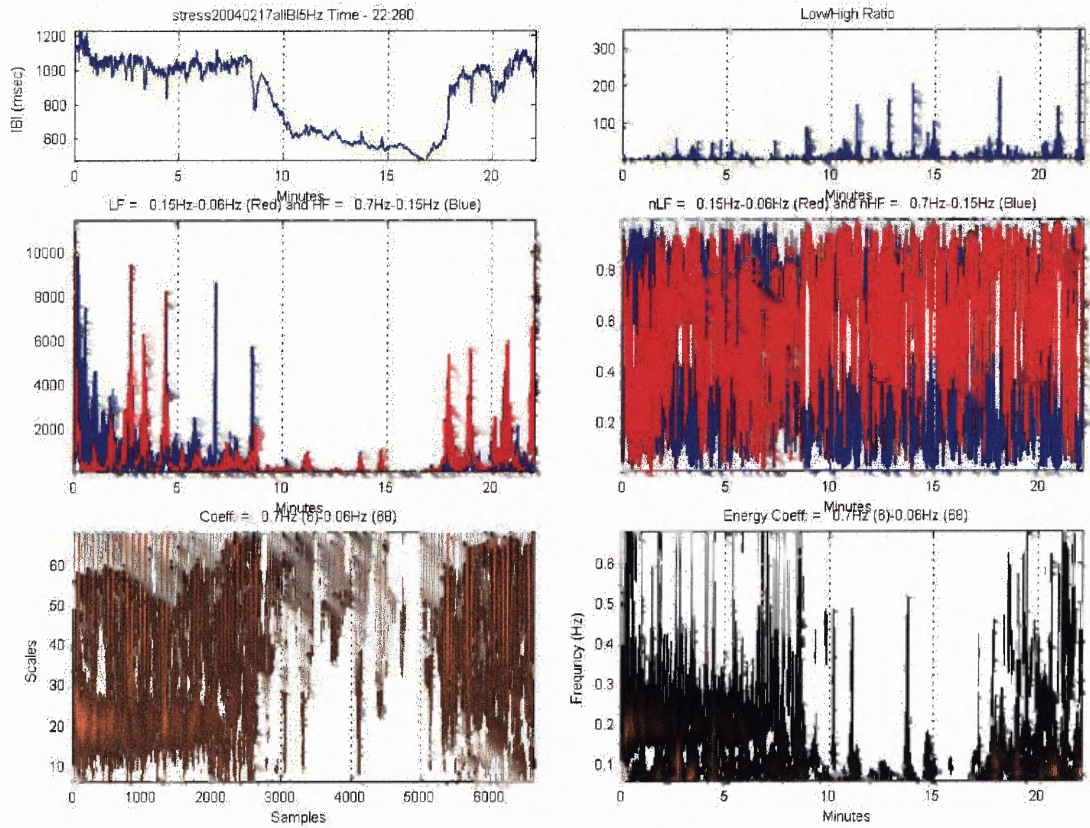


Figure H.21 STFT output for subject 21.

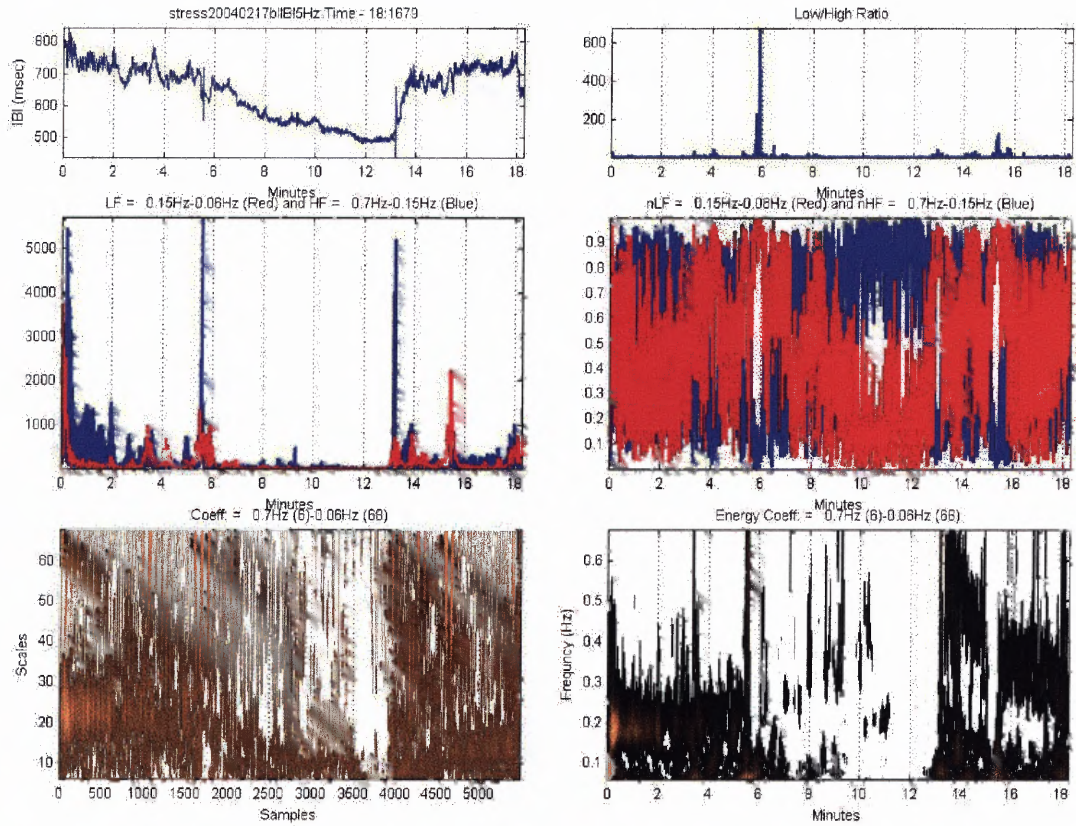


Figure H.22 STFT output for subject 22.

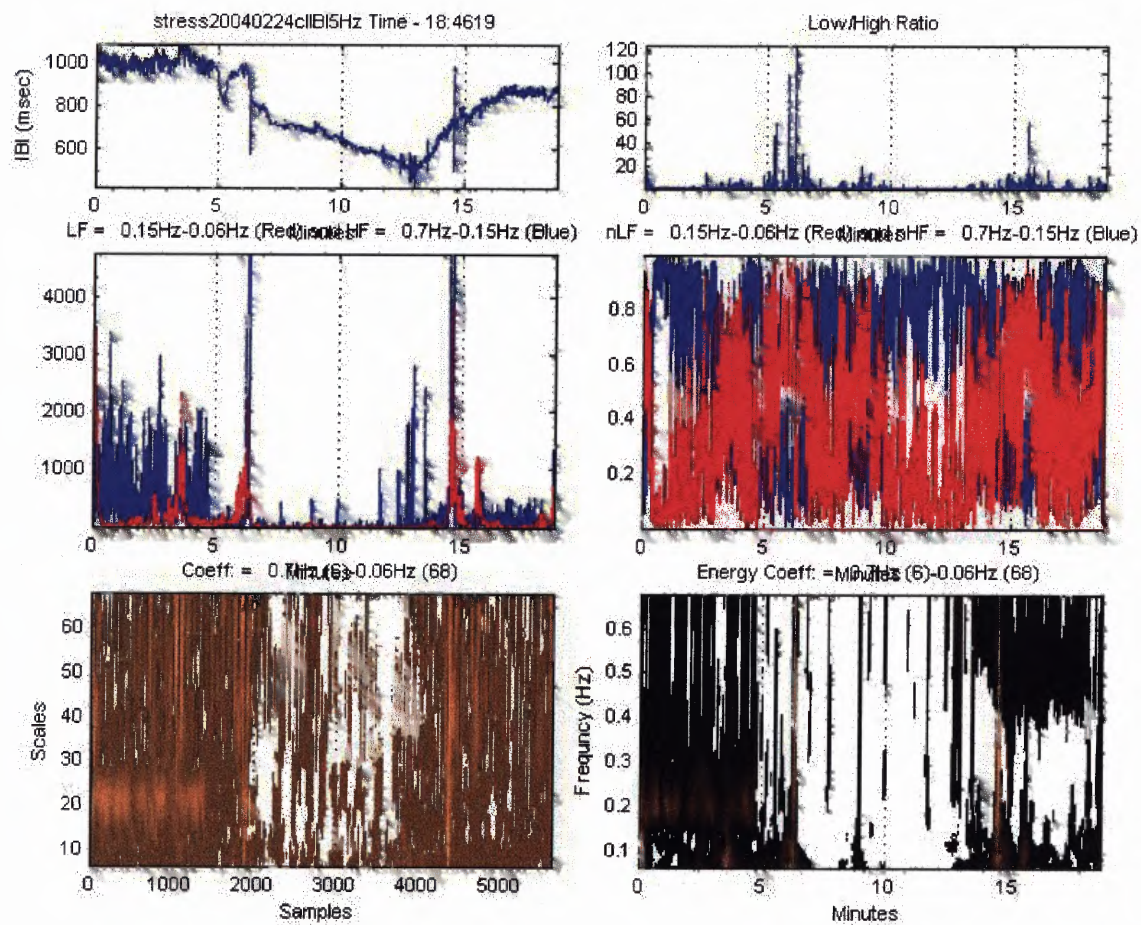


Figure H.23 STFT output for subject 23.

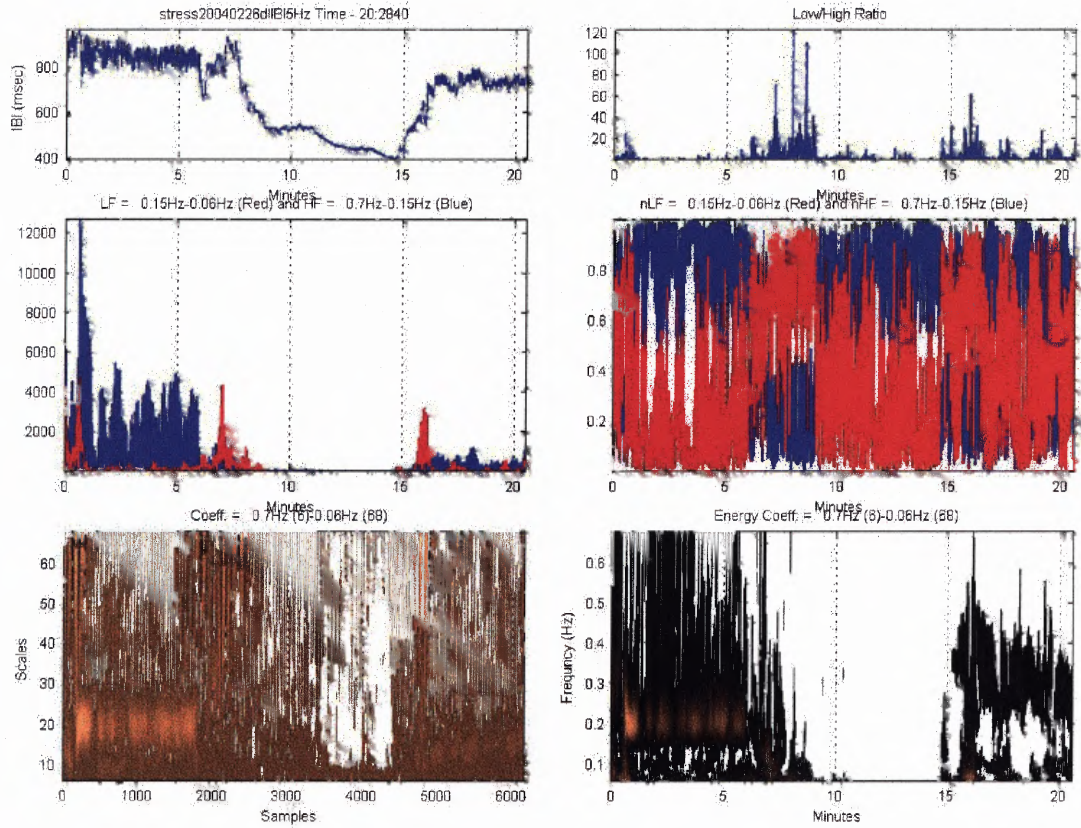


Figure H.24 STFT output for subject 24.

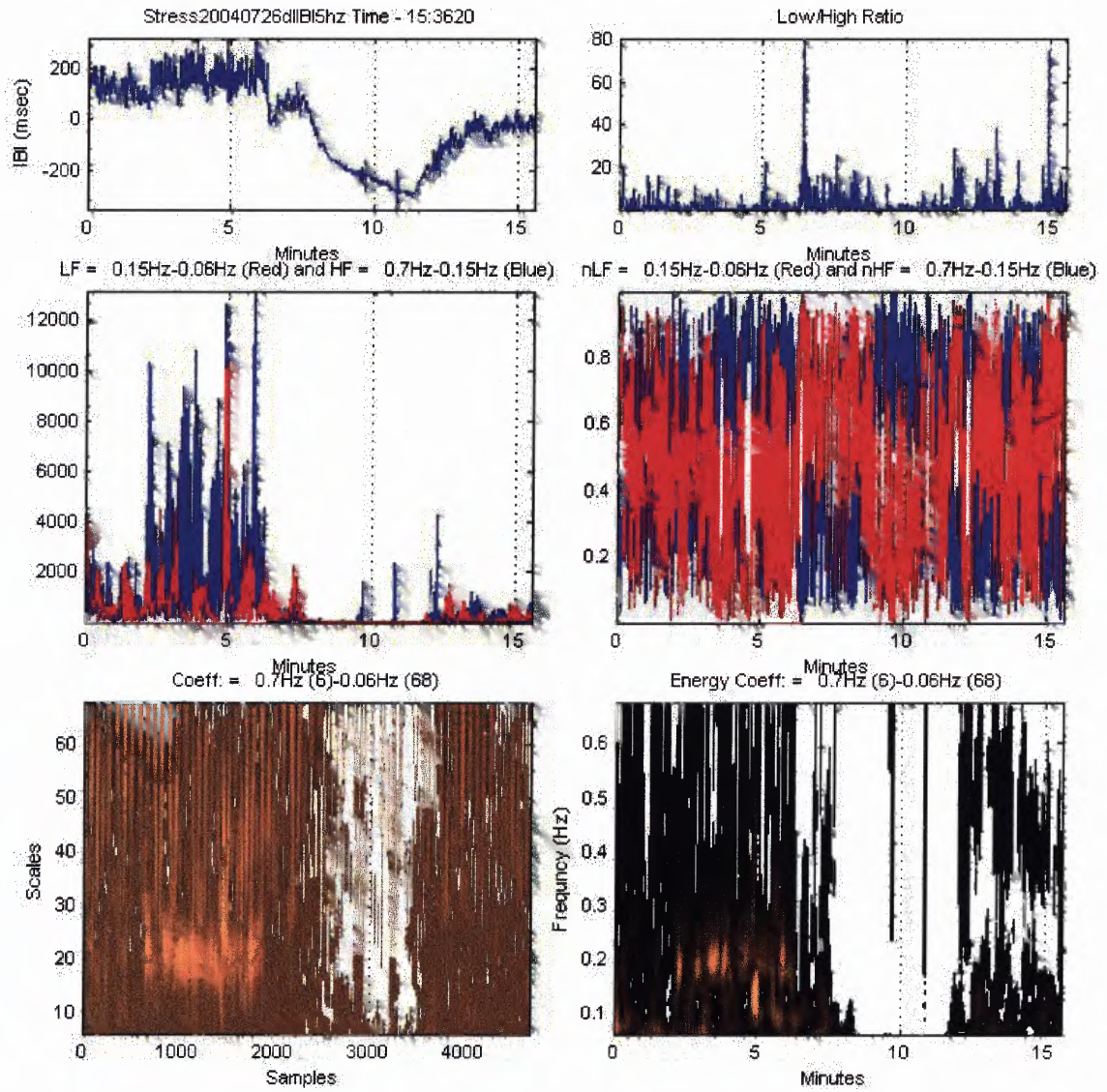


Figure H.25 STFT output for subject 25.

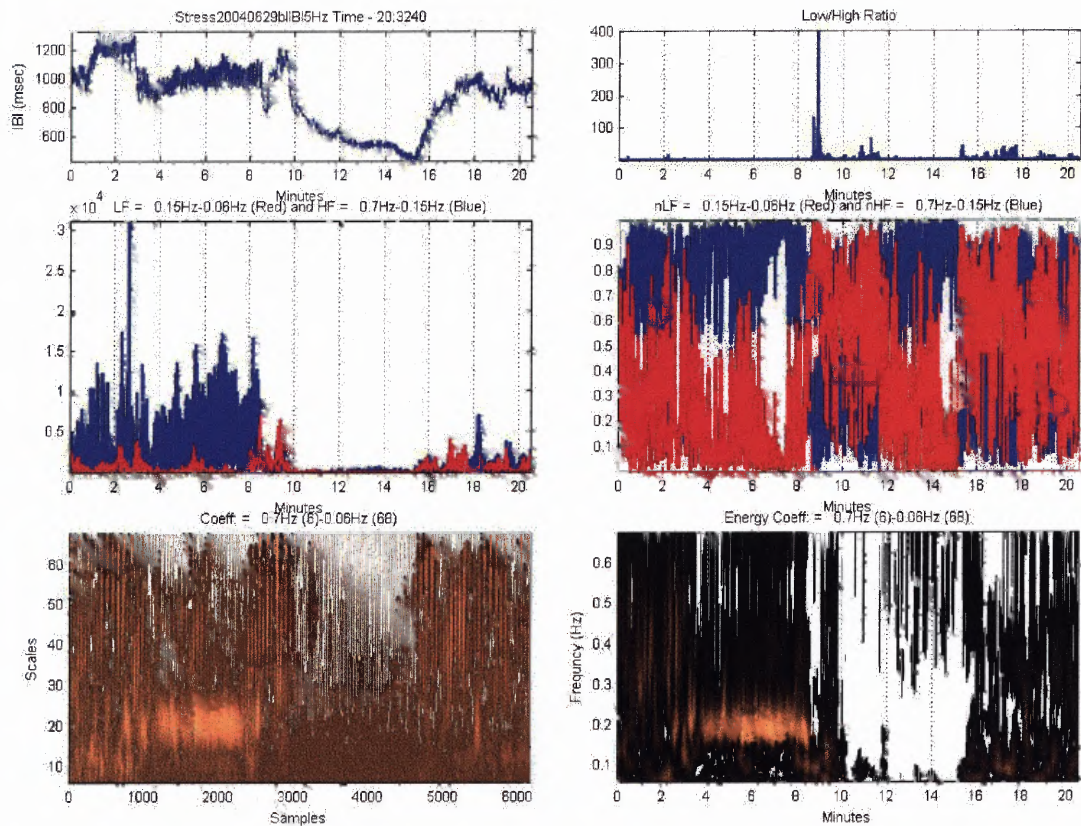


Figure H.26 STFT output for subject 26.

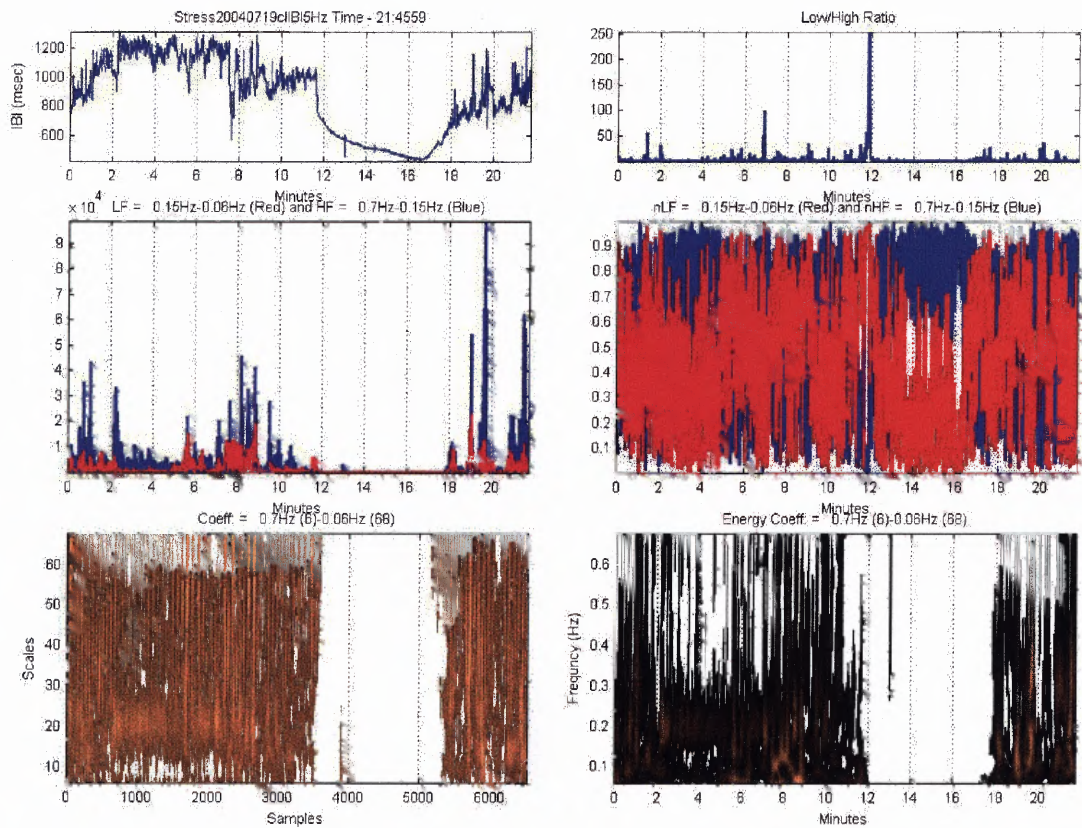


Figure H.27 STFT output for subject 27.

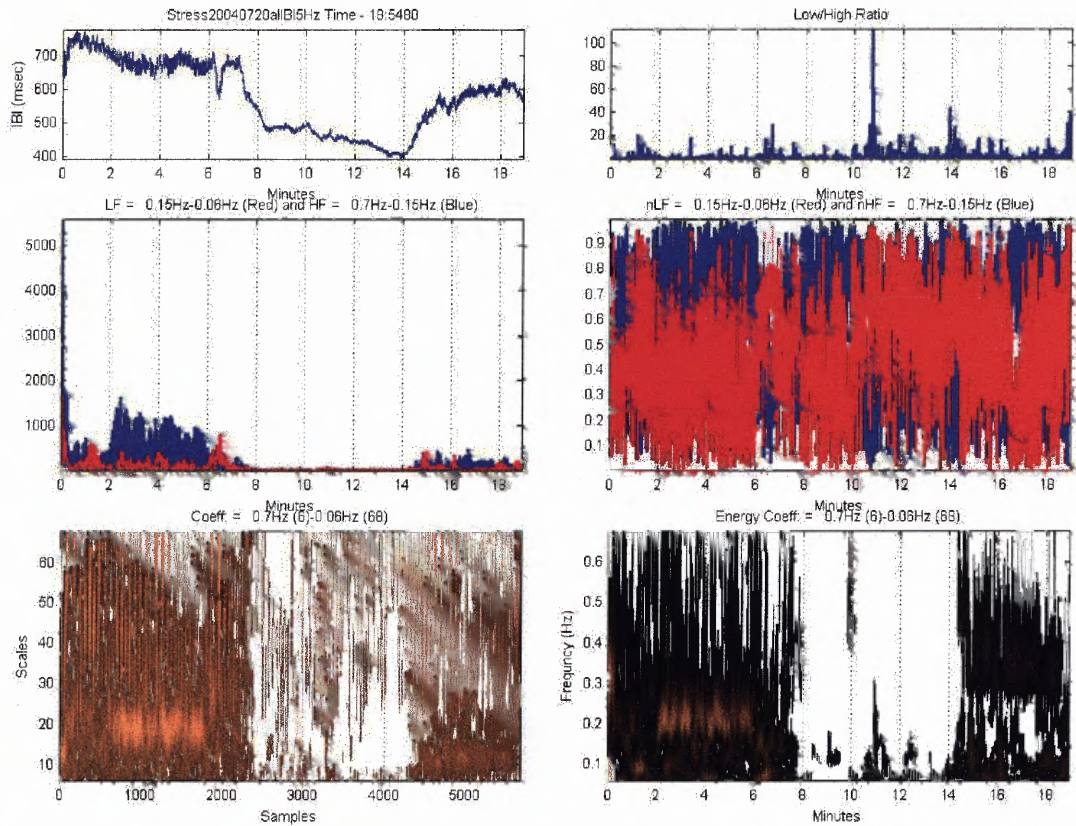


Figure H.28 STFT output for subject 28.

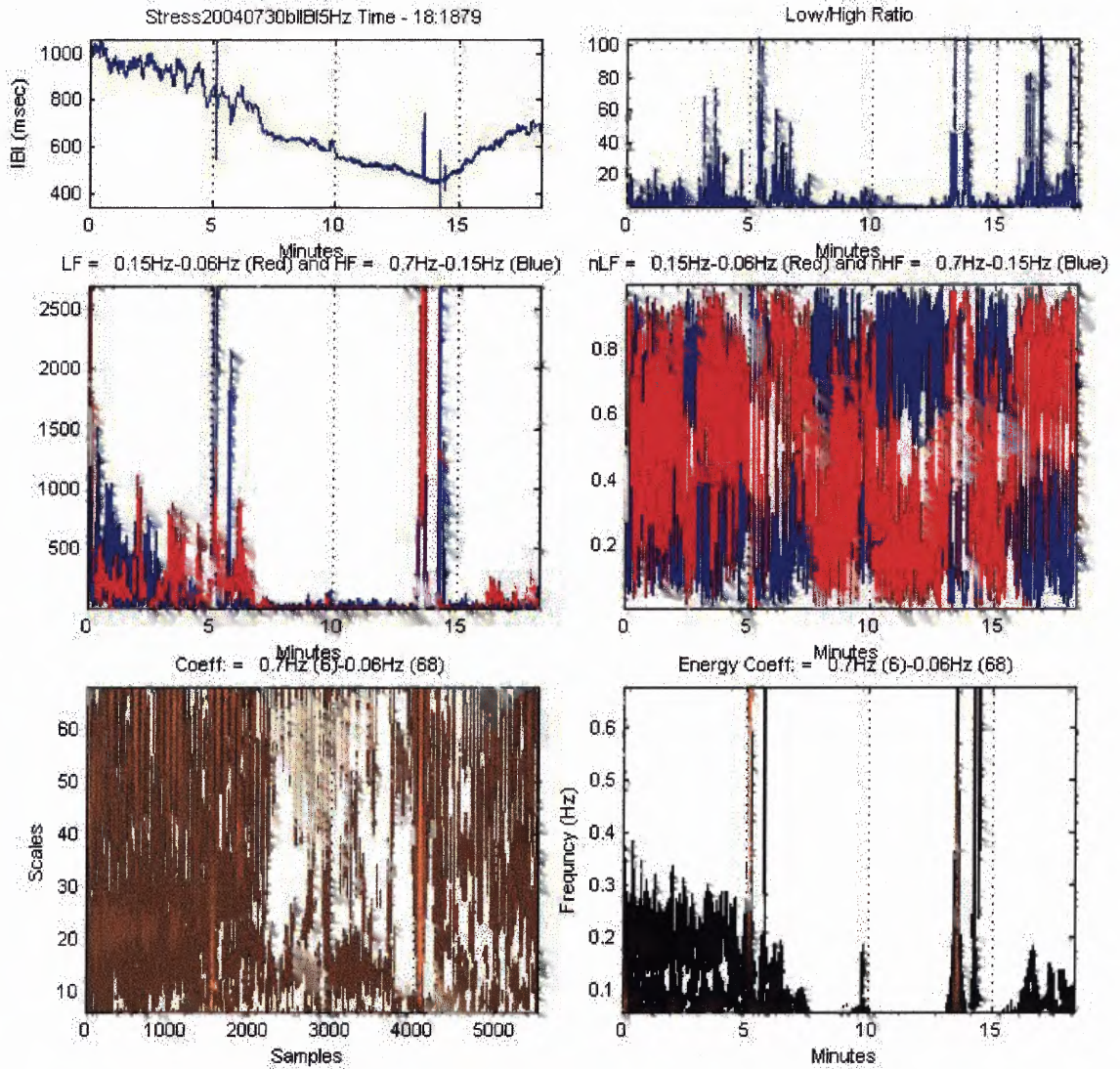


Figure H.29 STFT output for subject 29.

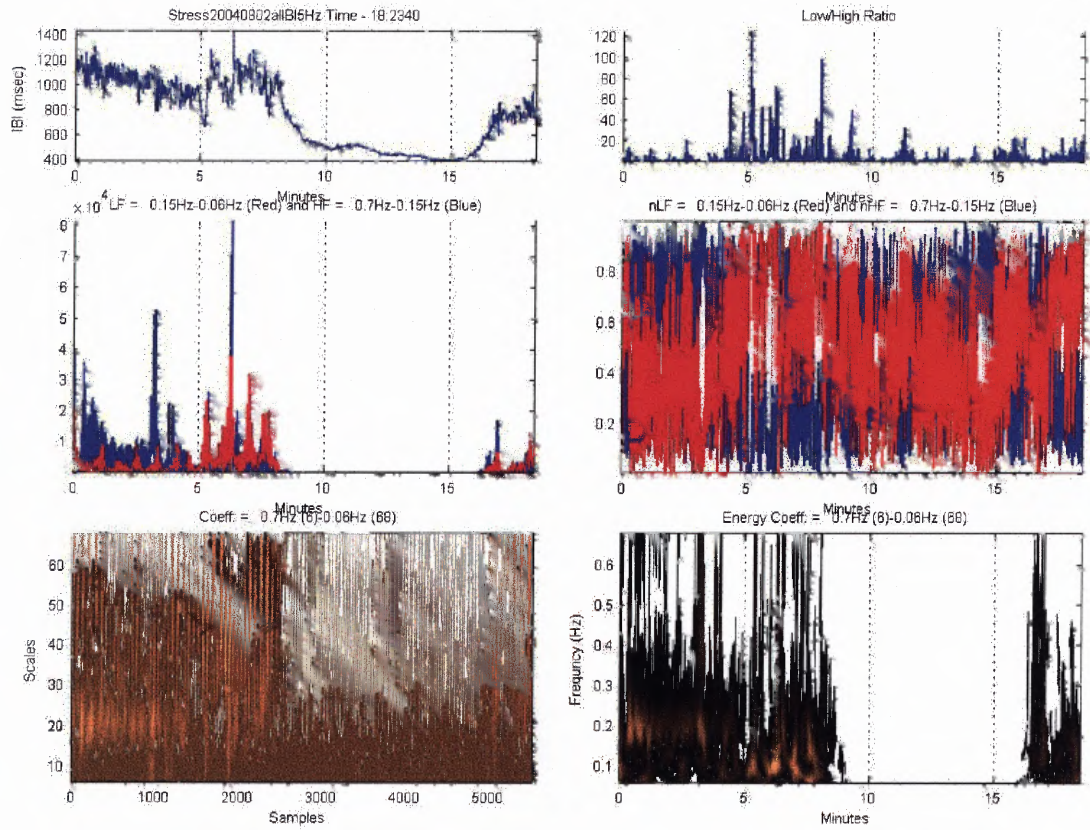


Figure H.30 STFT output for subject 30.

REFERENCES

- [1] D. M. Pober, B. Braun and P. S. Freedson. "Effects of a Single Bout of Exercise on Resting Heart Rate Variability." *Med. Sci. Sports. Exerc.*, vol. 36(7), pp. 1140-1148, Jul. 2004.
- [2] E. N. Marieb, *Human Anatomy and Physiology*, 3rd ed. New York: The Benjamin/Cummings Publishing Company, Inc., 1989.
- [3] S. E. O'Sullivan and C. Bell. "Training Reduces Autonomic Cardiovascular Responses to Both Exercise Dependent and Independent Stimuli in Humans." *Autonomic Neuroscience: Basic and Clinical*, vol. 91, pp. 76-84, April 2001.
- [4] W. M. Savin, D. M. Davidson and W. L. Haskell. "Autonomic Contribution to Heart Rate Recovery From Exercise in Humans." *J. Appl. Physiol.*, vol. 53, pp. 1572-1575, Dec.1982.
- [5] G. Pierpont and E.J. Voth. "Assessing Autonomic Function by Analysis of HR Recovery from Exercise in Healthy Subjects." *Am. J. Cardiol.*, vol. 94, pp. 64-68, Jul. 2004.
- [6] S. Shin, W. Tapp, S. Reisman and B. Natelson. "Assessment of Autonomic Regulation of Heart Rate Variability by the Method of Complex Demodulation." *IEEE Trans. Biomedical Eng.*, vol. 36, pp. 274-282, Feb. 1989.
- [7] E. H. Hon and S. T. Lee. "Electronic Evaluation of the Fetal Heart Rate VIII. Patters Preceding Fetal Death, Further Observations." *Am J Obstet Gynecol.*, vol.15, pp. 814-826, Nov. 1963.
- [8] M. Malik, J. T.Bigger, A. J. Cam, M. R. Kleiger, A. Malliani, A. Moss and P. Schwartz, "Heart Rate Variability: Standards of Measurement, Physiological Interpretation and Clinical Use." *European Heart Journal*, vol. 17, pp. 354-381, March 1996.
- [9] S. Akselrod, D. Gordon, F. A. Ubel, D. C. Shannon, A. C. Barger and R. J. Cohen. "Power Spectrum Analysis of Heart Rate Fluctuation: A Quantitative Probe of Beat-to-Beat Cardiovascular Control." *Science*, vol. 213, pp. 220-222, Jul. 1981.
- [10] S. Akselrod, D. Gordon, A. Ubel, D. Shannon, A. C. Barger and R. Cohen. "Power Spectrum Analysis of Heart Rate Fluctuations: A Quantitative Probe of Beat-To-Beat Cardiovascular Control." *Science*, vol. 213, pp. 220-222, Jul. 10, 1981.
- [11] U. Wiklund, M. Akay and U. Niklasson. "Short-Term Analysis of Heart-Rate Variability of Adapted Wavelet Transforms" *Engineering in Medicine and Biology Magazine, IEEE*, vol. 16, pp. 113 - 118, Sep. 1997.

- [12] E. Toledo, O. Gurevitz, H. Hod, M. Eldar and S. Akselrod. "Wavelet Analysis of Instantaneous Heart Rate: A Study of Autonomic Control During Thrombolysis." *Am. J. Physiol. Regul. Integr. Comp. Physiol.*, vol. 284, pp. R1079-R1091, Apr. 2003.
- [13] M. V. Kamath and E. L. Fallen. "Power Spectral Analysis of Heart Rate Variability: A Noninvasive Signature of Cardiac Autonomic Function" *Crit. Rev. Biomed. Eng.*, vol. 22, pp. 245-311, 1993.
- [14] R. Polikar. "The Engineer's Ultimate guide to Wavelet analysis." Internet: <http://users.rowan.edu/~polikar/WAVELETS/WTtutorial.html>, Jan. 12 2001 [Jan.13 2004].
- [15] L. B. Jackson. *Signals, Systems, and Transforms*. Reading, MA: Addison-Wesley Publishing Company, 1990, pp. 140-143,154.
- [16] F. Hlawatsch and G. F. Boudreaux-Bartels. "Linear and Quadratic Time-Frequency Signal Representations." *Signal Processing Magazine, IEEE*, vol. 9, pp. 21-67, Apr. 1992.
- [17] R. Atkins. "Heisenberg Uncertainty Principle and Quantum Mechanics." Internet: http://www.physics.utah.edu/~ratkins/lecture_notes_week8.pdf [Jan. 4, 2005].
- [18] P. Marmet. "Absurdities in Modern Physics: A Solution." Internet: <http://www.newtonphysics.on.ca/HEISENBERG/Chapter3.html> [Jan. 4, 2005].
- [19] D.A. Newandee and S. Reisman. "Wavelet Representation Comparison for Heart Rate Variability Analysis." *Proceedings of 29th Annual Bioengineering Conference, IEEE*, 2003, pp. 112-113.
- [20] J. Lewalle. "Tutorial on Continuous Wavelet Analysis of Experimental Data." Internet: <http://www.ecs.syr.edu/faculty/lewalle/tutor/tutor.html>, Apr. 1995 [Dec. 1, 2004].
- [21] P. Addison, J. Watson and T. Feng. "Low Oscillation Complex Wavelets." Internet: <http://www.cardiodigital.com/Publications/Low%20Osc%20S&V%20Preprint.pdf> [Dec. 1 2004].
- [22] C. Valens. "A Really Friendly Guide to Wavelets." Internet: <http://perso.wanadoo.fr/polyvalens/clemens/download/arfgtw.pdf> 1999 [Dec. 1, 2004].
- [23] Polar S810 manual <http://www.polarusa.com/manuals/s810.pdf> [Nov. 30,2004].
- [24] A. Loimaala, H. Sievanen, R. Laukkanen, et. al. "Accuracy of a novel real-time microprocessor QRS detector for heart rate variability assessment." *Clin. Physiol.*, vol.19, pp. 84-88, Jan. 1999.
- [25] <http://mathworld.wolfram.com/HanningFunction.html> [Nov. 2, 2004].

- [26] O. Faust, U. R. Acharya, S. M. Krishnan and L. C. Min. "Analysis of Cardiac Signals Using Spatial Filling Index and Time-Frequency Domain." *Biomed. Eng. Online*, vol. 30, Sep. 2004, Available: <http://www.biomedical-engineering-online.com/content/3/1/30> [Dec. 2, 2004].
- [27] V. I. Ponomarenko, M. D. Prokhorov, A. B. Bespyatov, M. B. Bodrov and V. I. Gridnev. "Deriving Main Rhythms of the Human Cardiovascular System From the Heartbeat Time Series and Detecting Their Synchronization Chaos." *Solitons & Fractals*, vol. 23, pp. 1429-1438, Feb 2005.
- [28] M. E. Torres and L. G. Gamero. "Relative Complexity Changes in Time Series Using Information Measures Physica A." *Statistical Mechanics and its Applications*, vol. 286, pp. 457-473, Nov. 2000.
- [29] M. Misiti, Y. Misiti, G. Oppenheim and J. M. Poggi. *Wavelet Toolbox User's Guide*. The MathWorks, 2004, pp. 8-208 – 8-217. Available: http://www.mathworks.com/access/helpdesk/help/pdf_doc/wavelet/wavelet_ug.pdf [Jan 9, 2005].
- [30] E. Pruvot, G. Thonet, J.M. Vesin, G. Van-Melle, K. Seidl, H. Schmidinger, J. Brachmann, W. Jung, E. Hoffmann, R. Tavernier, M. Block, A. Podczeck and M. Fromer. "Heart Rate Dynamics at the Onset of Ventricular Tachyarrhythmias as Retrieved From Implantable Cardioverter-Defibrillators in Patients With Coronary Artery Disease." *Circulation*, pp. 2398-2404, Dec. 1999.
- [31] D. J. Ewing, L. Hume, I.W. Campbell, A. Murray, J.M.M Neilson and B.F. Clarke. "Autonomic Mechanisms in the Initial Heart Rate Response to Standing." *J. Appl. Physiol.*, vol. 45, pp. 809-814, Nov. 1980.
- [32] J. Goldberger, S. Challapalli, R. Tumbg, M. Parker and A. Kadish. "Relationship of Heart Rate Variability to Parasympathetic Effect." *Circulation*, vol. 103, pp. 1977-1983, Jan. 2001.
- [33] J. Goldberger, M. Ahmed, M. Parker and A. Kadish. "Dissociation of Heart Rate Variability from Parasympathetic Tone." *Am. J. Physiol.*, vol. 266 pp. H2152-H2157, Feb. 1994.
- [34] C. Amara and L. Wolfe. "Reliability of Noninvasive Methods to Measure cardiac Autonomic Function." *Can. J. Appl. Physiol.*, vol. 23, pp. 396-408, Feb. 1998.
- [35] I. K. Brenner, S. Thomas and R. J. Shepard. "Spectral Analysis of Heart Rate Variability During Heat Exposure and Repeated Exercise." *Eur. J. Appl. Physiol. Occup. Physiol.*, vol. 76 pp. 145-156, Feb. 1997.
- [36] F. Cottin, C. Medigue, P.-M. Lepretre, Y. Papelier, J.-P. Oralsztein and V. Billat. "Heart Rate Variability During Exercise Performed Below and Above Ventilatory Threshold." *Med. Sci. Sports Exerc.*, vol. 36, pp. 594-600, Dec. 2004.

- [37] A.P. Pichon, C. De Bisschop, M. Roulaud, A. Denjean and Y. Papelier. "Spectral Analysis of Heart Rate Variability during Exercise in Trained Subjects." *Med. Sci. Sports Exerc.*, vol. 36, pp. 1702-1708, June 2004.
- [38] B. Pomeranz, R. Macaulay, M. Caudill, I. Kutz, D. Adam, D. Gordon, K. Kilborn, A. C. Barger, D. C. Shannon, R. J. Cohen and H. Benson. "Assessment of Autonomic Function in Humans by Heart Rate Spectral Analysis." *Am. J. Physiol.*, vol. 248, pp. H151-H153, 1985.
- [39] Y. Arai, J.P. Saul, P. Albrecht, L.H. Hartley, L.S. Lilly, R.J. Cohen and W.S. Colucci. "Modulation of Cardiac Autonomic Activity During and Immediately After Exercise." *Am. J. Physiol.*, vol. 256, pp. H132-41, Jan. 1989.
- [40] L.R. Davrath, I Pinhas, A. Beck, M. Scheinowitz, D. Elian and S. Akselrod. "Heart Rate Recovery After Exercise: A Study by Wavelet Analysis." *Computers in Cardiology*, vol. 30, pp. 453-456, 2003.